Institute for Molecular Medicine Finland (FIMM)

The Doctoral Programme in Biomedicine (DPBM)

Faculty of Medicine

University of Helsinki, Helsinki, Finland

Unravelling Lung Cancer Heterogeneity and Associated Therapeutic Responses using *in vivo* and *ex vivo* Model Systems

Ashwini S. Nagaraj

ACADEMIC DISSERTATION

To be presented, with the permission of the Faculty of Medicine,

University of Helsinki, for public examination in Lecture Hall 3,

Biomedicum Helsinki, Haartmaninkatu 8, Helsinki

On 7th of December 2018, at 12 o' clock noon.

Helsinki 2018

Supervised by

Emmy Verschuren, Ph.D.
FIMM-EMBL Group Leader
Institute for Molecular Medicine Finland (FIMM)
HiLIFE, University of Helsinki
Helsinki, Finland

Denis Kainov, Ph.D.
Associate Professor
Department of Clinical and Molecular Medicine
Norwegian University of Science and Technology (NTNU)
Trondheim, Norway

Thesis advisory committee

Prof. Elina Ikonen, M.D., Ph.D.
Institute of Biomedicine, Anatomy
University of Helsinki
Helsinki, Finland

Brendan Battersby, Ph.D.
Group leader, Institute of Biotechnology
University of Helsinki
Helsinki, Finland

Thesis reviewers

Prof. Anna-Liisa Levonen, M.D., Ph.D.
A.I.Virtanen Institute for Molecular Sciences
University of Eastern Finland
Kuopio, Finland

Aki Manninen, Ph.D.
Adjunct Professor, Oulu Center for Cell-Matrix Research
Biocenter Oulu and Faculty of Biochemistry and Molecular Medicine, University of Oulu
Oulu, Finland

Opponent

David Dankort, Ph.D.
Associate Professor
Department of Biology
McGill University
Québec, Canada

Custos

Prof. Jaakko Kaprio, M.D., Ph.D.
Faculty of Medicine
University of Helsinki
Helsinki, Finland

ISBN 978-951-51-4736-3 (paperback)
ISBN 978-951-51-4737-0 (PDF)
Printing house: Painosalama, Turku

ISSN 2342-3161 (print)
ISSN 2342-317X (online)

"*Vision without action is merely a dream; action without vision is merely passing time; but vision and action together can change the world."*

Sudha Murthy

Dedicated to my parents

TABLE OF CONTENTS

LIST OF ORIGINAL PUBLICATIONS

This thesis is based on following publications, and are referred in the text by their roman numerals:

I. **Ashwini S. Nagaraj***, Jenni Lahtela*, Annabrita Hemmes, Teijo Pellinen, Sami Blom, Jennifer R. Devlin, Kaisa Salmenkivi, Olli Kallioniemi, Mikko I. Mäyränpää, Katja Närhi, and Emmy W. Verschuren. Cell of Origin Links Histotype Spectrum to Immune Microenvironment Diversity in Non-Small Cell Lung Cancer Driven by Mutant *Kras* and Loss of *Lkb1*. *Cell Reports., 18 (3): 673-684, 2017.*

II. **Ashwini S. Nagaraj**, Jie Bao, Annabrita Hemmes, Mafalda Machado, Katja Närhi, and Emmy W. Verschuren. Establishment and analysis of tumor slice explants as a prerequisite for diagnostic testing. *Journal of Visualized Experiment. In Press.*

III. Katja Närhi, **Ashwini S. Nagaraj**, Elina Parri, Riku Turkki, Petra W. van Duijn, Annabrita Hemmes, Jenni Lahtela, Virva Uotinen, Mikko I. Mäyränpää, Kaisa Salmenkivi, Jari Räsänen, Nina Linder, Jan Trapman, Antti Rannikko, Olli Kallioniemi, Taija M. af Hällström, Johan Lundin, Wolfgang Sommergruber, Simon Anders, and Emmy W. Verschuren. Spatial Aspects of Oncogenic Signaling Determine Response to Combination Therapy in *Kras*-driven Lung Tumors. *Journal of Pathology., 245(1):101-113, 2018.*

IV. **Ashwini S. Nagaraj***, Sarang Talwelkar*, Jennifer R. Devlin, Annabrita Hemmes, Swapnil Potdar, Elina Kiss, Pipsa Saharinen, Kaisa Salmenkivi, Mikko I. Mäyränpää, Krister Wennerberg, and Emmy W. Verschuren. I*n situ* Oncogenic Signaling Activities Determine Sensitivity to Combinatorial MEK Inhibition and Stratify *Kras* mutant Lung Cancers. *Manuscript*.

* These authors contributed equally to the publication.

Publication I was included in the doctoral dissertation of Jenni Lahtela (Studying the functional relevance of lung cancer genetic drivers in their physiological niche, University of Helsinki, 2016).

Publication related to the thesis work but not included in the thesis:

- Emma J. Davies, Meng Dong, Matthias Gutekunst, Katja Närhi, Hanneke J. A. A. van Zoggel, Sami Blom, **Ashwini Nagaraj**, Tauno Metsalu, Eva Oswald, Sigrun Erkens-Schulze, Juan A. Delgado San Martin, Riku Turkki, Stephen R. Wedge, Taija M. af Hällström, Julia Schueler, Wytske M. van Weerden, Emmy W. Verschuren, Simon T. Barry, Heiko van der Kuip & John A. Hickman. Capturing complex tumour biology in vitro: histological and molecular characterisation of precision cut slices. *Scientific Reports., 9; 5:17187, 2015*.

ABBREVIATIONS

4EBP1	eukaryotic translation initiation factor 4E-binding protein 1
AAC	acinar adenocarcinoma
AAH	atypical adenomatous hyperplasia
AC	adenocarcinoma
Ad5-CC10-Cre	adenoviral vector expressing Cre-recombinase under CC10 promoter
Ad5-CMV-Cre	adenoviral vector expressing Cre-recombinase
Ad5-SPC-Cre	adenoviral vector expressing Cre-recombinase under SPC promoter
AIS	adenocarcinoma in situ
AKT	RAC-alpha serine/threonine-protein kinase
ALK	anaplastic lymphoma kinase
AMP	adenosine monophosphate
AMPK	AMP-activated protein kinase
Arg1	arginase 1
ASC	adenosquamous carcinoma
AT1 cell	alveolar type I cell
AT2 cell	alveolar type II cell
ATP	adenosine triphosphate
BADJ	bronchioalveolar duct junction
BASCs	bronchioalveolar stem cells
BRAF	B-Raf protooncogene, serine/threonine kinase
CC10	club cell-specific 10 kD protein
CCSP	club cell secretory protein
CDKIs	cyclin-dependent kinase inhibitors
Cdkn2ab	cyclin-dependent kinase Inhibitor 2A
CgA	chromogranin A
CGRP	calcitonin gene-related peptide
CK14	cytokeratin 14
CK5	cytokeratin 5
COPD	chronic obstructive pulmonary disease
CYP2F2	cytochrome P450 2F2
DNA	deoxyribonucleic acid
EGF	epidermal growth factor
EGFR	epidermal growth factor receptor
ERBB2	Erb-B2 Erythroblastic Leukemia Viral Oncogene Homolog
ERK	extracellular signal-regulated kinase
FAK	focal adhesion kinase
FGFR1	fibroblast Growth Factor Receptor 1
FOXJ1	forkhead box J1
GAP	GTPase-activating protein
GEF	guanine nucleotide exchange factors
GEMM	genetically engineered mouse model
Gr-1	myeloid differentiation antigen Gr-1
GTPase	small guanosine triphosphatase
H2-D1	histocompatibility 2, D region locus 1
H2-M2	histocompatibility 2, M region locus 2
HRAS	harvey Rat Sarcoma Viral Oncogene Homolog
IAC	invasive adenocarcinoma
IHC	immunohistochemistry
Il1b	interleukin 1 beta
ITH	intratumoral heterogeneity

KL	*Kras*$^{LSL\text{-}G12D/+}$*; Lkb1*$^{fl/fl}$
KP	*Kras*$^{LSL\text{-}G12D/+}$*;Trp53*$^{fl/fl}$
KRAS	Kirsten Rat Sarcoma Viral Oncogene Homolog
LCC	large cell carcinoma
LKB1/STK11	liver kinase B1 / serine/threonine-protein kinase 11
LY6C	lymphocyte antigen 6 complex locus C
LY6G	lymphocyte antigen 6 complex locus G
MAC	mucinous adenocarcinoma
MAPK	mitogen-activated protein kinase
MDM2	mouse double minute 2 homolog
MDSC	myeloid-derived suppressor cells
MHC	major histocompatibility complex
mTOR	mammalian target of rapamycin
NGR1	Neuregulin 1
NKX2-1	NK2 Homeobox 1
NRAS	neuroblastoma RAS Viral Oncogene Homolog
NSCLC	non-small cell lung cancer
p63	tumor protein 63
PAC	papillary adenocarcinoma
PAS	periodic acid–Schiff
PD-1	programmed cell death protein 1
PD-L1	programmed death-ligand 1
PI3K	phosphoinositide 3-kinase
PJS	peutz–Jeghers syndrome
ProGRP	serum pro-gastrin releasing peptide
PTEN	phosphatase and tensin homolog
Q-PCR	quantitative polymerase chain reaction
RB1	retinoblastoma 1
RTK	receptor tyrosine kinase
SCC	squamous cell carcinoma
SCGB1A1	secretoglobin family 1A member 1
SCLC	small-cell lung cancer
SO2	sulphur dioxide
SOX2	SRY (sex determining region Y)-box 2
SPC	surfactant protein C
SRC	proto-oncogene tyrosine-protein kinase Src
TAN	Tumor-associated neutrophil
TNM	Tumor-Node-Metastasis system
Trp53/TP53	transformation related protein 53/tumor protein 53
TSC1/TSC2	tuberous Sclerosis 1 Protein/ tuberous Sclerosis 1 Protein

ABSTRACT

Lung cancer is the leading cause of cancer-related mortality worldwide. Non-small cell lung cancer (NSCLC) is the most common type of lung cancer (85%), and is histologically subdivided into adenocarcinoma (AC; 40%), squamous cell carcinoma (SCC; 30%) and adenosquamous cell carcinoma (ASC; 0,4-4%). Histologically, ASCs harbor both AC and SCC components. Although ASCs are rare, they constitute the most aggressive form of lung cancer with poor patient prognosis. While molecularly targeted therapies for *EGFR/ALK/ROS* are typically directed towards ACs, in which these mutations are predominantly detected, the majority of NSCLC patients carry mutations in *KRAS* and *LKB1*, for which no approved therapies exist thus far. Furthermore, while heterogeneity in tumor microenvironments and oncogenic signaling are major factors contributing to disease relapse, the histotype-specific etiology of tumor heterogeneity remains elusive. Using genetically engineered mouse models (GEMMs) of lung cancer it has been shown that the identity of niche-specific progenitors defines the phenotype of the tumors that arise. Therefore, an understanding of lung histopathology subtype-specific cell(s) of origins will help to dissect the evolution of tumor heterogeneity, and ultimately the development of histotype-specific therapies.

This thesis work investigated the role of the cell of origin in defining histotype diversity in a GEMM that harbors concurrent activation of $Kras^{G12D}$ with loss of *Lkb1* (hereafter called 'KL'). To do this, lung progenitor cells were targeted using cell-type directed Adenoviral Cre viruses (AdCre) to initiate tumorigenesis in bronchiolar Club cells (Club cell secretory protein; $CC10^{+}$) or alveolar type II cells (surfactant protein C; SPC^{+}). This approach led to the identification of $CC10^{+}$ cells as predominant progenitors of ASC tumors. In addition, transcriptome analysis together with intratumoral immune cell analysis revealed an ASC-specific immunosuppressive phenotype, marked by downregulation of antigen-presenting genes, infiltration of tumor-associated neutrophils (TANs), and reduced numbers of intratumoral T cells. This part of the thesis work thus demonstrated that progenitor cell-specific etiology links to the histopathology spectrum and histotype-specific immune microenvironments of KL-driven tumors.

The second part of this thesis work provides a visual demonstration of a methodology for the generation, cultivation, and analysis of precision-cut murine NSCLC tissue slices. This work showed that optimization for slice thickness was important to retain maximum viability of cultured slices. Additionally, this protocol describes how to identify optimal drug concentrations for treatment of tumor slices, and highlights that comparison of heterogeneous marker expression in cultivated and

neighboring uncultured slices is important to assess the preservation of tumor-specific biological functions in cultured slices.

The thesis next focused on understanding the role of both tumor histotypes in defining oncogenic signaling downstream of KRAS and LKB1, and how such insights can be used for drug testing and selection of optimal drug combinations. By utilizing *Kras*-driven NSCLC GEMMs we demonstrate that certain oncogenic signaling pathways are spatially active in a histotype-specific manner, namely: predominance of PI3K/AKT and SRC pathways in SCC subregion of ASCs, and enrichment of MAPK pathway in ACs. Short-term treatment of tumor tissue slice cultures with combinatorial PI3K/mTOR and MAPK inhibitors showed that cytotoxic responses correlated with spatially distributed co-occurrence of both pathways. This work highlighted that tumor histotype, rather than genotype, is the major determinant of oncogenic signaling heterogeneity, and that concomitant spatial activation of targeted signaling pathways is essential to achieve optimal cytotoxic response to combination therapy. In addition, it demonstrated the utility of tumor tissue slices in modeling spatial response to drug treatment.

Finally, this thesis investigated histotype- or genotype-specific drug vulnerabilities using epithelial cultures of murine NSCLC. We showed that KL tumor cells are unable to grow under standard conditions and require a use of a cell culture protocol called conditional reprogramming (CR). Drug sensitivity and resistance testing (DSRT) on murine NSCLC conditionally reprogrammed cells (CRCs), followed by *in vivo* validation of treatment responses, led to the identification of NSCLC subtype-specific acute responses to single or combinatorial inhibition of the MAPK pathway. We showed that NSCLC subtype-specific resistance to MEK inhibition in CRC cultures is mediated by intrinsic or adaptive activation of receptor tyrosine kinases (RTKs), specifically activation of ERBBs (in KL;ASC and KL;ACs) or FGFR (in ACs). Importantly, we assessed the ability of CRCs to model *in vivo* drug response by performing short-term (3 days) combined MEK/ERBB inhibition in *Kras* mutant lung cancer GEMMs. This *in vivo* combinatorial inhibition resulted in acute cytotoxic response selectively in ASCs (with strongest responses in the SCC subregions of ASC tumors) compared to ACs. This result was further supported by the predominance of ERBB activation specifically in SCC regions of *in situ* ASCs. Consistent with murine findings, we showed ASC and SCC histotype-specific predominance of selected ERBB family receptors in clinical NSCLC samples. Collectively, this work suggests that NSCLC-derived primary cultures could be used for the identification of subtype-specific acute therapeutic responses, and that the coupling of *in vivo* spatial signaling activities with *in vitro* drug sensitivities could aid in selection of tumor-specific combination therapies.

In summary, this thesis demonstrates that the tumor cell of origin defines histotype fate and a histopathology-specific immune microenvironment upon expression of oncogenic *Kras*^{G12D} and loss of the tumor suppressor *Lkb1*, and that activation of oncogenic signaling pathways are also stratified by tumor histotype. Therefore, in addition to genotype-based stratification, deeper understanding of tumor histotype-specific features will be of importance in clinical settings. This work also validates the utility of *ex vivo* models, namely tumor tissue slices and tumor-derived primary cell cultures, for functional diagnostics, permitting assessment of spatial drug response and identification of pathology-specific drug vulnerabilities, respectively.

INTRODUCTION

Cancer is a disease characterized by abnormal growth of cells in an uncontrolled manner. Certain cancer cells have the potential to invade or spread into surrounding tissues, by a process called metastasis. Cancer can arise from any part of the body. Carcinomas are the most common cancer type, and arise from epithelial cells that cover the skin and the body's internal organs. Globally, cancer is the leading cause of mortality. During 2012, 8.2 million cancer-related deaths were reported worldwide (Ferlay et al., 2015). Cancer develops following somatic genetic abnormalities in normal cells, or inherited cancer-causing genetic variations (Hanahan and Weinberg, 2000, 2011; Loeb and Loeb, 2000). Exposure to physical (e.g. ultraviolet and ionizing radiation), chemical (e.g. tobacco, asbestos, arsenic), or biological carcinogens (e.g. viral and bacterial infections) results in alteration of genes that regulate cell growth and differentiation, increasing the risk of cancer development (Anand et al., 2008). Furthermore, chronic inflammation, or carcinogen-induced disruption of the host microenvironment also facilitates cancer development (Casey et al., 2015; Multhoff et al., 2011). Genes contributing to cancer initiation and progression are categorized as oncogenes, which promote cell growth, and tumor suppressors, which promote cell death or inhibit cell division under cellular stress conditions. Cancer-causing genetic alterations can lead to inappropriate activation or overexpression of oncogenes, or inactivation or loss of tumor suppressor genes (Balmain, 2001; Knudson, 2001). Transformation of a normal cell into a malignant tumor is considered to occur via a multistep process during which cancer cells acquire abnormal biological capabilities, termed as 'hallmarks of cancer'. These include sustaining proliferative signaling, evading growth suppressors, activating invasion and metastasis, enabling replicative immortality, inducing angiogenesis, resisting cell death, reprogramming of energy metabolism, and evading immune destruction (Hanahan and Weinberg, 2000, 2011).

Lung cancer is the major cause of cancer-related deaths worldwide (Ferlay et al., 2015; Siegel et al., 2018). Tobacco smoking is the primary risk factor, contributing to nearly 85% of the lung cancer deaths (Furrukh, 2013). Lung cancer is histologically and genetically a heterogeneous disease (Gridelli et al., 2015). Comprehensive genomic profiling has led to the classification of lung cancer into distinct molecular subtypes, and the development of targeted therapies against specific genetic alterations (Bronte et al., 2010). However, as of yet, no clinically approved therapies available for the treatment of lung cancer patients carrying common driver genes, namely mutations in oncogenic *KRAS* (Kirsten Rat Sarcoma Viral Oncogene Homolog), and the tumor suppressor *STK11* (Serine/Threonine Kinase 11, also known as LKB1).

The average five-year survival of lung cancer patients is only 15%, and the majority of patients are diagnosed at late stages, when tumors contain pronounced genetic and histological heterogeneities.

This limits the effectiveness of treatment, leading to poor patient survival (Chen et al., 2014; Wang et al., 2010). Pharmacological management of advanced NSCLC patients is primarily based on molecular and histological subtyping, and most patients develop resistance to targeted therapies within one year of treatment (Facchinetti et al., 2017b). Moreover, driver gene alterations do not always predict clinical response, highlighting a need for the development of diagnostic methods linked to predictive biomarkers (Shepherd et al., 2005; Tsao et al., 2005). Multiple factors contribute to therapy resistance, including roles for the tumor microenvironment and infiltrating immune cells, and activation of compensatory pathways through rapid rewiring of cancer cell signaling (Rosell et al., 2013; Wang et al., 2017). Furthermore, pronounced functional heterogeneity caused by the landscape of genetic mutations induced in different tumor cells of origin, as well as branched molecular evolution during tumor progression, poses challenges on the success of cancer therapies (Blanpain, 2013; de Bruin et al., 2015). A deeper understanding of disease etiology leading to end-stage tumor heterogeneity, using physiologically relevant models with intact immune systems, may help to eventually tackle this complexity in clinical samples.

This thesis investigates the role of niche-specific lung progenitor cells in defining NSCLC histotype spectra and immune microenvironment heterogeneity, using a murine model driven by oncogenic *Kras* and loss of the tumor suppressor *Lkb1*. In addition, using *Kra*s-driven NSCLC GEM models, this thesis also demonstrates histotype-associated spatial oncogenic signaling heterogeneity and its importance in defining therapeutic responses. Furthermore, it establishes *Kras*-driven NSCLC tumor tissue slice cultures and shows their utility as *ex vivo* models in predicting spatial responses to drug combinations. Finally, by performing drug screening on murine NSCLC primary cell cultures coupled with *in vivo* acute drug response analysis, this thesis identifies tumor subtype-selective therapeutic sensitivity and resistance mechanisms, as well as effective drug combinations.

1. REVIEW OF LITERATURE

1.1. Structure and function of the lung

The lung is the principal respiratory organ and plays a vital role in the survival of mammals and some vertebrates. The primary function of the lung is gas exchange. It provides oxygen from the air into the venous blood and removes carbon dioxide from the blood. The lung is also involved in the metabolism of compounds, filtering of unwanted substances from the blood, and also acts as a reservoir of blood (Joseph et al., 2013). In addition, recent studies have identified the lung to be a primary site for platelet production, and a reservoir of hematopoietic progenitors (Lefrancais et al., 2017). Structurally, the human lung consists of five lobes: two on the left and three on the right side of the chest. The trachea or windpipe splits into the right and left lungs to form primary bronchi, which in turn divide to form bronchioles, terminal bronchioles, and finally respiratory bronchioles that terminate in gas exchange units called alveoli. The region between the primary bronchi and the terminal bronchioles constitutes the proximal conducting airways, which function to lead the air to and from the distal gas exchange regions of the lung.

1.1.1. Cell types in the adult lung

The adult lung consists of over 40 different cell types, each with specific functions. Proximal airways (trachea and bronchi) are lined by a pseudostratified columnar epithelium, consisting of basal cells (cytokeratin 5/14; $CK5^+$, $CK14^+$, tumor protein 63; $p63^+$), ciliated cells (forkhead box j 1; $Foxj1^+$), club cells (secretoglobin 1 a1; $Scgb1a1^+$, or club cell secretory protein; $CCSP^+/CC10^+$), neuroendocrine cells (calcitonin gene-related peptide; $CGRP^+$) and mucus-producing goblet cells. The distal airway consists of club cells, basal cells, ciliated cells, and neuroendocrine cells. The alveolar epithelium is composed of cuboidal surfactant-producing (surfactant protein C; SPC^+) alveolar type II cells (AT2) and gas-exchanging squamous type I cells (AT1) (podoplanin; $PDPN^+$, also known as T1α) (Leeman et al., 2014; Li et al., 2015b).

Studies involving lineage tracing of murine lung epithelial cells have been instrumental in understanding the role these different cell types in the regeneration and homeostasis of the adult lung. However, there are some key differences between the mouse and human lungs, both in terms of structure and cellular composition. Unlike humans, mice contain four lobes on the right and one on the left side of the thoracic cavity. In mice, mucin-producing submucosal glands are present only in the proximal trachea but in humans they penetrate deep into the bronchi. Furthermore, there are striking

differences with respect to cellular composition through the airways' proximal-distal axis. In humans, basal cells are present throughout the airways until the terminal bronchioles, whereas in mice these are largely restricted to the trachea. Similarly, mucin-producing goblet cells are rare in laboratory mice, but are abundant in the human lungs (Figure 1) (Rock et al., 2010). These findings suggest that inter-species differences in structure and cellular composition of the lung should be taken into consideration while performing mechanistic studies using murine models.

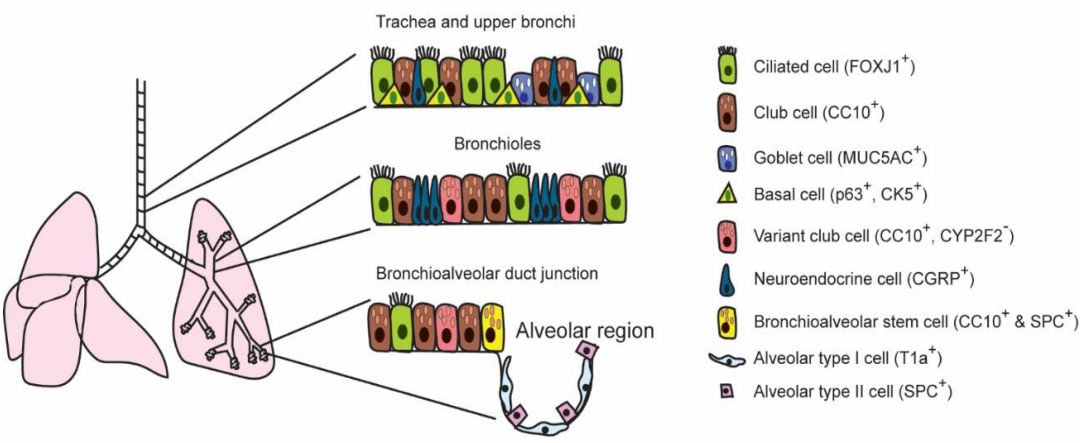

Figure 1. Structure and epithelial cell types in different compartments of the adult mouse lung. Modified from (Barkauskas et al., 2017).

1.1.2. Stem or progenitor cells of the adult lung

Stem cells are undifferentiated cells capable of self-renewal and differentiation into specialized cell types. Their progeny constitutes progenitor cells that commit to the formation of differentiated cell types. Unlike stem cells, which can undergo indefinite cell divisions, progenitor cells have limited replicative potential. In adult tissues, stem cells are involved in tissue repair upon injury, and hence regulate tissue homeostasis. Deeper understanding of the tissue-specific stem or progenitor cell biology majorly impacts on regenerative medicine and disease modelling such as cancer (Singh, 2012). Based on their ability to expand and differentiate into mature lung cells, different cell types residing in the distinct compartments have been proposed to be the progenitors of the adult mouse lungs. In the upper murine airways, tracheal basal cells have been shown to differentiate into ciliated and secretory club cells, both under steady state and upon sulphur dioxide (SO2)-induced injury (Rock et al., 2009), while club cells can differentiate in to ciliated cells upon SO2 injury (Rawlins et al., 2009). In the conducting airways, (bronchi and terminal bronchioles) naphthalene-resistant variant club cells that lack the cytochrome p450 enzyme (CYP2F2) that metabolizes naphthalene into a toxic derivative have been

shown to replenish ciliated and club cells upon naphthalene injury (Buckpitt et al., 1995; Li et al., 2011; Rawlins et al., 2009). Towards the distal part of the lung, SPC^+ AT2 cells have been shown to regenerate the damaged lung parenchyma following bleomycin injury (Rock et al., 2011). Subsequently, Chapman et al showed that integrin $\alpha6^+\beta4^+$ but SPC negative cells from distal lungs also have a capacity to expand after bleomycin injury, suggesting the additional existence of SPC^- progenitors in the distal lung (Chapman et al., 2011). Furthermore, also distal airway stem cells (DASC) marked by $p63^+$ $Krt5^+$ have been shown to regenerate both the bronchiolar and alveolar epithelium in response to H1N1 influenza virus infection (Zuo et al., 2015). Together, this indicates the existence of multiple tissue-regenerating stem cells, and shows that different injury types activate distinct progenitors.

In the bronchioalveolar duct junction (BADJ), CC10 and SPC co-expressing cells, also known as bronchioalveolar stem cells (BASCs), have been considered as stem cells with regenerative capacity following naphthalene (bronchiolar) or bleomycin (alveolar) injury (Giangreco et al., 2002). These BASCs have been shown to possess self-renewal capacity, and could differentiate into $CC10^+$ and SPC^+ cells when cultured on matrigel (Kim et al., 2005). Contrary to these findings, Rawlins et al did not find evidence supporting the role of BASCs in repair following hyperoxia-induced injury (Rawlins et al., 2009). Adenoviruses or lentiviruses expressing Cre recombinase-under the control of lung progenitor cell-specific promoters such as CC10- or SPC- have been used to investigate the cell of origin of lung cancer, and this will be discussed in section 1.8.

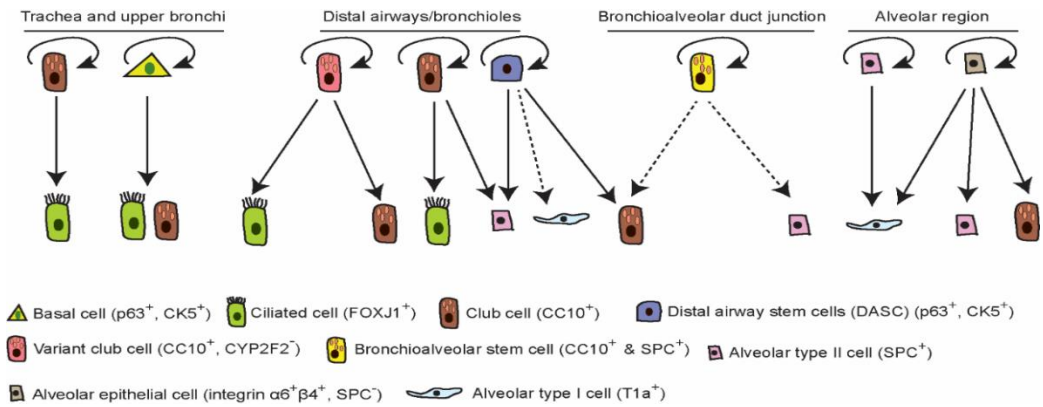

Figure 2. Epithelial stem or progenitor cells in different regions of the adult mouse lung. Solid arrows point at cells that are generated from indicated lineage, either in response to lung injury or during steady state. Dotted arrows indicate cells that are derived from a lineage still under debate. Cells with self-renewing capacity are indicated by curved arrows. Modified from (Chen and Fine, 2016).

1.2. Lung cancer

Lung cancer is one of the most common cancer types both in terms of incidence and mortality, and accounts for nearly 1.6 million deaths per year worldwide (Ferlay et al., 2015; Siegel et al., 2018; Wong et al., 2017). Initial lung cancer diagnosis is based on clinical symptoms, which include cough, dyspnea, and chest pain. Diagnostic tests to confirm lung cancer include imaging based positron emission tomography (PET)/computed tomography (CT) scans, or transesophageal and bronchoscopic ultrasound. In addition, a small tissue biopsy is routinely examined by microscopic means to establish disease diagnosis (Gridelli et al., 2015). Cancer stage is determined based on TNM classification: size of the primary tumor (T), regional lymph node involvement (N), and metastasis to distant organs (M) (Goldstraw et al., 2016). The overall survival of the patients diagnosed with lung cancer is strongly linked to clinical stage at the time of diagnosis. Patients who are presented at stage I have a five-year survival of appr. 73%, while patients with advanced stage IV disease have a poor survival of appr. 13% (Woodard et al., 2016). Treatment options depend on the clinical stage: surgery is the most effective treatment for stage I, II, and IIIA patients, while patients with stage IIIB or IV disease are mostly treated with chemotherapy or radiation therapy (Rocco et al., 2016). Diagnostic molecular profiling increasingly guides the prescription of targeted therapies as well as immunotherapies, particularly for treatment of metastatic lung cancer, and this will be discussed in detail in the following sections (Shojaee and Nana-Sinkam, 2017).

1.2.1. Lung cancer epidemiology

Lung cancer accounts for nearly 25% of all cancer-related deaths in men and women (Siegel et al., 2018). Nearly 25% of the lung cancers are detected in non-smoking people (Sun et al., 2007). In addition, lung cancer in never- smokers also varies in terms of geographic locations, non-smoking people developing lung cancer is higher in South and East Asia compared to Europe or United states (Pirie et al., 2016; Subramanian and Govindan, 2007; Thun et al., 2008). A never-smoker is defined as an individual who has had exposure to less than 100 cigarettes in a life-time (Sun et al., 2007). While smoking is associated with all histological lung cancer subtypes, stronger association has been shown for small-cell lung cancer (SCLC) and SCC (Khuder, 2001). Although the AC subtype is the most common in never smokers, a major global shift towards increased AC and decreased SCC has been observed in smokers (Gabrielson, 2006; Yang et al., 2002). This shift has been attributed to altered nicotine and carcinogen contents in cigarettes leading to changes in smoking behavior (Gray, 2006; Sun et al., 2007).

1.2.2. Histological subtypes of lung cancer

Lung cancer is broadly classified into two main subtypes; 1) NSCLC accounts for 85% of the diagnosed cases, 2) SCLC constitutes remaining 15% of the lung cancer (Gridelli et al., 2015). SCLC, previously known as oats cell carcinoma, is the most aggressive subset, and shows early and frequent metastasis (Bernhardt and Jalal, 2016). SCLC is a neuroendocrine carcinoma originating from neuroendocrine cells in the airways. Commonly used diagnostic markers, which distinguish SCLC from NSCLC, include serum pro-gastrin releasing peptide (ProGRP), chromogranin A (CgA) and synaptophysin (Taneja and Sharma, 2004).

NSCLC is further classified into sub-histotypes, according to commonly used pathology guidelines (Travis et al., 2013; Travis et al., 2011), and based on morphological characteristics as well as immunohistochemical markers. Specifically, NSCLC is classified into AC (~40%), SCC (~30%), and non-small cell carcinoma (NSCC) not otherwise specified (NOS) (NSCC-NOS: ~10%) (Gridelli wt al., 2015). A tumor is classified as adenosquamous carcinoma (ASC) if the resected specimens contain both AC and SCC biomarker expression; ASCs constitute appr. 4% of the NSCLC histotypes (Nakagawa et al., 2003; Travis et al., 2011).

An update to the AC classification was made in 2011 by the International Association for the Study of Lung Cancer/American Thoracic Society/European Respiratory Society (IASLC/ATS/ERS). According to this classification, surgically resected specimens are classified as pre-invasive, minimally invasive or invasive adenocarcinomas. Pre-invasive AC include, adenocarcinoma in situ (AIS), in which neoplastic cells grow along the pre-existing alveoli (lepidic growth), without stromal or endothelial cell infiltrations. Invasive ACs are characterized by disruption of normal alveolar structure and are further subtyped based on their lepidic, papillary, acinar, solid, or mucinous growth patterns (Travis et al., 2011).

NSCLC sub-histotypes are distinguished based on immunohistochemistry (IHC) markers. While thyroid transcription factor-1 (TTF-1), also known as NKX2-1, and napsin-A are the most widely used markers of ACs, SCCs are identified based on positivity for transcription factor p63, specifically DNp63 (also known as p40), a dominant negative isoform of p63 (Bishop et al., 2012; Terry et al., 2010). The cytoskeletal marker CK5/6 is also used as squamous histotype marker. If a tumor cannot be differentiated into AC or SCC it is classified as NSCLC-NOS. For ASCs, which are tumors that contain at least 10% of each SCC and AC components, p63 or CK5/6 positivity (SCC component) and NKX2-1 or napsin-A positivity (AC component) are used as diagnostic markers (Travis et al., 2011).

1.2.3. Genetic landscape of lung cancer

Comprehensive genomic analyses over the past decade have identified distinct molecular subtypes of lung cancer, characterized by DNA copy number alterations (CNAs), chromosomal rearrangements, and mutations in oncogenes or tumor suppressors. In addition to distinct morphological characteristics, NSCLCs and SCLCs harbor different sets of genetic alterations. Furthermore, NSCLC subtypes are also characterized by distinct genetic alterations (Campbell et al., 2016).

1.2.3.1. Genetic alterations in SCLC

SCLC is one of the deadliest lung cancer type, with a 5 year overall survival rate of 5-10% (Lassen et al., 1995). Almost all SCLC patients are smokers. These tumors show a high burden of carcinogen-induced mutations, amounting to around 8.62 non-synonymous mutations per million base pairs (George et al., 2015; Varghese et al., 2014). Bi-allelic inactivation of tumor suppressors TP53 (Tumor Protein 53) and RB1 (Retinoblastoma 1) are the most common genetic alterations in SCLC (George et al., 2015). In addition, inactivating mutations in *NOTCH1* (Notch homolog 1, translocation-associated), *PTEN* (Phosphatase and Tensin Homolog), copy number gain of *MYC* (MYC Proto-Oncogene, BHLH Transcription Factor), or amplification of *FGFR1* (Fibroblast Growth Factor Receptor 1) or *SOX2* (Sex Determining Region Y-Box 2) genes are reported in SCLC (Peifer et al., 2012; Rudin et al., 2012).

1.2.3.2. Genetic alterations in AC

Activating mutations in *KRAS* (32%) and *EGFR* (Epidermal Growth Factor Receptor: 15%) oncogenes are common in lung ACs (TCGA, 2014). The majority of *KRAS* mutations are detected in smokers (30-43%), as opposed to never smokers (0-7%). In contrast, *EGFR* mutations are more common in never smokers (45%) compared with smokers (0-7%) (Subramanian and Govindan, 2013). Moreover, the frequency of *EGFR* mutation in ACs vary depending on the geographic location, with the highest prevalence in Asia (47%) compared to Europe (15%) or the United States (23%) (Midha et al., 2015). This difference has been partially explained by differences in the prevalence of polymorphisms in the EGFR promoter region between Asian and Western populations (Nomura et al., 2007). *EGFR* alterations commonly are exon 19 deletions (60%) or missense mutations at exon 858 (L58R), resulting in constitutive EGFR activation (Jackman et al., 2006; Rosell et al., 2009). Due to redundancy in downstream signaling pathways, *KRAS* and *EGFR* mutations are mutually exclusive in ACs (Yang et al., 2009). Genetic alteration in *STK11/LKB1* is detected in 13-33% of ACs, and these often co-occur with *KRAS* mutations (10-67%) (Koivunen et al., 2008; Matsumoto et al., 2007; Sanchez-Cespedes et

al., 2002). Chromosomal translocations between the receptor tyrosine kinase gene *ALK* (Anaplastic Lymphoma Kinase) and *EML4* (Echinoderm Microtubule-associated Protein 4) are also common in AC patients (4-7%) with a history of never smoking (TCGA, 2014; Wong et al., 2009). In addition, nearly 4% of ACs harbor alterations in the receptor tyrosine kinase *ERBB2* (V-Erb-B2 Erythroblastic Leukemia Viral Oncogene Homolog (TCGA, 2014). Furthermore loss-of function mutations in *KEAP1* (Kelch-like ECH-associated protein 1) are also detected in approximately 20% of ACs (2012; Berger et al., 2017; Singh et al., 2006). Nearly 3-10% of lung ACs harbor activating mutations in *BRAF* (B-Raf Serine/Threonine-Protein), most commonly a glutamatic acid substitution for valine at codon 600 (TCGA, 2014; Litvak et al., 2014).

1.2.3.3. Genetic alterations in SCC

In SCC, alterations are detected in genes involved in growth factor signaling, namely, amplification of *FGFR1* (22%) (Weiss et al., 2010), loss of function mutation in *PTEN* (10%) (Jin et al., 2010), or copy number gains in *PIK3CA* (Phosphoinositide-3-Kinase, Catalytic, Alpha Polypeptide: 33-43%) (Okudela et al., 2007; Yamamoto et al., 2008). Furthermore, somatic mutations in *TP53* (81%) (2012), and amplification of *SOX2* (20-45%) (Bass et al., 2009; Sasaki et al., 2012) are also predominant in SCC. TP53 mutations are associated with cigarette smoking, and carcinogen-associated G-T transversions in *TP53* have been detected (Halvorsen et al., 2016; Pfeifer et al., 2002).

1.2.3.4. Genetic alterations in ASC

High prevalence of *EGFR* mutation has been reported in ASCs, with frequencies ranging from 13%-55% (Midha et al., 2015; Tochigi et al., 2011; Vassella et al., 2015), particularly in female never smokers (Song et al., 2013). Mutational analyses of micro-dissected AC and SCC components have revealed *EGFR* mutations in both the AC and SCC components (Midha et al., 2015; Powrozek et al., 2014; Tochigi et al., 2011), or shown divergence with glandular AC regions showing predominant *EGFR* mutation (Shi et al., 2016). In addition, mutations in *PI3KCA* have been detected in ASCs, particularly in the SCC component (Shi et al., 2016; Vassella et al., 2015). Compared to frequent overall *KRAS* mutation in ACs (32%), ASCs show lower incidence of *KRAS* mutation (7-13%) (TCGA, 2014; Shi et al., 2016; Tochigi et al., 2011; Vassella et al., 2015). Vassella et al also reported mutations in *LKB1*, *APC*, *KIT*, *TP53*, or *RB1*, in both the SCC and AC components of ASC (Vassella et al., 2015),

with 22% of all ASCs harboring *LKB1* mutation (Koivunen et al., 2008). These findings suggest that, as a hybrid of two histotypes, ASCs harbor select mutations specific to both the AC and SCC histotypes.

Table 1. **Selected genetic alterations in histological subtypes of NSCLC.** Information in the table has been derived from the following references: (TCGA, 2012; TCGA, 2014; Boch et al., 2013; Joshi et al., 2017; Koivunen et al., 2008; Li et al., 2012; Midha et al., 2015; Okudela et al., 2007; Sanchez-Cespedes et al., 2002; Shi et al., 2016; Tochigi et al., 2011; Vassella et al., 2015; Yamamoto et al., 2008).

Gene	Nature of genetic alteration	Frequency AC (%)	Frequency SCC (%)	Frequency ASC (%)
EGFR	M, C	11-40	4-7	13-55
KRAS	M	30-32	1-2	7-13
STK11	M	13-33	2-5	6-22
TP53	M	46	81	38
PIK3CA	M, C	3-6	4-43	13
ERBB2	M, C	3-20	4	NA

M: mutation, C: copy number alterations**,** NA: not available

Table 2. **Selected co-occurring gene mutations in histological subtypes of NSCLC.** Information has been derived from the following references: (Ji et al., 2007; Matsumoto et al., 2007; Schmid et al., 2009; Yang et al., 2009).

Co-occurring gene mutations	Frequency AC %	Frequency SCC %	Frequency ASC %
KRAS and *EGFR*	1-2	NA	NA
KRAS and *TP53*	12	7	NA
KRAS and *LKB1*	10-67	2	NA

1.2.4. KRAS and its downstream signaling

Ras (Rat sarcoma) family proteins are small guanosine triphosphatases (GTPases) that mediate intracellular signal transduction to regulate diverse cellular functions, including proliferation, survival, cytoskeletal integrity, migration, adhesion, and apoptosis (Wennerberg et al., 2005). Oncogenic functions of the *RAS* were first identified by the ability of retroviruses from leukemic rats to induce sarcomas in new-born rodents (Harvey, 1964; Kirsten and Mayer, 1967). Later, three independent studies discovered that human homologues of Kirsten and Harvey sarcoma viruses are found in cancer cell lines, and are capable of inducing transformation in mouse embryonic fibroblast NIH/3T3 cells (Der et al., 1982; Parada et al., 1982; Santos et al., 1982; Wennerberg et al., 2005).

RAS genes are highly conserved across different species. The *RAS* family consists of three members, or isoforms, namely *HRAS*, *KRAS*, and *NRAS*, and these are frequently mutated in various human cancers (Hobbs et al., 2016). Interestingly, RAS isoforms show tissue-specific differences in mutations and context-dependent transformation potential (Castellano and Santos, 2011). Furthermore, of the three isoforms, only *Kras* is essential for the development of mouse embryos; *Kras* null embryos die due to defects in the development of heart and neurons (Koera et al., 1997).

Among the three *RAS* isoforms, only *KRAS* forms two alternate splice variants, giving rise to two protein products, KRAS4A and KRAS4B, which differ in their 25 carboxyl terminal residues (Hobbs et al., 2016; Tsai et al., 2015). All RAS proteins are membrane localized, and a series of biochemical reactions involving C-terminal prenylation, farnesylation, and geranylation mediate the anchoring of RAS proteins to the plasma membrane (Casey et al., 1989; Prior and Hancock, 2012; Schaber et al., 1990). The GTPase activity, or activated form of KRAS, is regulated by two regulatory proteins: i) guanine nucleotide exchange factors (GEFs) that mediate the exchange of GDP to GTP, and ii) GTPase activating proteins (GAPs), which mediate GTP hydrolysis and conversion to GDP. In the GTP-bound active state, KRAS shows high affinity for downstream effector molecules and mediates a cascade of signaling events (Wennerberg et al., 2005). Activation of growth factor receptors or receptor tyrosine kinases (RTKs) via extracellular cues drives activation of KRAS via KRAS-GEF, which leads to the activation of a spectrum of downstream effectors. One of the canonical pathways downstream of KRAS is initiated by translocation of the Raf proto-oncogene, a serine/threonine-protein kinase to the plasma membrane, followed by its phosphorylation. Activated Raf phosphorylates a dual specificity kinase MEK1/2 (mitogen-activated protein kinase), which in turn phosphorylates and activates ERK1/2 (extracellular signal-regulated kinase). Activated ERK1/2 translocate to the nucleus, where it

phosphorylates Ets family transcription factors which regulate cell proliferation, differentiation, tissue remodeling and apoptosis (Figure 3) (Kar and Gutierrez-Hartmann, 2013; Repasky et al., 2004).

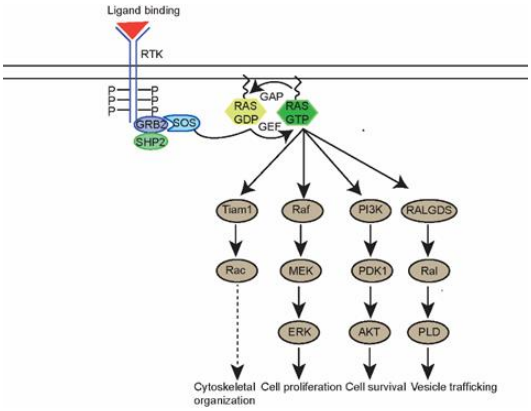

Figure 3. RAS-associated signaling pathways. RTKs are activated through phosphorylation upon ligand binding, which creates binding sites for adaptor proteins, including GRB2 and SHP2. These in turn recruit SOS, a RAS GEF, to the membrane to activate RAS via exchange of GDP for GTP. Activated RAS propagates various downstream effector pathways to regulate diverse cellular processes such as proliferation, survival, vesicle trafficking, and cytoskeletal organization. Modified from (Westcott and To, 2013).

1.2.4.1. KRAS in lung cancer

As mentioned, *KRAS* is among the most frequently mutated genes in lung cancer, particularly in ACs of patients with a history of tobacco smoking. *KRAS* mutations are also observed in SCC (~2%) and ASC (7-13%) with less frequency, and very rarely in SCLC (TCGA, 2012; Boch et al., 2013; Mitsudomi et al., 1991; Tochigi et al., 2011; Vassella et al., 2015). In lung cancer, *KRAS* mutations are more frequent than *HRAS* or *NRAS* mutations (Suzuki et al., 1990). The *KRAS* gene is located on chromosome 12p.12.1. Mutations leading to single amino acid substitutions are commonly found at codon 12, and also at codon 13 or 61, though at a lower frequency (Ahrendt et al., 2001). It is thought that metabolically active carcinogens in tobacco smoke, such as polycyclic aromatic hydrocarbons (PAH) or nicotine-derived nitrosamine ketone (NNK), forms reactive intermediates that bind to the DNA and cause point mutations in *KRAS* leading to G-C and G-T nucleotide transversions (Hecht, 2012). In line with this, the G12C (~40%) and G12V (~22%) *KRAS* point mutations in lung cancers constitute G/T transversions (Forbes et al., 2011; Gautschi et al., 2007). Some reports suggest poorer prognosis of patients with G12C and G12V mutations compared to other KRAS mutations (Ihle et al., 2012). Furthermore, the nature of the amino acid substitution has an effect on downstream signaling: mutant KRAS with a G12D substitution preferentially activates the PI3K/AKT pathway, while KRAS G12C, or G12V signals through the Raf-MEK pathway (Ihle et al., 2012). In addition, due to redundancy in downstream signaling, *KRAS* mutations confer resistance to anti-EGFR therapies (Eberhard et al., 2005; Pao et al., 2005).

1.2.5. LKB1

LKB1 is located on chromosome 19p13.3, and encodes for a serine threonine kinase (Manning et al., 2002). It was first identified as a gene whose germline mutation is responsible for Peutz-Jeghers syndrome (PJS) (Hemminki et al., 1998; Hemminki et al., 1997; Jenne et al., 1998). PJS is an autosomal-dominant disorder distinguished by gastrointestinal hamartomatous polyps and melanocytic macules of the lips (Hemminki, 1999). Patients with PJS are at increased risk for cancer, including gastrointestinal cancers (Giardiello et al., 1987; Hearle et al., 2006). The tumor suppressor function of LKB1 was first identified by overexpression of wild type LKB1 in HeLa and G361 cells, which leads to growth suppression via a G1 cell cycle arrest (Tiainen et al., 1999). The same study also showed that catalytically inactive *LKB1* mutants, including those found in PJS patients, were unable to cause growth arrest, confirming the role of kinase activity in blocking cell growth. Mice heterozygous for *Lkb1* do not display defects in embryonic or postnatal development. However, homozygous deletion of *Lkb1* is embryonic lethal, and *Lkb1* null embryos die in utero between E8.5-E9.5 due to neural tube and heart development defects, as well as vascular abnormalities, suggesting that LKB1 plays an important role in embryonic development (Jishage et al., 2002; Ylikorkala et al., 2001). *LKB1* is mutated in many human cancers, with the highest incidence in lung AC (~30%), followed by cervical cancers (Sanchez-Cespedes, 2007; Sanchez-Cespedes et al., 2002; Wingo et al., 2009).

1.2.5.1. LKB1 signaling

LKB1 exerts its function by forming a complex with two other proteins, the pseudo kinase STRAD (STE20-related adaptor) and scaffold protein MO25 (mouse protein 25) (Baas et al., 2003; Boudeau et al., 2003). LKB1 acts as a master kinase to regulate cell metabolism, differentiation, proliferation and polarity via a set of 14 downstream kinases (Vaahtomeri and Makela, 2011). AMP-activated protein kinase (AMPK), the best characterized LKB1 substrate, is a heterotrimeric kinase composed of a catalytic (α) subunit and two regulatory (β and γ) subunits (Novikova et al., 2015). AMPK is an energy-sensing kinase that is activated upon low cellular energy conditions, when cellular ATP levels are decreased and AMP levels are increased, mediated by LKB1-dependent phosphorylation of AMPK (Hardie, 2007). Activated AMPK activates catabolic pathways, including glucose uptake, glycolysis, and fatty acid oxidation. At the same time, AMPK inhibits anabolic processes such as protein synthesis, to restore cellular energy levels (Alexander and Walker, 2011). While the mTOR (mammalian target of rapamycin) pathway stimulates cell growth-associated processes in response to growth factor signaling, activated AMPK executes growth inhibitory effects, inhibiting mTOR activity through

phosphorylation of the tuberculosis sclerosis (TSC1/TSC2) complex, and phosphorylation of raptor, a component of mTORC1 (Figure 4) (Gwinn et al., 2008; Inoki et al., 2003).

LKB1 was first shown to regulate cell polarity in studies performed in *C. elegans* and *Drosophila*. The *C. elegans* LKB1 homologue Par-4 was shown to maintain the anterior-posterior polarity of the embryo (Kemphues et al., 1988). In Drosophila, *Lkb1* mutation affects the anterior-posterior axis as well as epithelial polarity (Martin and St Johnston, 2003). Using mammalian intestinal epithelial cells, it was later shown that activated LKB1 mediates actin cytoskeleton remodeling and formation of apical brush borders (Baas et al., 2004). Other AMPK-related kinases, namely MARK1-MARK4 (microtubule affinity-regulating kinases) and SAD-A and SAD-B (synapses of amphid-defective kinases), are known to control cell polarity by regulating microtubule assembly (Hezel and Bardeesy, 2008). Another AMPK-related kinase downstream of LKB1, NUAK (AMPK-Related Protein Kinase 5), has anti-apoptotic functions, and is activated upon oxidative stress. Upregulation of NUAK1 has been associated with aggressiveness in colorectal cancers (Port et al., 2018; Suzuki et al., 2003).

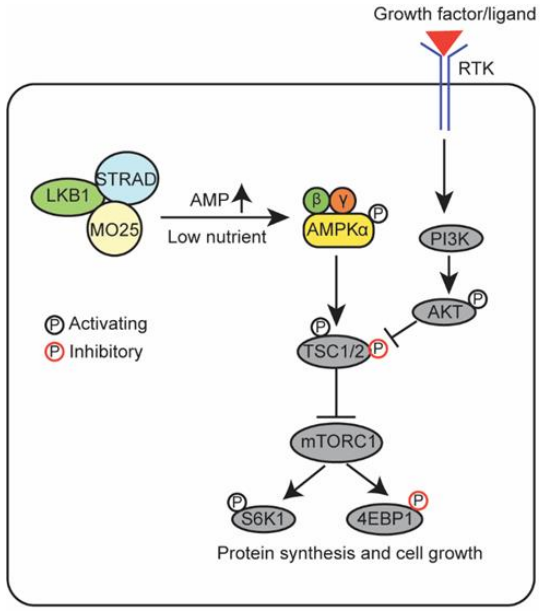

Figure 4. AMPK-mediated effector functions of LKB1. When cellular energy levels are low and AMP levels are high, LKB1 phosphorylates and activates AMPK. Activated AMPK inhibits protein synthesis and cell growth by inhibiting mTORC1 function. On the other hand, growth factor-mediated activation of the PI3K/AKT pathway leads to activation of mTORC1 by relieving negative regulation by TSC1/TSC2, and this results in cellular growth and protein synthesis. Modified from (Ochocki and Simon, 2013).

1.2.5.2. LKB1 in lung cancer

Loss of heterozygosity (Khosravi et al.) of chromosome 19 were initially observed in 80% of the analyzed NSCLC cell lines, compared to less than 30% of the analyzed SCLC cell lines (Virmani et al., 1998). Subsequent studies showed that biallelic loss of *LKB1* at chromosome 19.13, and loss of function mutation in *LKB1* (10-50%), are common events in lung cancer (Sanchez-Cespedes et al.,

2002). The *LKB1* gene is more frequently altered in lung ACs (30%) or ASCs (22%) compared with SCCs (1.4-5%); it is never altered in SCLC (TCGA, 2012; TCGA, 2014; Koivunen et al., 2008; Sanchez-Cespedes et al., 2002; Vassella et al., 2015). Most of the *LKB1* mutations are nonsense, frameshift or large intragenic deletions that result in the generation of a truncated protein. Missense mutations in the kinase domain have also been reported (Sanchez-Cespedes, 2007). Concurrent *LKB1* loss-of-function mutation and *KRAS* activating mutations are reported in 67% of analyzed lung cancer cell lines, while no significant association exists between *LKB1* mutation and *EGFR* or *TP53* mutations (Matsumoto et al., 2007). Clinical lung cancers with concomitant *KRAS* mutation and *LKB1* alterations (52%) constitute an aggressive subset of NSCLCs, more often found in smokers, and associated with poor patient survival (Calles et al., 2015; Facchinetti et al., 2017a; Matsumoto et al., 2007).

1.2.6. TP53

Tumor protein 53 (TP53) belong to the p53 superfamily of transcription factors. It was discovered nearly 40 years ago as the cellular partner of the viral oncoprotein simian virus 40 large T-antigen (Kress et al., 1979; Lane and Crawford, 1979). Other members of the p53 family transcription factors include p63 and p73 (Levrero et al., 2000). p53 functions as a tumor suppressor in response to various cellular stress conditions, including DNA damage, hypoxia, nutrient starvation, oncogene expression and ribosome dysfunction, by mediating cell cycle arrest and apoptosis. Murine embryos lacking *p53* (*p53-/-*) are developmentally normal, but adult mice develop tumors, predominantly lymphomas (Donehower et al., 1992). On the contrary, p63 and p73 are involved in development and differentiation, and homozygous deletion of *p63* (*p63-/-*) or *p73* (*p73-/-*) leads to embryonic defects (Bieging et al., 2014; Levrero et al., 2000; Mills et al., 1999; Yang et al., 2000). TP53 was originally thought to function as an oncogene, as it accumulated in the nuclei of the cancer cells. Later discoveries showed that it is only the mutated form of p53 cooperated with RAS in inducing cellular transformation, assigning it as a tumor suppressor (Finlay et al., 1989; Hinds et al., 1989). *TP53* mutations are found in the vast majority of human cancers, whereas *TP63* or *TP73* mutations are uncommon (Hagiwara et al., 1999; Hollstein et al., 1991; Melino et al., 2002).

1.2.6.1. p53 regulations and its biological functions

The transcription factor p53 regulates various biological processes, including DNA repair, cell cycle arrest, autophagy, senescence, apoptosis, cellular stem-ness, and metabolic reprogramming (Bieging et al., 2014). p53 mediates its function through transcriptional activation, or repression, as well as regulation of homologous DNA recombination and protein translation (Zilfou and Lowe, 2009). p53

functions as a tetrameric complex, and its function is regulated by affecting protein stability, activity, and subcellular localization. Post-translational modifications, which include phosphorylation, acetylation, sumoylation, and ubiquitination, play an important role in stabilization of p53. For example, p53 activation via protein stabilization is achieved by disruption of its interaction with Mdm2 (Mouse double minute 2 homolog), a ubiquitin ligase that mediates p53 protein destruction (Hu et al., 2012). Upon DNA damage, post-translational modification and phosphorylation of p53 by upstream kinases such as ATM and ATR disrupt the Mdm2 interaction, leading to protein stabilization (Appella and Anderson, 2001). In addition, upon exposure to γ radiation, ATM mediates phosphorylation of MDM2, resulting in impaired p53-MDM2 interaction (Khosravi et al., 1999). Following stabilization, p53 regulates gene expression by binding to DNA sites that contain two decameric palindromic sequences (half-sites) 5′-RRRCWWGYYY-3′, where R is purine, Y is pyrimidine, and W is either A or T (el-Deiry et al., 1992; McLure and Lee, 1998). Effector functions regulated by p53 include cell cycle checkpoint activation, cellular senescence, and apoptosis (Zilfou and Lowe, 2009). The cell cycle effects of p53 are executed via regulation of cyclins and cyclin-dependent kinase inhibitors (CKIs) (Brugarolas et al., 1995; St Clair and Manfredi, 2006). One of the p53 target genes, the p21 (waf-1/cip-1) CKI, negatively regulates the cell cycle by mediating G1 arrest via inhibiting cyclin/cyclin dependent kinases. In normal cells, wild type p53 can mediate cellular senescence in response to overexpression of oncogenic KRAS (Yang et al., 2006), as a form of cell-intrinsic tumor suppression. This phenomenon was later confirmed to occur also *in vivo*, in a lung cancer model driven by oncogenic BRAF, where loss of p53 bypassed senescence in the context of oncogenic $BRAF^{V600E}$ expression, resulting in adenoma to AC progression (Dankort et al., 2007). Recently, it was shown that p53 loss before the induction of $BRAF^{V600E}$ oncogene-induced senescence (OIS) permits adenocarcinoma progression, but p53 loss after the establishment of OIS fails to rescue senescence, and hence does not permit tumor progression (Garnett et al., 2017). These results suggest that in the $BRAF^{V600E}$ lung cancer model, the timing of p53 loss is crucial for prevention of OIS and hence progression from adenoma to adenocarcinoma.

1.2.6.2. TP53 in lung cancer

Genetic analysis of the bronchial epithelium from chronic smokers revealed frequent LOH on chromosome 17p3, which contains the *TP53* gene, suggesting a possible link between cigarette smoking and *TP53* alterations in the lung (Mao et al., 1997). In line with this, the frequency of *TP53* mutations is higher in lung tumors of bronchial origin such as SCLC (100%) and SCC (87%) compared to distally arising AC (50%) (TCGA, 2012; TCGA, 2014; D'Amico et al., 1992; George et al., 2015; Kishimoto et al., 1992; Takahashi et al., 1991). The high frequency of *TP53* mutations in smokers (67%

vs 19-26% in never smokers) has been attributed to carcinogen-induced DNA adducts within *TP53* exons (Denissenko et al., 1996; Takagi et al., 1998; Vahakangas et al., 2001). The majority of the mutations reside in the DNA binding region of TP53 (Olivier et al., 2002). Clinically, *TP53* mutations are significant predictor of poor outcome in stage I NSCLC patients (Ahrendt et al., 2003).

1.2.7. ERBB family receptors, ligands and their roles in cancer

Epidermal growth factor receptor (EGFR) or ERBB family receptors are a group of transmembrane tyrosine kinase receptors, consisting of four members: EGFR (ERBB1), HER2 (ERBB2), HER3 (ERBB3) and HER4 (ERBB4), and regulate cell growth, survival, differentiation, adhesion, and migration (Yarden and Sliwkowski, 2001). While inactive ERBB receptors constitute monomeric forms, ligand binding to the extracellular domain (ECD) results in homo- or heterodimerization of the receptors. In their monomeric state, an intracellular protein kinase (PTK) domain exist in an inactive conformation, which is activated in response to receptor dimerization (Fuller et al., 2008). Auto or trans-phosphorylation of multiple tyrosine residues within the intracellular domains of dimerized partners propagates intracellular signaling, through RAS/RAF/MEK/ERK and PI3K/AKT/mTOR signaling, and activation of SRC kinases and STAT transcription factors (Fuller et al., 2008; Yarden and Sliwkowski, 2001; Zhang et al., 2006). Although ERBB receptors are structurally similar to each other, they show differences in ligand binding and tyrosine kinase activity (Figure 5). ERBB2 is an 'orphan' receptor which lacks a specific ligand, while ERBB3 lacks an intracellular kinase domain. However, both can function as heterodimers with other ERBB receptors. Despite lacking functional kinase domain ERBB3 can undergo transphosphorylation and transduce intracellular signaling events (Citri et al., 2003; Garrett et al., 2003; Guy et al., 1994; Klapper et al., 1999). Ligands of ERBB family receptors possess a high affinity EGF-like domain required for receptor binding and activation. EGFR has been shown to bind with multiple ligands, which include EGF, transforming growth factor alpha (TGF-α), heparin-binding epidermal growth factor like factor (HB-EGF), amphiregulin, epiregulin or betacellulin. Of these, EGF, TGF-α and amphiregulin bind exclusively to EGFR, whereas HB-EGF, epiregulin and betacellulin also bind to ERBB4. One of the most recently described ERBB ligands, epigen, also binds to EGFR, but with lower affinity. Another family of ERBB receptor ligands, called neuregulins (NRGs, NRG1-NRG4) can bind to ERBB3 and ERBB4 (Figure 5) (Falls, 2003; Fuller et al., 2008).

Signaling events downstream of ERBB receptor activation involve docking of the adaptor proteins such as Grb2 or Shc via SH2/PTB domains to specific receptor phosphotyrosine residues on the cytoplasmic domain, followed by activation of RAS/RAF/MEK/ERK and PI3K/AKT/mTOR pathways, as well as activation of Src kinases and STAT transcription factors (Figure 5) (Yarden and Sliwkowski, 2001).

Interestingly, ERBB3 is a potent activator of the PI3K/AKT pathway, via its six docking sites for the PI3K regulatory subunit p85 (Hellyer et al., 1998). Studies using mouse models have shown that targeted deletion of each of the four ERBB receptors leads to embryonic or early postnatal lethality, implying that ERBB receptors have non-redundant functions during embryonic development (Lee et al., 1995; Miettinen et al., 1995; Threadgill et al., 1995; Tidcombe et al., 2003).

Emerging evidence suggests that ERBB receptors and their ligands play an important role in cancer initiation, progression as well as therapy resistance (Arteaga and Engelman, 2014). Oncogenic functions of ERBB receptors were first assigned to EGFR, as it is homologous to the retroviral protein v-ERBB that causes the avian erythroblastosis virus to transform chicken cells (Downward et al., 1984). Subsequent studies with laboratory models indicated the transforming ability of EGFR and its alterations in multiple malignancies (Arteaga and Engelman, 2014). Genetic alterations of ERBB receptors, as well as overexpression of certain ERBB ligands, have been detected in multiple cancer types (Arteaga and Engelman, 2014). Feedback activation of ERBB receptors, including activation of EGFR and ERBB3 following inhibition of MEK/ERK or PI3K/AKT pathways, confer resistance mechanisms. In such cases, the combined inhibition of ERBB/MEK or ERBB/AKT signaling provided greater anti-tumor effects (Chakrabarty et al., 2012; Chandarlapaty et al., 2011; Corcoran et al., 2012; Katayama et al., 2012; Kitai et al., 2016; Prahallad et al., 2012; Turke et al., 2012).

1.2.7.1. ERBB receptors and their ligands in lung cancer

Genetic alterations in all four ERBB receptors have been detected in human lung cancer. As mentioned, *EGFR* alterations are more common in AC (11-40%) than in SCC (4-7%) (Table 1). Similarly, genetic alteration in *HER2/ERBB2* (amplifications and mutations) are more prevalent in ACs (3-20%) compared to SCC (4%) (TCGA, 2012; TCGA, 2014; Kim et al., 2017; Li et al., 2012). In addition, intragenic kinase domain mutations in *ERBB2* are exclusively found in ACs and are not accompanied with protein overexpression (Stephens et al., 2004). Similar to *EGFR* mutations, *ERBB2* mutations are commonly found in female never smokers, accompanied with copy number gains of either *ERBB2* or *EGFR* (Li et al., 2012). ERBB2 protein overexpression in NSCLC has been controversial, and a poor association between gene copy number alteration and protein overexpression has been observed (Hirsch et al., 2002). Furthermore, some studies report that ERBB2 protein overexpression is more common in ACs (1.9-38%) (Hirsch et al., 2002a; Hirsch et al., 2002b; Nakamura et al., 2005), while others reported that ERBB2 overexpressing tumors are predominantly SCC (Ugocsai et al., 2005). Activating mutations in *ERBB3* and *ERBB4* have also been reported in NSCLC (TCGA, 2012; Kurppa et al., 2016). In addition, chromosomal rearrangements in *NRG1*, one of the ligands of ERBB3, is detected in NSCLC. Recurrent rearrangements in the *NRG1* gene that result in different fusion gene

products, such as CD74-NRG1, RBPMS-NRG1, WRN-NRG1, and SDC4-NRG1, have been identified in both AC and SCC, and a pro-tumorigenic effect of NRG1 gene fusions has been attributed to overexpression of full-length NRG1 protein driven by WRN promoter (WRN-NGR1), or CD74-NRG1 fusion protein inducing ERBB2/ERBB3 heterodimers (Dhanasekaran et al., 2014; Fernandez-Cuesta et al., 2014).

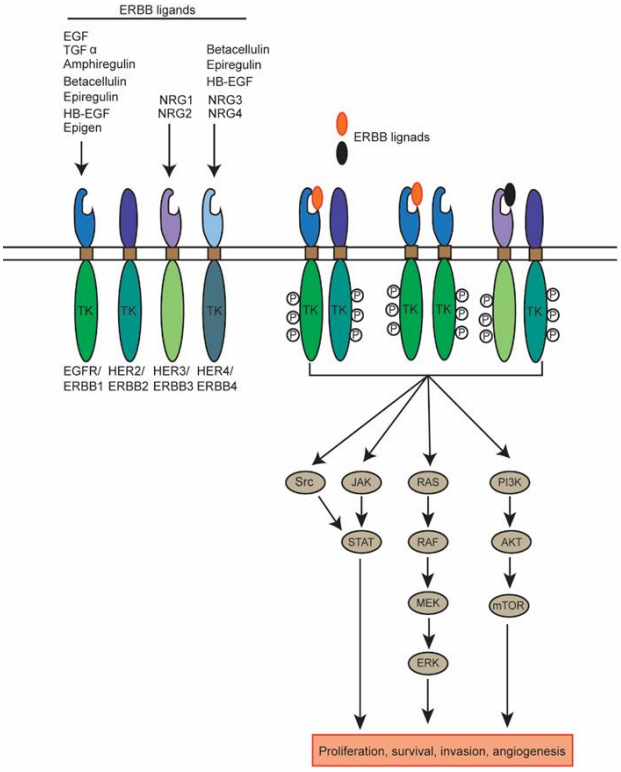

Figure 5. ERBB family receptors, ligands and signaling pathways. ERBB3 lacks a functional tyrosine kinase (TK) activity, and there are no specific ligands for ERBB2. Ligand binding to the extracellular domain of the ERBB receptors results in homo- or heterodimerization, transphosphorylation and receptor dimer activation. This in turn results in activation of downstream signaling pathways, namely RAS/RAF/MEK/ERK and the PI3K/AKT/mTOR, and activation of SRC family kinases and STAT transcription factors. Together, these pathways regulate cell proliferation, survival, invasion, and angiogenesis. Modified from (Modjtahedi et al., 2014).

1.3. Targeted therapies for NSCLC

The discovery of lung cancer driver genes has laid the foundation for implementation of targeted therapies against select gene alterations, such as *EGFR* mutations and *ALK* rearrangements. Mutations in *EGFR* lead to ligand-independent constitutive activation of the receptor and downstream effectors pathways, including activation of MAPK, and PI3K/AKT pathways (Sordella et al., 2004). Small molecule TKIs such as gefitinib and erlotinib, or monoclonal antibodies (mAbs) such as cetuximab have been developed against mutant EGFR (Pao et al., 2004). Gefitinib and erlotinib are reversible competitive inhibitors of ATP, inhibiting the tyrosine kinase activity, and hence downstream pathways. Clinical studies have shown improved response with EGFR TKIs in AC histotype tumors, and the response correlated with activating somatic mutations in EGFR (Lynch et al., 2004; Miller et al., 2004; Pao et al., 2004). Following a phase III clinical trial, both gefitinib and erlotinib were approved as first-line monotherapy for the treatment of EGFR mutation-positive NSCLC (Pao et al., 2004; Rosell et al., 2012). However, although EGFR inhibitors prolong patient survival, most patients developed resistance following 7-12 months of treatment. In the majority of the cases, acquired resistance was due to secondary gatekeeper mutations in exon 20 of EGFR, specifically T790M conversion (Yun et al., 2008). Other anti-EGFR resistance mechanisms include MET amplification, or mutations in HER2, PIK3CA, BRAF, STAT3, or AXL kinases (Serizawa et al., 2013; Sordella et al., 2004; Wu et al., 2013; Zhang et al., 2012). Efforts have focused on targeting EGFR T790M to treat EGFR TKI-resistant tumors. Towards this, several third-generation EGFR inhibitors are effective alone or in combination with anti-EGFR mAbs in EGFR T790M-positive and EGFR T790M-negative TKI-resistant tumors (Politi et al., 2015).

Clinically, TKIs are not the therapeutic choice after the failure of first-line platinum-based therapy in SCC patients (Figure 6). Also, since EGFR alterations are sporadic in the SCC histotype, molecular testing for EGFR mutation is not routinely done in patients with SCC. Interestingly, a recent phase III trial comprising of molecularly unselected lung SCC patients pretreated with chemotherapy reported improved progression-free survival and overall survival of the patients treated with afatinib, an irreversible EGFR/ERBB2 inhibitor, compared to erlotinib (Soria et al., 2015). Furthermore, Song et al reported that ASC patients treated with erlotinib or gefitinib showed improved progression-free survival (ASC: 4.4 months vs SCC: 1.9 months) and overall survival (ASC: 17.6 months vs SCC: 12.2 months) compared to SCC patients (Song et al., 2013).

Anaplastic lymphoma kinase (ALK) belongs to the insulin receptor tyrosine kinase family. In lung cancer, ALK/EML4 gene fusion is commonly detected in AC (7%) from younger and non-smoking patients (Soda et al., 2007; Takahashi et al., 2010; Wong et al., 2009). *ALK* rearrangements are mutually

exclusive with *EGFR* or *KRAS* mutation, and at least 27 *ALK* fusion variants have been reported (Sasaki et al., 2010). According to the International Association for the Study of Lung Cancer (IASLC) and the European Society for Medical Oncology (ESMO) guidelines, all patients diagnosed with lung AC should be tested for *ALK* rearrangements. The small molecule TKI crizotinib has been approved as a first-generation ALK inhibitor, and its mechanism of action is similar to EGFR TKIs. Clinically, crizotinib has shown better efficacy compared to standard chemotherapy in ALK positive NSCLC patients (Shaw et al., 2013). Crizotinib is also effective against ROS1 and MET tyrosine kinases (Ou et al., 2011), (Bergethon et al., 2012). However, similar to first-generation EGFR inhibitors, resistance to crizotinib is typically developed within one year of treatment, and 20% of the patients treated with crizotinib were diagnosed with brain metastasis following treatment, while no prior metastases were present at first diagnosis (Costa et al., 2015). Acquired resistance mechanisms to crizotinib include secondary mutations in the ALK kinase domain, copy number gain of the ALK fusion gene, and bypass mechanisms consisting of activation of EGFR, KRAS, and c-kit (Choi et al., 2010; Doebele et al., 2012; Katayama et al., 2012; Sasaki et al., 2011). Second-generation ALK inhibitors such as ceritinib and alectinib have been approved for the treatment of crizotinib-resistant *ALK* positive tumors (Friboulet et al., 2014; Sullivan and Planchard, 2016).

1.4. Immunotherapy for NSCLC

Cancer immunotherapy involves activation of the patient's immune system to inhibit tumor progression. Immunotherapies can function by breaking so-called immune checkpoints, which are generally defined as the set of immune signals required to establish self-tolerance and to prevent the immune system from randomly killing cells. Most checkpoint signals are mediated by ligand receptor interactions, and they can be grouped as stimulatory or inhibitory. Immune checkpoint molecules can be expressed on tumor cells, antigen presenting cells, or T cells. While interactions between stimulatory molecules expressed on T cells and antigen presenting cells promote the expansion and effector functions of the T cells, interactions between inhibitory checkpoint molecules suppress the activity of T cells. For example, interaction between inhibitory checkpoint molecules expressed on the cancer cell or tumor-infiltrating immune cells (e.g. Programmed death-ligand 1; PD-L1), and on the T cell (e.g. Programmed cell death protein 1; PD-1, or cytotoxic T-lymphocyte-associated protein 4; CTLA-4) are known to inhibit T cell proliferation and activation, resulting in escape from anti-tumor immune response (Li et al., 2016).

Immune checkpoint blockade has revolutionized lung cancer therapy. Recently, clinical trials showed improved efficacy of mAb PD-1 inhibitors, nivolumab and pembrolizumab, compared to standard-of-care docetaxel chemotherapy. The CheckMate 017 phase III clinical trial reported an extended median

overall survival (OS) of SCC patients treated with nivolumab (9.2 months) compared to docetaxel alone (6.0 months). Interestingly, in this study PD-L1 expression was not predictive of response to nivolumab therapy, as patients with PD-L1 negative tumors also showed improved response (Brahmer et al., 2015). A different phase III study on non-squamous lung tumors showed similar responses to nivolumab, although in this case response correlated with tumor PD-L1 expression status (Borghaei et al., 2015). Similarly, a clinical study evaluated the efficacy of anti-PD-1 pembrolizumab compared to docetaxel in pre-treated advanced NSCLC patients. A significantly improved OS was observed in the pembrolizumab vs the chemotherapy group (median OS 14.9 vs 8.2 months), with a positive correlation between OS and tumor PD-L1 expression status (Herbst et al., 2016). A phase II clinical (POPLAR) trial using the anti-PD-L1 mAb atezolizumab has also shown a longer median OS compared to docetaxel alone (12.6 vs 9.7 months), and response was associated with increased expression of PD-L1 (Fehrenbacher et al., 2016). Contrary to this finding, a more recent phase III trial showed that anti-PD-L1 therapy improved the OS of NSCLC patients regardless of histotype or PD-L1 status (Rittmeyer et al., 2017). Based on these clinical trial results, PD-1 and PD-L1 inhibitors have been approved for immunotherapy of advanced NSCLC patients.

Despite the emergence of immune checkpoint inhibitors as powerful approach for treatment of advanced NSCLC, response remains limited to a small proportion of the patients (Gettinger et al., 2015). Moreover, evidence from murine and human tumors show that the subset of NSCLC that harbors *KRAS* and *LKB1* mutations lack PD-L1 expression, and hence are not suitable for immune checkpoint inhibition (Calles et al., 2015; Koyama et al., 2016; Skoulidis et al., 2015). This suggest the need for alternate effective therapies to treat NSCLC patients who are non-responsive to immunotherapy.

1.5. Combination therapies for NSCLC

Combination therapy combines two or more therapeutic agents. As opposed to a monotherapy approach, drug combinations can show improved efficacy by simultaneously inhibiting pathways that are synergistic or additive in promoting tumor growth and metastasis. In addition, it was shown more recently that inter-patient variability in response to a single drug and independent drug actions can also explain combination therapy benefit, without involving synergistic drug effects (Palmer and Sorger, 2017).

For lung cancer, FDA approved combination therapies currently include chemotherapy combined with targeted therapy or immunotherapy (Ruiz-Ceja and Chirino, 2017). The TRIBUTE randomized phase III clinical study showed that the combination of the EGFR TKI erlotinib with carboplatin and

paclitaxel showed improved response compared to chemotherapy alone, and EGFR mutation carriers showed improved response to the combination (53%) than wild type EGFR (18%) (Eberhard et al., 2005). As expected, *KRAS* mutation in this study was negatively associated with response to combination therapy. Recently, the combination of the MEK inhibitor trametinib and the B-Raf inhibitor dabrafenib was FDA-approved for the treatment of *BRAF* mutant metastatic NSCLC. Owing to the high incidence ERBB family receptor alterations in NSCLC, (Hendler and Ozanne, 1984; Hirsch et al., 2003; Ugocsai et al., 2005), combinations with the pan-ERBB inhibitor afatinib are currently being evaluated (Bennouna and Moreno Vera, 2016). Preclinical evidence using NSCLC cell lines has shown ERBB3 activation following MEK inhibition (Kitai et al., 2016), and the combination afatinib and MEK inhibitor selumetinib treatment for *KRAS* mutant advanced NSCLC is under clinical investigation (Bennouna and Moreno Vera, 2016). The combination of afatinib with the PI3K/mTOR inhibitor sirolimus did not provide any therapeutic benefit in a recent phase Ib clinical trial (Moran et al., 2017), and the combination of afatinib with the SRC inhibitor dasatinib and the pan-JAK inhibitor ruxolitinib are still under clinical investigation (Bennouna and Moreno Vera, 2016).

Direct targeting of KRAS has been challenging, due to a number of reasons, including absence of known allosteric binding sites, the high affinity of KRAS for GTP over GDP, as well as parallel compensatory pathways that provide alternate signaling (Gysin et al., 2011). Attempts to inhibit KRAS using farnesyl transferase inhibitors (FTI), which interfere with the post-translational addition of a farnesyl group, lead to escape mechanisms via post-transcriptional activation of geranyl-geranylation (Adjei et al., 2003; Sousa et al., 2008). Similarly, salirasib, which dislodges farnesylated RAS from the cell membrane, was also ineffective in NSCLC patients (Tsimberidou et al., 2010). A recent study reported on a new KRAS G12C inhibitor, ARS-1620, and showed it caused tumor regression in patient derived xenograft models, but its effect on clinical samples has yet to be investigated (Janes et al., 2018). The MEK protein downstream of KRAS has also been considered as a potential target to inhibit MAPK signaling. However, combinations of docetaxel and the MEK inhibitor selumetinib or trametinib in *KRAS* mutant NSCLC patients did not show favorable outcomes compared to docetaxel alone (Blumenschein et al., 2015; Janne et al., 2013). Furthermore, the combination of selumetinib plus erlotinib in advanced *KRAS* mutant or wild type NSCLC patients was not beneficial over monotherapy (Carter et al., 2016). Clinical trials evaluating the efficacy of immunotherapy in combination with EGFR or ALK TKI in advanced NSLC are ongoing (Moya-Horno et al., 2018), and may give encouraging results. Overall, these results highlight an unmet need for effective combinations to treat molecularly-defined advanced NSCLC, and particularly its link to companion diagnostics that may better stratify the patients.

Despite significant advances in the discovery of targeted therapies for the treatment of advanced NSCLC, patients eventually develop resistance, culminating in poor clinical outcomes. Despite the discovery of select targetable drivers, traditional chemotherapy is the only first-line treatment of choice for treating locally advanced or metastatic SCC (Figure 6). In addition to genotype-based patient subtyping, efforts must be focused on the identification of histotype-specific predictive biomarkers to achieve NSCLC subtype-specific effective therapies.

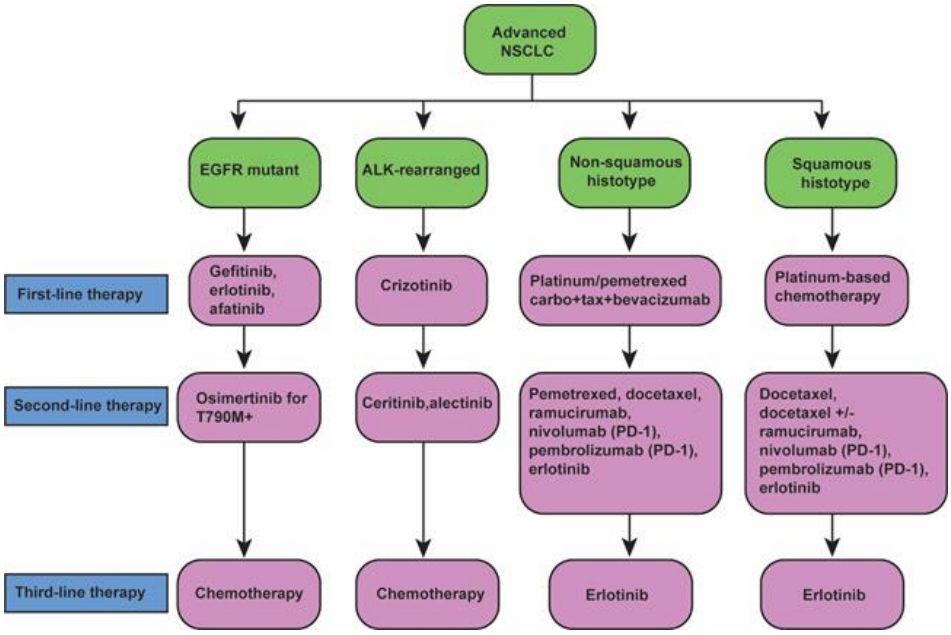

Figure 6. **Pharmacological management of advanced NSCLC. Treatments are based on histological and molecular features.** Platinum-based chemotherapy is recommended as first-line treatment for non-squamous and squamous lung cancer, and second-line treatments are either docetaxel alone, or in combination with the anti-VEGFR2 antibody ramucirumab, or anti-PD1 antibodies nivolumab and pembrolizumab. Anti-EGFR TKIs erlotinib, gefitinib, and afatinib are approved as first-line therapy in patients carrying EGFR mutations. Osimertinib, a third-generation EGFR TKI, is applied as second-line therapy for T790M carriers following first-line anti-EGFR therapies. Patients with ALK rearrangements are treated with crizotinib as first-line therapy. Progressive disease after second-line therapy is treated with chemotherapy. Adapted from (Rocco et al., 2016).

1.6. Tumor heterogeneity

Tumor heterogeneity refers to differences in the genetic, phenotypic and functional profiles of distinct cell populations found in a single tumor (intratumor heterogeneity: ITH), or between different tumors (intertumor heterogeneity). Tumor heterogeneity is detected at various levels: i) genetic heterogeneity, in which each tumor has its own genetic or epigenetic profile, or genetic differences exist between subpopulations of the same tumor, ii) microenvironmental heterogeneity, where tumors exhibit distinct stromal features composed of, for example, varying immune cell infiltrates, fibroblasts, or vasculature, iii) differences in biomarker expression, such as oncogenic signaling activities (de Bruin et al., 2015; Hanahan and Coussens, 2012; Liu et al., 2016; Spagnolo et al., 2016). The second and third heterogeneity types are considered to represent phenotypic heterogeneity, and all three heterogeneity types can be distributed in a spatial manner within the same tumor, referred to as spatial ITH (Hao et al., 2016; Spagnolo et al., 2016; Yuan, 2016). Both genetic and phenotypic heterogeneity have been implicated in sensitivity to therapies or drug resistance (Junttila and de Sauvage, 2013; Turner and Reis-Filho, 2012).

Two different models have been proposed to explain tumor heterogeneity: i) the cancer stem cell model, suggesting that only a subpopulation of tumor cells, called stem cells, possess an ability to self-renew and differentiate into non-tumorigenic cells, with heterogeneity arising from differences in genetic and epigenetic changes among different stem cells, and ii) the clonal evolution model, suggesting that tumors originate as a result of mutation in a single cell of origin, and by temporally accumulating mutations, this gives rise to heterogeneous populations which can divide and mutate further (Nowell, 1976; Reya et al., 2001). The mechanisms by which tumor heterogeneity arises during the patient's life time is currently an intensely investigated subject. Multiregion sequencing analysis pioneered by Swanton and Gerlinger suggests that tumor evolution is accompanied with spatially and temporally distinct genetic alterations, with subclonal mutations leading to intratumor genetic and phenotypic heterogeneity (de Bruin et al., 2015; Gerlinger et al., 2012)

1.6.1. NSCLC heterogeneity and therapeutic implications

Multiregional analysis of human lung AC for spatial distribution of *KRAS* and *EGFR* mutation has identified high level of intratumor and intertumor heterogeneity in gene mutations. In addition, analysis of tumor subregions has identified correlations between higher variant allele frequencies (VAF) of *KRAS* and *EGFR* with solid AC growth pattern compared to other histological AC subtypes (Dietz et al., 2017). Recent multiregional gene expression analysis of human NSCLC has also shown significant inter and intratumor heterogeneity, of gene signatures related to epithelial-to-mesenchymal transition

(EMT), and resistance to PD-1 checkpoint inhibitors (Lee et al., 2018). Furthermore, by doing multi-region exome/whole genome sequencing of NSCLC patients, Swanton and colleagues showed spatial and temporal heterogeneity in driver gene alterations. They found decrease in smoking-associated mutations over time and increase in apolipoprotein-B mRNA editing catalytic polypeptide-like (APOBEC) cytidine deaminase mediated mutations, and this was more prevalent in lung ACs compared to SCC, suggesting histotype-specific regulatory effects of APOBEC (de Bruin et al., 2015).

The process of tumorigenesis involves a complex interplay between tumor cells and the host immune system, in a way that favors tumor cells to escape from host immune surveillance. Tumor infiltrating immune cells can either be pro-tumorigenic, and this category includes tumor associated macrophages (TAMs), myeloid derived suppressor cells (MDSCs), and regulatory T cells (Tregs). Anti-tumorigenic immune cells include cytotoxic T cells (CTL) (CD8+) and natural killer cells (NK cells). The density of tumor-infiltrating lymphocytes, particularly CTL, is associated with response to chemotherapy and improved survival in patients with advanced NSCLC (Kilic et al., 2011; Liu et al., 2012a). On the contrary, an increase in MDSCs ($CD14^{+}HLA\text{-}DR^{-}$) in NSCLC patients is associated with metastasis and poor response to chemotherapy (Huang et al., 2013). Heterogeneity in signaling downstream of NSCLC driver genes has an impact on patient survival, therapeutic sensitivity and resistance mechanisms (Gerdes et al., 2013; Lee et al., 2013). However, intertumoral as well as spatial ITH in oncogenic signaling downstream of common driver genes, such as *KRAS*, *EGFR*, or loss of *LKB1* has thus far not been extensively studied in NSCLC.

1.7. Preclinical models of lung cancer

Various *in vivo* and *ex vivo* models have been established to dissect the physiological and molecular mechanisms that drive lung cancer pathogenesis. These models have also been used for preclinical investigation of promising monotherapy and drug combinations, and the discovery of potential new NSCLC targets.

1.7.1. *In vivo* models

In vivo mouse models can be categorized as xenografts, chemically-induced, syngeneic, and transgenic models (Kellar et al., 2015). Generation of classic xenograft models involves injection of established cancer cell lines into immunodeficient mice, either subcutaneously or orthotopically into the same organ from which cancer cells were derived. These classical models are mainly used for testing drug response *in vivo* prior to enrolling new compounds in clinical trials (Steiner et al., 2007). Recent efforts have however focused on the grafting of patient-derived tumor cells or tissue pieces (PDX models),

and these serve as an ideal model for personalized cancer therapy (Gao et al., 2015; Morgan et al., 2017). However, besides lacking physiologically relevant immune system, PDX models have been shown to undergo genetic drift during later passages, and hence may not recapitulate molecular and functional heterogeneity of the *in situ* tumor (Julien et al., 2012). Chemically-induced mouse models require exposure to carcinogens to initiate tumorigenesis. Typically, carcinogen-induced mouse models are inbred mice strains such as A/J or SWR known to be susceptible for spontaneous tumor development (Gordon and Bosland, 2009). Among carcinogen-induced models, lung adenocarcinomas driven by urethane has been shown to harbor *Kras* and *p53* mutations (Horio et al., 1996). Syngeneic mouse models enable the injection of immunologically compatible tumor cells into immunocompetent mice. Syngeneic mouse models of lung cancer are limited; one well-studied model is the lewis lung carcinoma (LLC), originally established by injecting primary LCC cells derived from the spontaneous lung tumor of C57BL mouse into the lung of recipient C57BL mouse (Rask et al., 2013). Due to the aggressiveness of the cell line, this model is used to for metastasis studies and for *in vivo* testing of chemotherapeutic agents (Papageorgiou et al., 2000; Sakai et al., 2006). Genetically engineered mouse models (GEMMs) are transgenic models that carry conditional or inducible genetic alterations, and are created by microinjection of the desired DNA construct into fertilized mouse oocytes, followed by homology-based genomic recombination to generate genetically-modified offspring (Gordon et al., 1980). Another method, developed by Oliver Smithies and Mario Capecchi, involves modifying embryonic stem cells (ES) with DNA constructs homologues to the gene of interest, followed by implantation of ES cells with the desired genomic DNA into murine blastocysts (Thomas and Capecchi, 1987). A variety of GEMMs carrying clinically-relevant genetic alterations have been created to model human NSCLC, which will be discussed below.

1.7.1.1. Transgenic mouse models of lung cancer

Transgenic mice or GEMMs of lung cancer are powerful models to examine processes governing tumor initiation and progression (Meuwissen and Berns, 2005). Sophisticated genetic engineering tools have enabled the creation of a number of lung cancer models with somatic gene alterations, which can be activated or inactivated in a spatial and temporal manner. The widely used Cre/lox and FLP/frt recombinase system permits conditional activation of oncogenes or inactivation of tumor suppressors (Jackson et al., 2001; Lee et al., 2012; Meuwissen et al., 2001; Sadowski, 1995; Sternberg and Hamilton, 1981). The availability of intranasally or intratracheally deliverable adenoviral Cre (AdCre) particles, as well as lentiviral Cre (LentiCre) particles, can mediate pulmonary tissue-specific genetic recombination (Gierut et al., 2014). These particles also permit the study of the role of different lung

epithelial cells in tumor initiation and progression, through the incorporation of cell type-specific promoters to drive Cre expression (Sutherland et al., 2011; Sutherland et al., 2014).

1.7.1.2. GEM models of lung adenocarcinoma

A number of transgenic mouse models model AC, the most common subtype of lung cancer. The earliest transgenic mouse model developing AC was expressing simian virus large T-antigen (SV40Tag) under the control of the CC10 or SPC promoter (DeCaprio et al., 1988; Dobbelstein and Roth, 1998). Later, expression of the oncogene *c-Myc* under the control of SPC promoter was shown to drive bronchioalveolar adenoma and then AC, with an average latency of 9.2 months (Ehrhardt et al., 2001). On the other hand, when *c-Myc* was driven by CC10 promoter, only bronchioloalveolar hyperplasias were observed (Geick et al., 2001). Transgenic mice carrying genetic alterations that are commonly found in lung ACs include models with *Egfr* mutation and *Eml4-Alk4* fusion genes; mice harboring human EGFR kinase domain mutations, the exon 19 deletion and the exon 21 point mutation L858R, under the CCSP promoter develop ACs (Ji et al., 2006a; Politi et al., 2006). Expression of the *Eml4-Alk4* fusion gene in SPC^{+} cells leads to development of multiple ACs within a few weeks of birth (Soda et al., 2008).

The first oncogenic *Kras*-driven lung AC models were developed by Jacks and colleagues, and one model used a latent allele of $Kras^{G12D}$ ($Kras^{LA}$) which is activated by spontaneous recombination. In addition to lung ACs, these mice also developed intestinal crypt foci, and skin papilloma (Johnson et al., 2001). Two additional inducible $Kras^{G12D/+}$ GEMMs were created, one with a reverse tetracycline-controlled transactivator (rtTA), and the other one with the $Kras^{G12D}$ stop codon flanked by Cre-loxP sites (Fisher et al., 2001; Jackson et al., 2001). Both these *Kras* models have been extensively used, and include the combination of $Kras^{G12D}$ together with genes involved in cell cycle regulations, such as $p53^{fl/fl}$, $Rb1^{fl/fl}$, $Rb12^{fl/fl}$, and $Map2k7^{fl/\Delta}$, or genes involved in controlling cellular metabolism and polarity, such as $Lkb1^{fl/fl}$, or genes that regulate cell growth and proliferation, such as $Pten^{fl/fl}$ (Ho et al., 2009; Iwanaga et al., 2008; Ji et al., 2007; Schramek et al., 2011). With exception of the model harboring concomitant $Kras^{G12D}$ activation and loss of *Lkb1* ($Kras^{G12D/+}$;$Lkb1^{fl/fl}$, KL), which produces lung SCC, ASC, and NSCLC-NOS (previously known as large cell carcinoma) in addition to AC, all models exclusively develop AC histotype tumors. Recently, a GEM model carrying clinically common *KRAS* mutation, $KRAS^{G12C}$ ($hKRAS^{G12C}$) has been established (Li et al., 2018).

A transgenic model carrying the $Kras^{G12V}$ mutation commonly found in lung ACs, has been established (Meuwissen et al., 2001). To elucidate the bioequivalence of oncogenic functions of *Kras* and *Hras* isoforms, Barbacid and colleagues generated transgenic mice expressing $Hras^{G12V}$ under the *Kras* locus,

and demonstrated differential effects of oncogenic *Kras*^{G12V} and *Hras*^{G12V} in lung tumorigenesis. Unlike *Kras*^{G12V}, lung-specific expression of *Hras*^{G12V} from the *Kras* locus did not result in lung tumors due to overactivation of MAPK signaling, resulting in a senescent-like state. However, it was also shown that the expression of *Kras* locus-driven *Hras*^{G12V} was 2.5 fold higher than that of *Kras*^{G12V}, suggesting that differences could be due to differences in their expression levels (Drosten et al., 2017).

The transcription factor NKX2-1 is a master regulator of cell fate determination during embryonic development of pulmonary tissue, and is frequently lost in poorly differentiated ACs (Herriges and Morrisey, 2014). Homozygous loss of *Nkx2-1* alters AC differentiation in *Kras*$^{G12D/+}$ mice, and deletion of *Nkx2-1* leads to mucinous AC as well as gastric differentiation of lung ACs marked by expression of the transcription factor, Hnf4α (Hepatocyte nuclear factor 4-alpha) (Snyder et al., 2013). These results suggests that NKX 2-1 has an important role in determining tumor differentiation and establishment of the AC sub-histotypes.

Homozygous loss of *p53* (*p53*$^{fl/fl}$) or expression of a mutant form of p53 (structural mutant; *p53*$^{R172H/-}$, or contact mutant; *p53*$^{R270H/-}$) accelerates *Kras*^{G12D}-induced lung AC development, and increases metastasis to lymph nodes and distant organs (Table 3) (Jackson et al., 2005). Tumors in the *Kras*^{G12D}*;p53*$^{fl/fl}$, *Kras*^{G12D}*;p53*$^{R172H/-}$, or *Kras*^{G12D}*;p53*$^{R270H/-}$ GEMMs show characteristics of human tumors, including high grade ACs characterized by nuclear atypia, and desmoplastic stroma. Interestingly, AdCre-mediated loss of p53 (*p53*$^{fl/fl}$) alone drives AC with a longer latency (1-1.5 years) suggesting that *p53* alteration itself is not sufficient to initiate lung tumorigenesis; instead the oncogenic *Kras* drives tumor initiation and loss of *p53* accelerates tumor progression (Meuwissen et al., 2003).

Table 3. Select mouse models of lung AC

Genetic modifications	Initiation method	Tumor burden	Reference
Kras $^{LSL\text{-}G12D/+}$	Ad5-CMV-Cre	AC spectrum	(Jackson et al., 2001)
Kras $^{LSL\text{-}G12D/+}$*;Trp53* $^{fl/fl}$	Ad5-CMV-Cre	Advanced AC with lymph node metastasis	(Jackson et al., 2005)
Kras $^{LSL\text{-}G12D/+}$*;Trp53* $^{LSL\text{-}R172H/-}$	Ad5-CMV-Cre	Advanced AC with lymph node metastasis	(Jackson et al., 2005)
Kras $^{LSL\text{-}G12D/+}$*;Trp53* $^{LSL\text{-}R270H/-}$	Ad5-CMV-Cre	Advanced AC with lymph node metastasis	(Jackson et al., 2005)
Kras $^{LSL\text{-}G12D/+}$*;Pten*$^{fl/fl}$	CC10-Cre	Advanced AC	(Iwanaga et al., 2008)
Kras $^{LSL\text{-}G12D/+}$*;Lkb1*$^{fl/fl}$	Ad5-CMV-Cre	AC	(Ji et al., 2007)
Kras $^{LSL\text{-}G12D/+}$*;Nkx2-1*$^{fl/fl}$	Ad5-CMV-Cre	Increased AC burden and additional mucinous AC	(Snyder et al., 2013)
Kras$^{LSL\text{-}G12D/+}$*;Pik3r2-/-; Pik3r1*$^{fl/fl}$*;*	Ad5-CMV-Cre	Decreased AC burden	(Engelman et al., 2008)
Kras $^{LSL\text{-}G12D/+}$*;Tgfbr2*$^{fl/fl}$	K5-CrePR	Increased AC burden	(Malkoski et al., 2012)
Kras $^{LSL\text{-}G12V/+}$	*CMV-Cre*$^{+/T}$	Adenomas and AC	(Meuwissen et al., 2001)
hKRAS $^{LSL\text{-}G12C/+}$	Ad5-CMV-Cre	AC	(Li et al., 2018)

1.7.1.3. GEM models of lung squamous cell carcinoma

Only very few GEMMs exist to model lung SCC. Lung-specific loss of *Lkb1* together with bi-allelic inactivation of *Pten* (LP) leads to SCC formation (Xu et al., 2014). In addition, using bi-cistronic lentiviral vectors expressing Sox2 and Cre recombinase, it has been shown that Sox2 expression cooperates with *Lkb1* loss (*Sox2;Lkb1*) to promote lung SCC formation (Mukhopadhyay et al., 2014). Concomitant loss of *Pten* and *Tgfrb2* (transforming growth factor beta type II receptor) in airways by Cre recombinase under the control of *K5* (keratin 5) promoter results in SCC with low incidence (Malkoski et al., 2012). A recent study by Berns and colleagues showed that SOX2, but not FGFR1, overexpression is critical for establishing squamous tumors in mice harboring conditional loss of *Pten* and *Cdkn2ab* (PC). This study demonstrated that both FGFR1 and SOX2 expression can drive lung tumorigenesis in PC mice but, only SOX2 (*Sox2;PC* model) overexpression promotes SCC formation, whereas FGFR1 overexpression results in sporadic SCCs (Ferone et al., 2016). These findings suggest that FGFR1, despite being frequently amplified (22%) and overexpressed (27%) in lung SCC, is not critical for driving SCC tumorigenesis, at least in the mouse (Table 4) (TCGA, 2012; Ferone et al., 2016; Weiss et al., 2010).

A lung cancer model harboring homozygous loss of *Lkb1* was shown to cooperate with oncogenic $Kras^{G12D}$ to generate an expanded histopathology spectrum compared to $Kras^{G12D}$ mice, including SCC and ASC tumors. Furthermore, KL mice treated with AdCre exhibited a shorter latency compared to $Kras^{G12D/+}$ mice (median survival, KL: 63 days vs *Kras*: 168 days). In addition, these mice also demonstrated enhanced metastasis to regional lymph node (61%), or axial cytoskeleton (7%) compared to $Kras^{G12D/+}$ (0%) mice (Ji et al., 2007). Interestingly, $Kras^{G12D}$ activation or *Lkb1* loss alone did not produce SCC, suggesting cooperative effects of oncogenic *Kras* and *Lkb1* loss in SCC tumorigenesis (Ji et al., 2007). Furthermore, spontaneously arising SCCs in a mouse model harboring kinase dead *IKKα* (an inhibitor of the nuclear factor kappa-B kinase subunit alpha) showed significant downregulation of LKB1 compared to adjacent normal lung tissue, further supporting a mechanistic role of LKB1 loss in SCC differentiation and tumorigenesis (Xiao et al., 2013). In the KL model, transdifferentiation of AC to SCC via an ASC intermediate stage has been reported (Han et al., 2014), and suggested to mechanistically involve the extracellular matrix remodeling enzyme lox (lysal oxidase), the YAP (yes-associated protein) hippo pathway protein, as well as oxidative stress in regulating the AC-SCC transition (Gao et al., 2014; Han et al., 2014; Li et al., 2015a).

Despite the low incidence of *LKB1* genetic alterations in lung SCC (Table 1), above murine studies thus show that *Lkb1* loss plays an important role in the establishment of SCC together with genes

predominantly altered in SCC, namely *PTEN* and *SOX2*, and that these tumors thus represent a small subset of clinical SCC.

1.7.1.4. GEM models of lung adenosquamous cell carcinoma

ASC is one of the rarest but most aggressive subtype of lung cancer, with poor patient prognosis (Nakagawa et al., 2003). Only limited mouse models have been shown to give rise to ASCs, with the already mentioned KL model being one of these (Ji et al., 2007) (Table 4). As mentioned, in the KL model, transdifferentiation of SPC^{+} cell-derived AC to SCC tentatively suggested to involve ASC as an intermediate stage (Han et al., 2014). In addition to the KL model, also loss of *Pten* and a transcription factor *Smad4* in CC10 expressing airway epithelial cells results in ASCs, showing increased activation of AKT and ERBB2 compared to normal airway epithelium (Liu et al., 2015). Mechanistically, deletion of *Pten* and *Smad4* led to transcriptional repression of *Errfi1*, a negative regulator of ERBB2 leading to increased ERBB2 signaling. Interestingly, transgenic expression of the mutant human *HER2* gene ($hHER2^{YVMA}$) in the lung epithelium drives ASC formation (Perera et al., 2009), suggesting that ERBB2 receptor-mediated signaling suffices to initiate and establish ASC tumors.

Table 4. Select mouse models of lung SCC and ASC

Genetic modifications	Initiation method	Tumor burden	Reference
Kras$^{LSL\text{-}G12D/+}$*; Lkb1*$^{fl/fl}$ (KL)	Ad5-CMV-Cre	AC, SCC, ASC, and LCC	(Ji et al., 2007)
Lkb1$^{fl/fl}$*;Pten*$^{fl/fl}$ (LP)	Ad5-CMV-Cre	SCC	(Xu et al., 2014)
Ikka$^{KA/KA}$		Spontaneous SCC	(Xiao et al., 2013)
Tgfbr2$^{fl/fl}$*;Pten*$^{fl/fl}$	K5-CArePR	AC and rare SCC	(Malkoski et al., 2012)
Lkb1$^{fl/fl}$ *Lenti-Sox2-Cre (Sox2;Lkb1)*	Lenti-Sox2-Cre	SCC	(Mukhopadhyay et al., 2014)
Pten$^{fl/fl}$*;Cdkn2ab*$^{fl/fl}$ *;LSL-Sox2* (*Sox2;PC*)	Ad5-K5-Cre Ad5-K14-Cre	SCC	(Ferone et al., 2016)
Pten$^{fl/fl}$ *;Cdkn2ab*$^{fl/fl}$ *;LSL-Fgfr1*^{K656E}	Ad5-K5-Cre Ad5-K14-Cre	Sporadic SCC	(Ferone et al., 2016)
Pten$^{fl/fl}$ *;Smad4*$^{fl/fl}$	CCSPiCre	ASC	(Liu et al., 2015)
hHER2^{YVMA}	CC10-rTA	ASC and occasional AC	(Perera et al., 2009)

1.8. Cellular origin(s) of lung cancer

Tumorigenesis is a multistep process. Transforming events lead to alterations of stem/progenitor cell functions. In this, the precise cell of origin has been suggested to define phenotypic heterogeneity of the tumor lesions (Blanpain, 2013). Thus, improved understanding of the tumor progenitor cell can help in uncovering the source of tumor heterogeneity. As mentioned, anatomically distinct stem/progenitor cells have been identified based on their ability to self-renew and/or differentiate into specific lung epithelial cells. These include tracheal basal cells and club cells, bronchiolar club cells, BASCs in the BADJ, and alveolar AT2 cells (Figure 2) (Leeman et al., 2014). To explore the role of progenitor cells in progression of NSCLC, two different approaches have been used in GEM models: i) adenoviruses that contain epithelial cell type-specific promoter to drive expression of the Cre recombinase (Ad5-CC10-Cre, Ad5-SPC-Cre, Ad5-K5-Cre,and Ad5-K14-Cre), and ii) inducible knock-in mouse models (Sftpc-CreER, or CC10-CreER), in which cell type-specific genetic recombination is achieved following tamoxifen treatment (Sutherland et al., 2011; Sutherland et al., 2014; Xu et al., 2012)

1.8.1. Studies on the cell of origin of NSCLC

The progenitor cells of lung AC have been defined during recent years. Studies using the $Kras^{G12D/+}$ and $Kras^{G12D/+};p53^{fl/fl}$ GEMMs have identified club cells, AT2 cells, and BASCs as progenitors of murine AC (Kim et al., 2005; Sutherland et al., 2014; Xu et al., 2012). By using Ad5-CC10-Cre and Ad5-SPC-Cre, Sutherland et al showed that both $CC10^+$ and SPC^+ cells can drive AC progression upon activation of $Kras^{G12D/+}$ alone, or in combination with loss of *p53* (Sutherland et al., 2014). Despite an absence in survival differences between $Kras^{G12D/+}$ or KP mice infected with SPC-Cre or CC10-Cre viruses, Sutherland et al reported that $CC10^+$ cell-derived ACs showed invasive characteristics and expressed Hmga2, a transcription factor involved in the regulation of proliferation, EMT, and metastasis in many cancers and also expressed in poorly differentiated tumors (Gao et al., 2017; Sutherland et al., 2014). Similarly, using tamoxifen-inducible SPC-Cre-ER or CC10-Cre-ER mouse models, Xu et al showed that both $CC10^+$ and SPC^+ positive cells are progenitors of AC in $Kras^{G12D/+};p53^{fl/+}$ mouse model (Xu et al., 2012). The role of BASCs as progenitors of AC is under debate: while Kim et al showed expansion of BASCs as measured by immunofluorescence (IF) staining, following Ad5-CMV-Cre mediated $Kras^{G12D/+}$ expression, Sutherland et al did not observe SPC and CC10 dual positive cells in the BADJ/BASC region of Ad5-SPC-Cre infected $Kras^{G12D/+}$ mice (Kim et al., 2005; Sutherland et al., 2014). Possible explanations could be that either the SPC promoter activity in SPC/CC10 dual positive BASC cells is too low to initiate $Kras^{G12D}$ activation, or BASCs are not AC progenitors. Interestingly, an AdCre-mediated inflammatory response, consisting of increased

infiltration of T and B cells, has been linked to $CC10^+$-driven AC progression in the $Kras^{G12V/+}$ model (Mainardi et al., 2014). This inflammatory response was essential for progression of epithelial hyperplasia to low grade adenomas, but not for progression to advanced ACs. These findings show that the tumor cell of origin, together with the genetic drivers and microenvironmental factors influence the tumor progression and aggressiveness of the established tumors.

Recently, Ferone et al demonstrated that basal cells, club cells, and AT2 cells have the capacity to give rise to SCC in the *Sox2;PC* mouse model. While SCCs induced from basal cells using Ad5-K14-Cre were detected in the bronchi or bronchioles, leading to centrally-localized tumors, Ad5-CC10-Cre- or Ad5-SPC-Cre driven SCCs were distributed in the peripheral regions of the lung. In addition to morphological similarities, SCCs derived from different progenitors exhibited striking similarity in their gene expression profiles. The authors therefore concluded that peripheral SCCs in humans may originate from both SPC^+ or $CC10^+$ cells, and also that SOX2 expression is a determining factor for SCC tumorigenesis (Table 5). (Ferone et al., 2016). Using CC10 promoter-driven knock-in mice or AdCre viruses, previous studies have shown that $CC10^+$ cells can drive ASC tumorigenesis (Liu et al., 2015; Perera et al., 2009). However, the relative roles of progenitors in establishing lung ASC remains unclear. Moreover, in the study by Han et al addressing the transdifferentiation of KL AC to SCC via ASC, the human SPC promoter was used to drive Cre-ER expression, and this promoter has been shown to be active in bronchiolar and alveolar cells (Glasser et al., 1991; Han et al., 2014), suggesting that cellular origins of diverse NSCLC histotypes observed in the KL model are unlikely restricted to the alveolar compartment.

Table 5. Select mouse model studies addressing the cell of origin of NSCLC

Genetic modifications	Initiation method	Tumor burden	Reference
Kras $^{LSL\text{-}G12D/+}$	Ad5-CC10-Cre	Papillary hyperplasia, papilloma, and papillary carcinoma	(Sutherland et al., 2014)
Kras $^{LSL\text{-}G12D/+}$	Ad5-SPC-Cre	AAH, mixed AC	(Sutherland et al., 2014)
Kras $^{LSL\text{-}G12D/+}$*;Trp53* $^{fl/fl}$	Ad5-CC10-Cre	Invasive, metastatic Hmga2 positive AC	(Sutherland et al., 2014)
Kras $^{LSL\text{-}G12D/+}$*;Trp53* $^{fl/fl}$	Ad5-SPC-Cre	Mixed AC	(Sutherland et al., 2014)
Kras $^{LSL\text{-}G12D/+}$*;Trp53* $^{+/fl}$	CC10-CreER	Hyperplasia at BADJ, AC in alveoli	(Xu et al., 2012)
Kras $^{LSL\text{-}G12D/+}$*;Trp53* $^{+/fl}$	SPC-CreER	AC in alveoli	(Xu et al., 2012)
Kras $^{LSL\text{-}G12D/+}$*; Lkb1* $^{fl/fl}$	SPC-CreER	AC which transdifferentiate into SCC via ASC	(Han et al., 2014)
Kras $^{LSL\text{-}G12D/+}$*; Lkb1* $^{fl/fl}$	Ad5-SPC-Cre	AC, SCC, and, ASC	(Li et al., 2015a)
Pten $^{fl/fl}$*;Cdkn2ab* $^{fl/fl}$ *;LSL-Sox2*	Ad5-CC10-Cre	Central SCC	(Ferone et al., 2016)
Pten $^{fl/fl}$*;Cdkn2abf* $^{fl/fl}$ *;LSL-Sox2*	Ad5-SPC-Cre	Peripheral SCC	(Ferone et al., 2016)
Pten $^{fl/fl}$*;Cdkn2abf* $^{fl/fl}$ *;LSL-Sox2*	Ad5-K14-Cre	Central SCC	(Ferone et al., 2016)

1.9. Modeling of immune functions in lung cancer

Tumorigenesis involves a complex interplay between malignant cells and the host environment, which consists of vasculature, stromal cells, and cells of the innate and adaptive immune system (Junttila and de Sauvage, 2013). The tumor immune contexture, which is defined as the functional identity, density, and spatial distribution of immune cells, is regarded as an important factor affecting patient prognosis and therapeutic efficacy (Fridman et al., 2013). Immunosurveillance is a mechanism by which the host immune system recognizes neoantigens, and destroys transformed cells. Some of the effector cells that mediate immunosurveillance are NK cells, macrophages, and tumor-infiltrating lymphocytes (TILs), mainly represented by $CD8^+$ T cells and interferon gamma (IFN-γ)-producing γδ T cells (Figure 7) (Dunn et al., 2002). Conversely, tumors employ various strategies to escape from the host immune system, a process called immunoediting. Various soluble factors and cytokines secreted by the tumor cells favor the recruitment of cells with immunosuppressive functions, which includes MDSCs capable of inhibiting T cell-mediated immunosurveillance (Marvel and Gabrilovich, 2015). Another immune evasion mechanism is altered antigen presentation by downregulating expression of class I major histocompatibility complex (MHC) molecules, or alterations in the antigen-processing machineries, amounting to escape form CTL-mediated recognition and tumor attack (Garrido et al., 1997; Maeurer et al., 1996). A subset of $CD4^+$ T cells called Tregs, marked by expression of the FoxP3 transcription factor, also act immunosuppressively, by suppression of antigen presentation and secretion of T cell inhibitory cytokines (Facciabene et al., 2012). Tregs have been implicated in lung cancer progression and metastasis (Marshall et al., 2016). In addition, significant enrichment of Tregs in lung ACs compared to SCCs has been observed in clinical samples suggesting histopathology-selective functions of Tregs and AC patients might benefit from anti-Treg therapies (Black et al., 2013).

Hematopoietic stem cells give rise to myeloid progenitors, which then differentiate into immature myeloid cells (IMCs). Under normal conditions, IMCs are produced in the bone marrow, and these cells then differentiate into macrophages, dendritic cells (DCs) and granulocytes. However, in disease conditions including cancer, differentiation of IMCs can be blocked, resulting in the expansion of IMCs with immunosuppressive functions which are referred to as MDSCs (Gabrilovich and Nagaraj, 2009). In mice, MDSCs are identified based on cell surface expression of CD11b (integrin alpha M) and Gr-1. A monoclonal antibody that binds to cell surface antigen Gr-1 recognizes two different epitopes, namely lymphocyte antigen 6 complex locus G and C (LY6G and LY6C), with higher affinity for LY6G (Fleming et al., 1993). Subsequently, development of isotope-specific antibodies led to the identification of two subsets of MDSCs, namely granulocytic MDSCs identified as $CD11b^+LY6G^+LY6C^{low}$, and monocytic MDSCs identified as $CD11b^+LY6G^-LY6C^{hi}$ (Youn et al.,

2008). Importantly, granulocytic MDSCs share similarity with neutrophils/tumor-associated neutrophils (TANs) in terms of morphology and cell surface markers (Pillay et al., 2013).

Human MDSCs are identified as cells that co-express CD11b and CD33, but lacking HLA-DR. The granulocytic counterpart of human MDSCs are $CD15^+$, whereas monocytic MDSCs are $CD14^+$. In recent years, molecules that regulate MSDC's immune suppressive functions have been identified, including Arginase-1 (Arg-1), indoleamine 2, 3-dioxygenase (IDO1), reactive oxygen species (ROS), and nitric oxide synthase (NOS) (Elliott et al., 2017). Inflammatory signals, and the pro-inflammatory cytokines interleukin 1b (IL1β) and interleukin-6 (IL-6), as well as the bioactive lipid prostaglandin (PGE2), are known to induce MDSC accumulation and activation (Ostrand-Rosenberg and Sinha, 2009; Song et al., 2005; Tu et al., 2008). In addition, the S100 Calcium Binding Proteins A8 and A9 (S100A8 and S100A9) regulate MDSC mobilization (Sinha et al., 2008). One of the well-described mechanisms of MDSC-mediated immunosuppression relates to the metabolism of L-arginine, which acts as a substrate for two enzymes, iNOS (generating NO) and arginase 1 (converting L-arginine to urea and L-ornithine). MDSCs express high levels of both of these enzymes, and the specific T cell suppressive ability of MSDCs is attributed to depletion of extracellular arginine required for the proliferation and expansion of T cells (Munder et al., 2006; Rodriguez and Ochoa, 2008; Rodriguez et al., 2002). In addition to immunosuppressive functions, MDSCs can also assist in tumor invasion, angiogenesis and migration by secreting growth factors such as MMPs (matrix metalloproteinases) and VEGFA (vascular endothelial growth factor A) (Ye et al., 2010).

Importantly, analysis of granulocytic MDSCs isolated from the peripheral blood of lung cancer patients showed an inverse relationship between the abundance of MSDC and $CD3^+CD8^+$ CTLs, and MDSC infiltration correlated with as poor patient prognosis (Liu et al., 2010). Furthermore, increases in monocytic MDSCs were reported in NSCLC patients treated with chemotherapy, and this was associated with disease progression and poor response to therapy (Koinis et al., 2016). Recently, it was shown that elevated neutrophil-to-lymphocyte ratio (NLR) negatively correlates with patient survival and response to anti-PD1 therapy in metastatic NSCLC patients (Diem et al., 2017). In addition, using murine breast cancer models, neutrophils have been shown to provide a pre-metastatic microenvironment in the lungs facilitating lung metastasis of breast cancer cells (Wculek and Malanchi, 2015). These finding imply that targeting MDSCs and neutrophils may help in controlling primary and metastatic disease. Various strategies are being tested in preclinical and clinical settings to therapeutically target MDSC function, such as molecules affecting MDSC recruitment (anti-CSF-1 and anti-G-CSF antibodies), expansion (cyclooxygenase (COX-2 and PGE2), differentiation (trans-Retinoics; ATRA, vitamin D3), and immune suppression (inhibitors of reactive nitrogen species) (Albeituni et al., 2013; Gabrilovich, 2017).

The role of the immune microenvironment in tumor progression has been extensively studied using GEMMs. For example, in the KP GEMM, exogenous expression of T cell antigens elicited a substantial anti-tumor immune response marked by increase in number of T and B cells (DuPage et al., 2011). This response was not sustained at later time points, due to loss of anti-tumor functional and memory T cells, as well as expression of the T cell exhaustion marker PD-1, and tumors eventually escaped from T cell attack. Despite lack of T cell response in the later phase, significant delay in the tumor development was observed in immunogenic KP mice compared to poorly immunogenic control mice, suggesting early anti-tumor responses can delay disease progression (DuPage et al., 2011). In addition, the role of Tregs in lung tumorigenesis has been studied using murine models, $Foxp3^+$ Treg cells promote tumor growth in CC10-Tag transgenic lung AC mouse model. Specifically, anti-CD25-mediated depletion of Tregs led to reduction in tumor burden accompanied by increased cleaved caspase-3-marked cell death and enhanced $CD8^+$ T cell infiltration, indicating that in this model Tregs promote lung cancer development by restraining anti-tumor immunity (Ganesan et al., 2013).

Tertiary lymphoid structures (TLS) are immune cell aggregates that are often found near the site of an inflammatory infection, or near cancerous tissue. TLSs contain T and B lymphocytes, and dendritic cells. The role of tumor associated (TA)-TLS in tumor development has been deeply studied in the KP NSCLC GEMM. Specifically, Joshi et al demonstrated that depletion of Tregs located in TA-TLS resulted in an increased number of tumor infiltrating $CD8^+$ lymphocytes and triggered an anti-tumor immune response against established ACs (Joshi et al., 2015).

Profiling of the immune cell phenotypes in ACs driven by mutant *Kras*, mutant *Egfr* or mutant *Kras* with *p53* loss, revealed immune cell signatures unique to each of these models. Specifically, flow cytometry and IHC analysis showed expansion of $CD8^+$ lymphocytes in mutant *Kras*- and KP-driven tumors, but not in *Egfr* mutant tumors, and this was further validated in human *KRAS* and *EGFR* mutant NSCLC. On the contrary, murine *Kras* and KP ACs, but not *Egfr* mutant ACs, showed a significant decrease in NKG2D (natural killer group 2, member D receptor) expression required for suppression of NK cell-mediated cytotoxicity, suggesting NSCLC subtype-specific immune cell composition (Busch et al., 2016).

A recent study by Faget et al reported that particularly the large and advanced tumors in the KP model exhibited high $Gr\text{-}1^+$ neutrophil and low $CD8^+$ T cell infiltration, and $Gr\text{-}1^+$ neutrophils were shown to promote tumor progression by enhancing tumor hypoxia and Snail expression (a transcription factor involved in EMT) by the cancer cells. Anti-Gr1-mediated neutrophil depletion reversed hypoxia, decreased Snail expression, and sensitized tumors for PD-1 inhibition, resulting in tumor regression. Authors further validated this finding in human NSCLC samples, by showing that patients with low

$CD8^+$ T cell and high $CD15^+$ neutrophils showed reduced overall survival (Faget et al., 2017). These findings suggest that immune cell signatures correlate with the histological grade or aggressiveness of the tumor, and that immunosuppression by neutrophils is predominant in advanced lung ACs.

In a mouse model harboring kinase dead *IKKα*, which develops spontaneous SCC, macrophage-induced inflammation was shown to regulate the development of SCC (Xiao et al., 2013). Another lung SCC model driven by loss of *Lkb1* and *Pten* showed immunosuppressive features marked by PD-L1 expression and high tumor-associated neutrophil (TAN) infiltration (Xu et al., 2014). Similarly, SCCs in the *Sox2;PC* model showed abundant LY6G and myeloperoxidase (MPO) positive TANs, and conversely, TAMs were poorly represented in these tumors. Furthermore, while membranous PD-L1 expression was variable in human SCC, *Sox2;PC*-derived SCCs showed strong PD-L1 positivity, suggesting immunosuppression in *SOX2;PC*-driven SCC (Ferone et al., 2016). Together, these reports indicate that TAN infiltration might be characteristic of lung SCC and advanced ACs, while lymphocyte functions vary depending on the AC subtype.

Loss of *Lkb1* has also been linked to an immunosuppressive microenvironment, characterized by pro-inflammatory cytokine and chemokine production favorable for TAN infiltration. Koyama et al reported that tumors from the KL model show increased $CD11b^+$ $Gr\text{-}1^+$ TANs and decreased PD-L1 expression compared to *Kras* tumors. In addition, expression of the pro-inflammatory cytokine *Il6* was higher in TANs isolated from KL tumors compared to neutrophils from the normal lung. Therapeutic benefit was observed only upon TAN inhibition via IL-6 neutralizing antibody, whereas treatment with anti-PD1 antibody did not show measurable response in KL mice. This study also reported that *LKB1* inactivating mutations in human NSCLC were associated with reduced PD-L1 expression and low $CD3^+/CD8^+$ T cells compared to *Kras* mutant tumors (Koyama et al., 2016). Given the observation that SCCs as well as advanced ACs in the KP model exhibit TAN infiltration, it remains to be investigated if TAN-mediated immunosuppression in the KL model is histotype-specific.

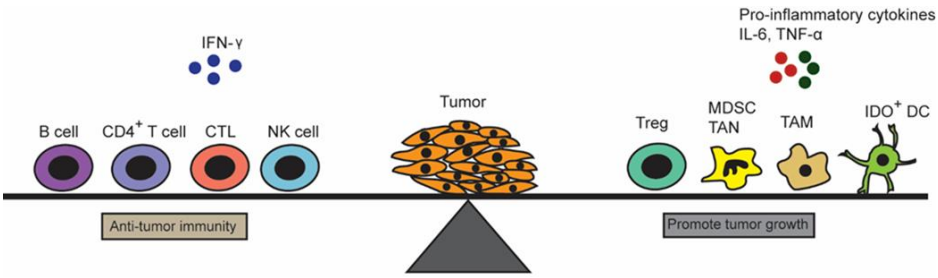

Figure 7. **The balance between anti-tumor and tumor promoting functions of the immune system.** Both innate and adaptive immune cells mediate anti-tumor immunity, and these include B cells, $CD4^+$ T cells, CTLs, and NK cells that can be activated by interferon gamma (IFN-γ). On the other hand, tumor promoting immune cells, including Tregs, MDSCs, TANs, TAMs, and IDO^+-dendritic cells are activated by pro-inflammatory cytokines IL-6, and TNF- α (tumor necrosis factor alpha). Adapted from (Smith et al., 2014).

1.10. Oncogenic signaling heterogeneity in murine NSCLC

Deregulation of signaling pathways that govern cell proliferation, survival, and migration such as MAPK and PI3K/AKT pathways are frequently found in cancers (McCubrey et al., 2012). Surprisingly, oncogenic signaling heterogeneity has been studied only to a limited extent using lung cancer GEMMs. Integrative genomic and proteomic analysis identified activation of SRC (proto-oncogene tyrosine-protein kinase) and FAK (focal adhesion kinase) in primary and metastatic KL tumors compared to $Kras^{G12D}$ tumors. This was suggested to have functional consequences, as interference with SRC and FAK signaling in LKB1 wild type and LKB1 null human NSCLC cell lines using the small molecule inhibitors dasatinib (SRC inhibitor) or PF573228 (FAK inhibitor) resulted in decreased cell adhesion and migration. Furthermore, LKB1 null cell lines grew faster as subcutaneous xenografts compared to wild type cells, and showed vimentin positivity in the tumor periphery, suggesting that loss of LKB1 could promote EMT. These findings indicate that activation of SRC and FAK signaling could be one possible mechanism by which LKB1 loss activates cell migration and promotes metastasis (Carretero et al., 2010).

Loss of *PTEN* is generally known to activate PI3K/AKT pathway. Interestingly, however, Curry et al showed that, depending on the bronchiolar or alveolar origins, $Kras^{G12D}$-driven *Pten*-null murine tumors showed differential AKT activation and resistance to dietary restriction. *Pten* lacking, bronchiolar, high-grade tumors showed AKT activity and resistance to dietary restriction. On the other

hand, alveolar tumors were sensitive to dietary restriction and displayed low AKT activity. This difference was attributed to bronchiolar cells intrinsically expressing high levels of IGF-IR (insulin-like growth factor-I receptor) and the enzyme ENTPD5 (endoplasmic reticulum enzyme, ectonucleoside triphosphate diphosphohydrolase 5), known to modulate growth factor receptor levels (Curry et al., 2013). These findings imply that cell autonomous growth factor signaling in the bronchiolar vs alveolar compartments of the lungs may influence signaling activities in the tumors derived from different progenitors.

Murine squamous tumors in the LP model exhibited high AKT activity, as well as low ERK activity compared to *Kras*^{G12D}-driven tumors, suggesting that LP SCC tumors rely on PI3K/AKT signaling, while *Kras*^{G12D}-driven AC tumors are more dependent on MEK/ERK signaling (Xu et al., 2014). Similarly, SCCs in the *Sox2;Lkb1* model showed weak activation of ERK compared to *Kras*^{G12D} and KL tumors. However, AKT activation was found to be variable in KL tumors as well as in SCCs in the *Sox2;Lkb1* model. Furthermore, *Sox2;Lkb1*-driven SCCs showed significantly higher nuclear pSTAT3 compared to AC or SCC tumors in the *Kras*^{G12D} or KL model, respectively (Mukhopadhyay et al., 2014). These studies linked PI3K/AKT and MAPK signaling heterogeneity to tumor genotype. However, oncogenic signaling heterogeneity in a genetically homogeneous KL model with mixed NSCLC pathologies remained to be investigated.

1.11. Organotypic tumor slice cultures as a preclinical model

Predicting patient responses to anticancer therapies remains as a major challenge, especially for solid tumors such as lung cancer, where pronounced genetic, phenotypic and microenvironmental heterogeneity influences treatment efficacy (Mumenthaler et al., 2015; Xue et al., 2017). As opposed to conventional two-dimensional (2D) and three-dimensional (3D) models, in which tumor complexities can be partially retained, organotypic cultures known as precision-cut slices retain the complexities of the *in situ* tumors such that intact tumor-stroma interactions which can be studied in a spatial manner (Meijer et al., 2017). In addition, tumor tissue slices offer a low-throughput but high-content platform for pharmacological drug testing. The first organotypic cultures were generated from heart and brain tissues of chick embryos and adult rats, respectively (Bousquet and Meunier, 1962; Loffredo Sampaolo, 1956). Initially, precision-cut slices were generated using a Krumdieck tissue slice machine that punches cylindrical tissue cores, which are further sliced by a rotating knife (Krumdieck, 2013). More recently, a vibratome machine Leica VT1200 S, which uses a vibrating blade microtome to generate precision-cut slices has been developed. The latter generates reproducible and more precise slices compared to the Krumdieck tissue slicer, and also enables to follow the order of slicing (Zimmermann et al., 2009).

The most widely used tissue slice culture method is the air-liquid interphase, which involves placing the slices on top of 0.4 μm pore size membrane inserts immersed in the culture medium. Some studies have cultivated slices on top of titanium grids inserted into culture medium in rotating 6-well plates, and this method ensures intermittent exposure of tissue slices to oxygen and nutrients (Kiviharju-af Hallstrom et al., 2007). Careful optimization of the tissue slice culture conditions is a prerequisite for long-term culturing. Slices with varying thickness (250 μm -500 μm) have been shown to preserve the morphological and histological tissue features up to 16 days (Das et al., 2015; Davies et al., 2015; Kiviharju-af Hallstrom et al., 2007; Merz et al., 2013; Naipal et al., 2016; Vaira et al., 2010). Davies et al performed a systematic comparison of culture conditions using tumor slices derived from lung, breast and prostate cancer models. This showed that atmospheric oxygen and membranous supports are required for the preservation of the tissue slice viability. They further showed that stress response genes were elevated in cultured slices compared to freshly section uncultured 0 h slices, and that an intra-slice gradient in viability, proliferation and biomarkers formed during cultivation; the region of the slice exposed to the culture medium had reduced viability, and accumulated HIF1α as a result of poor oxygenation. This suggests that intra-slice viability gradients, as well as DNA damage responses, likely affecting tumor-specific biological functions, and should be taken into consideration when performing perturbation studies on slice cultures (Davies et al., 2015).

Precision-cut tumor slices from a variety of tumor tissues have been established for testing anti-cancer agents (Carranza-Torres et al., 2015; Gerlach et al., 2014; Koerfer et al., 2016; Vaira et al., 2010). Breast cancer-derived tissue slices were established for *ex vivo* diagnostics to test RAD51 accumulation at DNA double strand breaks, and authors suggest that this assay could be used to guide selection of patients for treatment with PARP inhibitors (Naipal et al., 2014). In addition, Muzumder et al developed an *ex vivo* tumor slice model established from clinical biopsies of Head and neck squamous cell carcinoma (HNSCC), or colorectal cancer, this model composed of slices cultured with tumor grade-matched matrix and autologous patient serum. They evaluated the functional drug response (viability, and proliferation) to targeted drug (cetuximab) and or chemotherapy agents on these cultures and integrated the responses obtained in *ex vivo* engineered cultures with response from matched patients. This permitted the development of an algorithm that could accurately predict clinical response in a new group of 55 patients (Majumder et al., 2015). Furthermore, Vaira et al established tissue slices from human lung, colon, and prostate cancers, and showed that viability and proliferation in these cultures are preserved up to 4 days. Pharmacological inhibition of the PI3K/AKT pathway in slices effectively inhibited phosphorylation of AKT and S6RP (S6 ribosomal protein), and resulted in a partial reduction in viability and proliferation (Vaira et al., 2010). The authors also show an increase in the levels of phosphorylated S6RP (pS6RP) in cultured slices as compared to uncultured T0 tissue slices, suggesting altered signaling in the cultured slices. This highlights the importance of careful analysis of the cultured

slices for the preservation of targeted pathway activities of *in situ* tumors before evaluating *ex vivo* drug responses. The utility of slice cultures has also been extended for the prediction of response to combination treatments; slices established from clinical glioblastoma tumors from patients harboring the ROS1-FIG fusion gene showed a synergistic response to combination treatment with crizotinib and the chemotherapy agent temozolomide (Das et al., 2015). Together, these findings suggest that precision-cut tumor slices could be a valuable tool for evaluating functional drug response.

1.12. Preclinical studies using *in vivo* models

The utility of *in vivo* and *ex vivo* cancer models extends from understanding disease biology to testing the efficacy of anticancer regimens prior to their clinical application. Preclinical studies have been carried out with lung cancer GEMMs, human NSCLC cell lines, and more recently also with patient-derived primary cells. A study conducted by Johnson and colleagues showed that combination of chemotherapy (carboplatin) and erlotinib has no effect on the survival of KP mice, and this observation was in line with the response to same combination in *Kras* mutant NSCLC patients. In addition, they also showed that similar to human NSCLC, KP mice obtain significant survival benefit from combination of chemotherapy with anti-VEGFR therapy compared to chemotherapy alone (Singh et al., 2010). This highlights the preclinical utility of lung cancer GEMM in predicting therapeutic responses and identifying novel drug combinations. TKIs were shown to be effective in an *Egfr* mutant transgenic lung cancer model (Ji et al., 2006b; Politi et al., 2006). In addition, the anti-EGFR mAb cetuximab was shown to mediate effective tumor regression in a mutant *Egfr*-driven lung AC model (Ji et al., 2006a). Another lung AC GEM model, driven by expression of the H1047R kinase domain mutation of the PI3K p110α catalytic subunit (PIK3CA), was used to show that treatment with the dual PI3K and mTOR inhibitor NVP-BEZ235 (dactolisib) effectively caused tumor regression. Interestingly, while the same inhibitor was not effective in $Kras^{G12D}$ mice, combined treatment with NVP-BEZ235 and the MEK inhibitor ARRY-142886 caused efficient tumor regression, suggesting that two major effector pathways downstream of KRAS need to be perturbed to achieve tumor regression in mutant *Kras*-driven murine lung tumors (Engelman et al., 2008). On the other hand, KL tumors were found to be unresponsive to combined PI3K/mTOR and MEK inhibition (dactolicib+AZD2644/selumetinib) (Carretero et al., 2010). Based on the observation that KL tumors showed increased SRC and FAK activation, Carretero et al hypothesized that interference with SRC signaling might restore sensitivity in KL tumors. In line with this hypothesis, they observed that the triple combination of dactolisib, selumetinib, and the SRC inhibitor dasatinib caused tumor regression in KL mice. These findings imply that KL tumors are resistant to combined PI3K/mTOR and MEK inhibition, at least partly due to activation of SRC (Carretero et al., 2010). Another murine study

conducted in parallel with an ongoing human clinical trial, comparing the response of standard-of-care docetaxel monotherapy with the combination of docetaxel and the MEK inhibitor selumetinib in *Kras* mutant NSCLC patients (Chen et al., 2012). This co-clinical study used tumor-bearing $Kras^{G12D}$, KP, and KL mice. Similar to the observations by Carretero et al, KL tumors were shown to be non-responsive to docetaxel/selumetinib combination therapy, while significant decreases in tumor volume accompanied by increased apoptosis and decreased proliferation were detected in $Kras^{G12D}$ and KP tumors. These authors thus suggested that resistance to combination therapy in KL tumors could be associated with low MAPK activity and increased AKT and SRC activity, indicating that multiple pathways in addition to MAPK appear to drive proliferation of KL tumors (Chen et al., 2012). In addition, $hKRAS^{G12D}$ mice showed prolonged progression-free survival to combination of selumetinib and chemotherapy, while the same combination was not effective in $hKRAS^{G12D;}$ $p53^{R270H}$ mice. These results suggests that the *KRAS* and *p53* mutation status may define sensitivity to MEK inhibition plus chemotherapy (Li et al., 2018).

Resistance to targeted therapies can be categorized as: i) primary resistance, where some of the tumor-inherent features in pose resistance to therapy, for example *KRAS* mutation confers resistance to anti-EGFR therapies, ii) adaptive resistance in which bypass signaling is activated upon blockade of driver-gene induced oncogenic signaling, iii) acquired resistance occurs when cancer cells obtain additional mutations following therapy. Towards the identification of effective combination therapies to treat *Kras* mutant lung cancer, and to understand adaptive resistance mechanisms, Manchado et al employed an *in vitro* shRNA screen on *Kras* mutant NSCLC cell lines to identify genes whose downregulation sensitizes to MEK inhibition following trametinib treatment. This showed that feedback activation of RTKs, via activation of FGFR1-mediated signaling, was involved in adaptive resistance to MEK inhibition. Subsequent *in vivo* treatment using combinatorial treatment with trametinib and the FGFR1 inhibitor ponatinib in KP mice showed significantly increased tumor regression compared to single treatment (Manchado et al., 2016), implying FGFR activation is an adaptive signal mediating resistance to MEK inhibition.

Metabolic rewiring is considered as one of the hallmarks of cancer in which cancer cells continue to grow and survive in harsh environmental condition by altering their metabolism and nutrient requirements (Hanahan and Weinberg, 2011). Martins and colleagues reported that high grade, but not low grade, tumors in the KP model exhibit $Kras^{G12D}$ allelic amplification, which results in metabolic rewiring accompanied by altered glucose and glutathione metabolism. Combined inhibition of glycolysis, using the glucose analogue 2-deoxy-d-glucose (2DG), and inhibition of glutathione using buthionine sulfoximine (BSO, an inhibitor of gamma-glutamylcysteine synthetase, an enzyme required for glutathione synthesis), proved to be effective in advanced KP tumors (Kerr et al., 2016). LKB1-

deficient NSCLC cell lines and tumors in the KL model are sensitive to the anti-diabetic drug phenformin (Shackelford et al., 2013). Under normal conditions, phenformin mediates its effect by inhibiting the mitochondrial complex I, and thereby increases intracellular AMP levels, which results in LKB1-dependent phosphorylation of AMPK. Activated AMPK in turn directs defective mitochondria towards autophagy (Dykens et al., 2008; Egan et al., 2011; Hawley et al., 2010; Owen et al., 2000). Shackelford et al demonstrated that lack of AMPK activation in KL tumors confers sensitivity to phenformin due to defective mitochondria and autophagy, but not in *Kras*^{G12D} and KP tumors. In addition, long-term treatment with phenformin also provided survival benefit to KL, but not KP, mice (Shackelford et al., 2013). Interestingly, it was found that AC and SCC tumors in KL mice responded differently to combination treatment with phenformin and the mTOR inhibitor MLN0128: while this combination induced apoptosis and inhibited proliferation in KL-derived ACs (KL;ACs), squamous tumors in the same mice were resistant to combination therapy. MLN0128 treatment induced AKT activation in KL-derived SCCs, suggesting a possible resistance mechanism (Momcilovic et al., 2015). This suggests that combinatorial strategies involving AKT inhibition could be effective specifically in KL squamous tumors.

As discussed previously, transgenic mice expressing an inducible form of human mutant *HER2*^{YVMA} in mouse airway epithelium give rise to ASCs (Perera et al., 2009). Combinatorial treatment with the irreversible dual EGFR/HER2 inhibitor BIBW2992/afatinib and rapamycin caused effective tumor shrinkage, suggesting possible therapeutic combinations for *HER2* mutant NSCLC. Similarly, ASCs in the *Pten;Smad4* conditional mouse model, which showed ERBB2 and AKT activation, were found to regress following combinatorial treatment with the PI3K inhibitor GDC-094 and the ERBB2/EGFR dual kinase inhibitor lapatinib (Liu et al., 2015).

Collectively, these preclinical studies utilizing lung cancer GEMMs have addressed tumor genotype and signaling pathway activity directed therapeutic responses. In KL mice, Momcilovic et al identified AC histotype-selective sensitivity to combination of phenformin and mTOR inhibitor (Momcilovic et al., 2015). However, in the KL model, histotype-specific drug sensitivity and resistance mechanisms including drugs targeting PI3K/mTOR, MAPK, or SRC pathways have not been investigated. Moreover, it is unknown if the previously described PI3K/mTOR and SRC pathway signatures in the KL model are selective to a particular histotype, or whether histotype-selective signaling differences confer differential drug sensitivities. Furthermore, spatial ITH in oncogenic signaling and its importance in predicting therapeutic responses have thus far not been addressed.

1.13. Preclinical studies using *in vitro* models

Despite the fact that two-dimensional (2D) monolayer cell cultures fail to represent the complexities of the *in situ* tumors, cancer cell lines have been extensively used in preclinical studies to identify new targets and gene signatures predicting drug response (Greshock et al., 2010; Sos et al., 2009). Compared to complex *in vivo* models, 2D models are advantageous due to the fact that they are amenable to i) high-throughput functional assays, including drug sensitivity screening, ii) relatively straightforward investigation of mechanisms of drug resistance, and iii) easier genetic manipulation compared with *in vivo* models.

Pharmacological targeting of mutant KRAS remains challenging. Alternatively, inhibition of the RAS effector pathways including MAPK pathway has been considered in clinical settings. However, targeting MEK a downstream effector of the KRAS has proven to be ineffective, due to adaptive activation of several other pathways including PI3K/AKT (Blumenschein et al., 2015; Cox et al., 2014; Janne et al., 2013) . Furthermore, MEK inhibition relieves the negative feedback regulation of upstream RTKs leading to survival and proliferation of cancer cells (Turke et al., 2012). Towards identification of adaptive resistance to MEK inhibition in *KRAS* mutant lung cancer cells, Kitai et al demonstrated epithelial or mesenchymal cell-specific adaptive activation of RTKs leads to resistance to MEK inhibition. While epithelial-like cell lines showed activation of ERBB3 as a feedback mechanism, mesenchymal-like cell lines showed FGFR1 activation as a resistance mechanism upon trametinib treatment. Furthermore, combination treatment with the pan-ERBB inhibitor afatinib and MEK inhibitor trametinib was found to be effective only in epithelial-like cell lines and corresponding xenograft models, whereas mesenchymal-like cell lines and xenograft tumors were sensitive to combinatorial blockade of MEK together with FGFR inhibitor NVP-BGJ398 (Kitai et al., 2016). Similarly, Sun et al identified synergistic effects of the MEK inhibitor AZD6244 and the pan-ERBB inhibitor afatinib in *KRAS* mutant NSCLC and colon cancer cell lines. Mechanistically, they showed that AZD6244 treatment relieves MYC-mediated transcriptional repression of ERBB2 and ERBB3, leading to their increased expression, and resistance to MEK inhibition (Sun et al., 2014). Collectively these studies imply that feedback activation of ERBB and FGFR1 RTKs is one of the mechanisms of resistance to MEK inhibition in KRAS mutant lung cancer cells (Figure 8).

While establishment of conventional 2D cell cultures derived from patient lung tumors have been reported, the success rate was low at 2.6% (Sugaya et al., 2002). Primary cultures have also been derived from murine NSCLCs, although in this case mice were always crossed with the $p53^{fl/fl}$ GEMM to derive KP or KPL tumor-derived cell lines (Koyama et al., 2016; Liu et al., 2013; Meylan et al., 2009; Pfirschke et al., 2016). However, promising recent advancements in cell culture technology have

improved the ability to establish primary epithelial cell cultures from a variety of normal and tumor tissues. This method was originally developed by Schlegel and colleagues, known as the conditional reprogramming (CR) protocol (Liu et al., 2012b). This methodology involves the culturing of primary cells together with irradiated 3T3 feeder cells, in the presence of media containing the Rho-associated protein kinase inhibitor or ROCK inhibitor Y-27632. This protocol has been suggested to achieve cell immortalization by: i) induction of telomerase expression by factors secreted by the feeder cells, and ii) ROCK inhibitor-mediated deregulation of cytoskeleton and Rb/p16 pathway (Liu et al., 2012b). Various studies have identified novel therapies, even applied to clinical translation, using the CR technology (Beglyarova et al., 2016; Crystal et al., 2014; Liu et al., 2017; Liu et al., 2012b; Saeed et al., 2017; Yuan et al., 2012). Crystal et al established conditionally reprogrammed cells (CRCs) from biopsies of lung cancer patients treated with EGFR or ALK TKIs, following acquired resistance to therapy. By combining genetic analysis with pharmacological screens on patient-derived CRCs, they were able to identify effective combinations against resistant tumors and validated their findings in PDX *in vivo* models (Crystal et al., 2014). For example, they showed that an *ALK*-positive resistant tumor with MAP2K1 activating mutation was sensitive to combination treatment with ALK and MEK inhibitors. Similarly, combinatorial treatment with EGFR and FGFR inhibitors was effective in *EGFR* mutant resistant CRCs that had acquired a novel FGFR3 mutation. This suggests that CRCs may offer a unique tool for use in precision medicine, to identify lesion-specific therapeutic sensitivities. However, it remains unaddressed in how far the *in vitro* drug responses observed in CRCs are predictive of response of native tumors. In addition, lung cancer GEMM tumor-derived CRC cultures have not been established thus far.

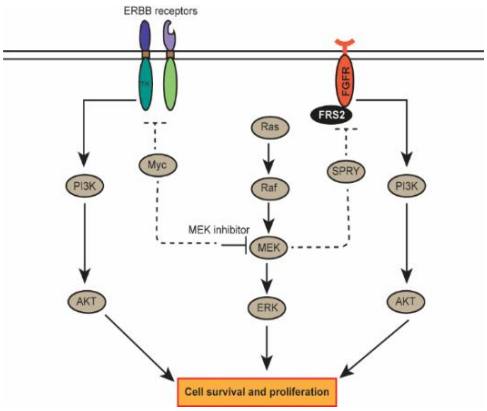

Figure 8. Feedback RTK activation following MEK inhibition. In *KRAS* mutant NSCLC cell lines, MEK inhibitor treatment relieves negative regulation of ERBB and FGFR receptors by Myc and Sprouty (SPRY), respectively. This in turn leads to activation of PI3K/AKT signaling and adaptive resistance to MAPK inhibition. Modified from (Sun et al., 2014).

Taken together, cancer genome analyses have revolutionized our understanding of lung cancer at the genetic level, and this information has been integrated in the development of targeted therapies against a set of driver genes. So far, targeted therapies, particularly tyrosine kinase inhibitors against EGFR or ALK1, are however mainly been directed towards AC histotype tumors, in which these genetic alterations are predominantly detected. Despite gained understanding of the genetic landscape of SCC and ASC histotype tumors, effective therapies to treat these subtypes are still underway. Moreover, resistance to targeted therapies occur eventually leading to poor clinical outcomes. Therefore, better understanding of intrinsic and adaptive resistance mechanisms as well as the investigation of predictive markers beyond genetic drivers is necessary to design effective single or combination therapies. The evolution of cancer from pre-malignant lesions to heterogeneous tumors is a multistep process, and various factors, including the nature of cancer-initiating oncogenic events and the tumor cell of origin, determine the fate of end-stage tumors (Blanpain, 2013). Furthermore, the complex interplay between malignant cells, stromal and immune cells can also influence therapy response (Junttila and de Sauvage, 2013). Hence, understanding of tumor immunity, particularly tumor immune suppression, is necessary for guiding optimal immunotherapy. Therefore, in addition to understanding of the heterogeneity at genetic level, improved understanding of the phenotypic and functional heterogeneity may help in designing lung cancer subtype-specific effective therapies. Despite the development and utilization of various *ex vivo* models for testing drug responses, their ability to maintain molecular and functional features of the native tumor remains poorly characterized. This highlights the importance of careful characterization of *ex vivo* models in order to reliably predict drug responses of the native tumors.

2. AIMS OF THE STUDY

Genetic alterations in cancer cells of origin lay the foundation for initiation and establishment of tumors. In addition, intrinsic and extrinsic factors related to the tumor cell of origin influence the heterogeneity of the established tumors. Hence, it is important to investigate the niche-specific tumor progenitors of different cancer subtypes. Using mouse models driven by oncogenic *Kras*^{G12D} alone, or in combination with loss of the tumor suppressor p53, it has been established that multiple cells of origin, namely CC10^{+} and SPC^{+} cells, serve as progenitors of lung ACs. However, the relative roles of different lung progenitors in establishing other NSCLC histotype tumors has remained obscure. Given that a mouse model harboring conditional expression of *Kras*^{G12D} together with loss of the tumor suppressor *Lkb1* (KL) produces all four subtypes of NSCLC, it serves as an excellent model to study the etiology of NSCLC histotypes. Furthermore, as all of the histotypes in this model are derived from common genetic drivers, the model allows the investigation of histotype-specific functions of lung cancer.

Tumor heterogeneity plays an important role in drug sensitivity and resistance; therefore, understanding the cellular and molecular basis of tumor heterogeneity is fundamental in disease control. However, the investigation of tumor heterogeneity, including intratumor spatial heterogeneity, is challenging in surgically-resected clinical samples or small biopsies. GEMMs that mimic the genetic and biological aspects of patient tumors offer an excellent opportunities to expand our knowledge on tumor heterogeneity, and to investigate effective drugs or drug combinations. Furthermore, the balance between pro-tumorigenic and anti-tumor tumor immune functions influence on disease outcome, as well as the response to immunotherapies. The objectives of this thesis were to unravel how the cell of origin influences histotype spectra and immune function heterogeneity. In addition, this thesis work also set out to investigate intertumoral and intratumoral spatial heterogeneities and associated drug sensitivities. These aims were addressed using the KL and KP lung cancer GEMMs, representing a range of NSCLC histotypes, as well as *ex vivo* tumor slices and primary cell cultures derived from KL and KP tumors.

Specific aims of this thesis were:

I. To investigate the role of the cell of origin in determining NSCLC histopathology and associated immune function heterogeneity upon activation of *Kras*^{G12D} together with loss of the tumor suppressor *Lkb1*.

II. To set up a methodology for the establishment and analysis of precision-cut murine NSCLC slice cultures as a prerequisite for drug testing

III. To investigate oncogenic signaling heterogeneity in *Kras*-driven murine NSCLC, and test signaling heterogeneity-related functional drug responses, using tumor tissue slice cultures.

IV. To identify histotype-specific drug sensitivities using murine NSCLC cell cultures, and investigate the effectiveness of primary cultures to predict acute *in vivo* drug response.

3. MATERIALS AND METHODS

3.1. Materials used in this thesis work

3.1.1. Mouse strains

Mouse Strain	Description	Reference	Study
Kras$^{LSL\text{-}G12D/+}$	Mice carrying conditional allele of mutant *Kras*	(Jackson et al., 2001)	I, II, III, & IV
Lkb1$^{fl/fl}$	Mice carrying conditional allele for *Lkb1*	(Bardeesy et al., 2002)	I, II, III, & IV
p53$^{fl/fl}$	Mice carrying conditional allele for *p53*	(Marino et al., 2000)	I, III, & IV
Rosa26$^{mT/mG}$	Membrane-targeted tandem dimer Tomato/membrane-targeted tandem dimer	(Muzumder et al., 2007)	I, III, & IV
Pten$^{LoxP/LoxP}$	Mice carrying conditional allele for Pten loss-of-function	(Marino et al., 2002)	III
PSA-Cre	Mice carrying Cre recombinase under the control of PSA promoter	Ma et al., 2005)	III

3.1.2. Primary antibodies

Antibody	Description	Reference	Study
GFP	Rabbit polyclonal	Verschuren Laboratory	I
SPC	Rabbit polyclonal	Millipore, Ab3786	I
CC10	Rabbit polyclonal	Millipore, AB-07632	I
NKX 2-1 (TTF1)	Rabbit monoclonal	Abcam, ab133638	I, II, III, & IV
p63	Rabbit polyclonal	Abcam, ab124762	I, III, & IV
Ki67	Rabbit monoclonal	Thermo Fischer scientific, RM-9106-S0	I, III, & IV
LKB1	Rabbit monoclonal	Cell Signaling Technology, 13031	I, & IV
SOX2	Goat polyclonal	Santa Cruz Biotechnology, sc-17320	I
Cytokeratin 5	Rabbit monoclonal	Abcam ab52635	I
HMGA2	Rabbit polyclonal	Biocheck, BC-59210AP	I
Gr-1 (Ly6G)	Rat monoclonal	E-Bioscience, 145931	I
CD11b	Rabbit monoclonal	BioSB, BSB6441	I
CD3	Rabbit polyclonal	Abcam ab5690	I
CD45	Rabbit monoclonal	Cell Signaling Technology, 13917	I
CD8	Mouse monoclonal	Dako, M7103	I
CD4	Rabbit monoclonal	Abcam, 133616	I
CD33	Mouse monoclonal	LSbio, C338084	I
HLA-DR	Mouse monoclonal	Abcam, 20181	I
p44/22 (Erk1/2)	Rabbit monoclonal	Cell Signaling Technology, 4370	II, III, & IV
p4EBP1	Rabbit monoclonal	Cell Signaling Technology, 2855	II, III, & IV
pAMPK	Rabbit monoclonal	Cell Signaling Technology, 2535	III
pSRC(Y416)	Rabbit polyclonal	Cell Signaling Technology, 2101	III
E-cadherin	Rabbit monoclonal	Cell Signaling Technology, 3195	I, III, & IV
Vimentin	Rabbit monoclonal	Abcam, ab92547	IV
γ-H2AX	Rabbit monoclonal	Millipore,MABE205	III
CIdU	Rat monoclonal	Biorad, OBT0030	IV
pEGFR (Tyr 1068)	Rabbit polyclonal	Cell Signaling Technology, 2234S	IV
pERBB2 (Tyr1211/1222)	Rabbit monoclonal	Cell Signaling Technology, 2243	IV
pERBB3 (Tyr1289)	Rabbit monoclonal	Cell Signaling Technology, 4791	IV
Cleaved Caspase-3	Rabbit monoclonal	Cell Signaling Technology, Y9664	IV
CD45-PE	Rat monoclonal	E-Biosciences, 12-0451-82	I
CD3-APC	Mouse monoclonal	Biolegend, 100236	I
CD4-PerCP	Mouse monoclonal	BD Biosciences, 553052	I
CD8-FITC	Rat monoclonal	E-Biosciences, 11-0083-81	I
CD11b-FITC	Rat monoclonal	Biolegend, 101206	I
Ly-6c-PerCP	Mouse monoclonal	Biolegend,128027	I
Gr1-APC	Rat monoclonal	Biolegend, 108412	I

3.1.3. Quantitative PCR (q-PCR) probes and primers

Q-PCR probe	Nucleotide sequence	Source	Study
Mouse *l1b* fwd	5'TGCCACCTTTTGACAGTGATGAGA3'	Verschuren laboratory	I
Mouse *l1b* rev	5'CCTGGAAGGTCCACGGGAA3'	Verschuren laboratory	I
Mouse *Arg1* fwd	5'TCGTGTACATTGGCTTGCGA3'	Verschuren laboratory	I
Mouse *Arg1* rev	5'GCCAATCCCCAGCTTGTCTA3'	Verschuren laboratory	I
Mouse *H2-D1* fwd	5'CTGAAGAACGGGAACGCGAC3'	Verschuren laboratory	I
Mouse *H2-D1* rev	5'TGTAAGAGTCAGTGGACGGAGG3'	Verschuren laboratory	I
Mouse *H2-M2* fwd	5'GTGCCTTGGATGGAACAGAT3'	Verschuren laboratory	I
Mouse *H2-M2* rev	5'CCAGTCATCCTTTGGATGG3'	Verschuren laboratory	I
Mouse *Rpl19* fwd	5'CGGGAATCCAAGAAGATTA3'	Verschuren laboratory	I
Mouse *Rpl19* rev	5'CGGGAATCCAAGAAGATTGA3'	Verschuren laboratory	I

3.1.4. Human NSCLC samples (I, III, and IV)

Tissue microarrays (TMAs) were prepared from human NSCLC tissue blocks, and consisted of ASCs (n=13), ACs (n=25), and SCCs (n=28) operated during 2000-2015 at the Hospital District of Helsinki and Uusimaa (HUS), Finland under an approval of the ethics committees of Joint Authority for the HUS, Finland.

3.1.5. Growth factors and supplements

Name	Description	Source	Study
Insulin	Recombinant human expressed in yeast	Sigma, I2643	IV
EGF	Recombinant human expressed in E.coli	BD Biosciences, 354052	IV
Hydrocortisone		Sigma, H4001	IV
Adenine		Sigma: A2786	IV
Cholera toxin		List Biological laboratory, 100B	IV
ROCK inhibitor		ENZO, ALX-270-333	IV

3.1.6. Selected small molecule inhibitors used in study II, III and IV. List of all the compounds used in study IV can be found from supplementary Table S1 (IV)

Name	Mechanism/Target	Approval status	Source	Study
Selumetinib AZD6244	MEK inhibitor	Investigational (Phase 3)	Selleckchem, S1008	II, III, & IV
Dactolisib NVP-BEZ235	PI3K/mTOR inhibitor	Investigational (Phase 2)	Selleckchem S1009	II, III, & IV
Saracatinib AZD-0530	Src, Bcr-Abl inhibitor	Investigational (Phase 3)	LC Laboratories S-8906.	III
Trametinib GSK1120212	MEK1/2 inhibitor	Approved	ChemieTek CT-GSK112	IV
Afatinib BIBW2292	EGFR and ERBB2 inhibitor	Approved	Selleckchem, S11011	IV
Ponatinib AP24534	Broad TK inhibitor	Approved	Selleckchem, S1490	IV

3.2. Methods

3.2.1. Mouse cohort and adenovirus infections (I, II, III, and IV)

All mice experiments conducted in this thesis followed the guidelines from the Finnish National Board of Animal Experimentation and were approved by the Experimental Animal committee of the University of Helsinki and the State Provincial Office of Southern Finland (permit number ESAVI/9752/04.10.07/2015). Cohorts of *Kras*$^{LSL\text{-}G12D/+}$;*Lkb1*$^{fl/fl}$ (KL) were generated by breeding *Kras*$^{LSL\text{-}G12D/+}$ mice (C57Bl/6J background) with *Lkb1*$^{fl/fl}$ mice on a mixed genetic background (F4 ICR;BALB/cByJ;FVB/N). KL mice were also bred with Rosa26mT/mG reporter mice resulting in cohorts with mixed genetic background (C57Bl/6J, F4 ICR;BALB/cByJ;FVB/N, 29X1/SvJ;ICR). *Kras*$^{LSL\text{-}G12D/+}$ mice were also crossed with *Trp53*$^{fl/fl}$ mice to generate *Kras*$^{LSL\text{-}G12D/+}$; *Trp53*$^{fl/fl}$ mice. Eight to ten weeks old KL or KP mice were intranasally or intratracheally treated with 1-20 x10^7 pfu of Ad5-CC10-Cre or 2.5-7.5 x10^9 pfu of Ad5-SPC-Cre viruses under isofluorane anaesthesia (Viral Vector Core Facility, University of Iowa, USA). Animal experiments performed using *Pten* mice were approved by the animal experimentation committee of the Erasmus Medical Center (DEC-consult, permit number 106-05-11). Cohorts of *PSA-Cre;Pten-loxP/loxP* (*Pten*) mice, were generated by crossing *PSA-Cre* mice (strain FVB) with mice carrying *Pten-loxP* allele (strain 129Ola).

3.2.2. Tissue preparation immunohistochemistry and quantification (I, III, & IV)

Tumor bearing lungs from moribund mice were fixed in 4% formaldehyde overnight at 4°C followed by processing into paraffin blocks. Formalin-fixed paraffin-embedded (FFPE) lungs were sectioned into 4-5µm thickness and then processed for H&E staining or IHC analysis. IHC on murine paraffin sections were performed as follows: rehydrated sections were subjected to antigen retrieval method (either citrate buffer, pH 6.0 or tris-EDTA, pH 9.0) to expose antigenic epitopes. To block non-specific binding of primary antibody, sections were blocked with 1% BSA and 10% normal goat serum (NGS) in 1x PBS. Primary antibodies were stained for 1-1.5 h at ambient temperature or overnight at 4°C. Secondary antibodies, BrightVision poly-HRP Goat anti-rabbit (IL ImmunoLogic, AD Duiven, the Netherlands) or Peroxidase Goat anti-rat IgG (H+L) (Invitrogen Corporation, Camarillo, CA) were incubated for 30 min at ambient temperature. Immunodetection was done using DAB (Bright DAB, IL ImmunoLogic, Duiven, The Netherlands). IHC stained sections were scanned using Panoramic 250 3DHISTECH (3DHISTECH Kft., Budapest, Hungary) digital slide scanner using a 20x objective. Quantitation for H&E or IHC stained whole slide scans were performed using the Tissue StudioTM image analysis of the Definiens Developer XD 64 2.1-4.2 software (Definiens, Munich, Germany).

3.2.3. Immunohistochemistry quantification using CellProfiler (II)

Whole slide scans of the IHC-stained samples were acquired using Pannoramic 250 3DHISTECH scanner, and TIFF images were acquired using Pannoramic Viewer 3DHISTECH. Using Fiji-ImageJ, the images were converted into 16-bit images, and uploaded to CellProfiler™ (http://cellprofiler.org) 2.0.0 for analysis. The following pipeline was used for quantification: Identify Primary Objects -> Measuring Object Intensity -> Filter Objects (minimal value=0.0025) -> Calculate Math. The results were represented as percentages of DAB-stained nuclei of the total number of nuclei.

3.2.4. Immunofluorescence and quantification of human NSCLC TMA (I)

For fluorescent triple multiplex staining on human NSCLC TMA, tissue sections were rehydrated followed by antigen retrieval using 10mM Tris/1mM EDTA pH 9.0 buffer in a PT heating module (Thermo Scientific). Endogenous peroxidase activity was blocked using 0.9% H_2O_2 in TBS, followed by blocking with TBS containing 0.05% Tween-20 and 10% normal goat serum. Sections were incubated with primary antibodies for 1-2 h at ambient temperatures. The 488 fluorescent signal was developed first by applying HRP (1:10 diluted) conjugated secondary (Bright Vision, Immunologic, Duiven, the Netherlands) followed by enhancement of signal using the TSA-Alexa Fluor-488 substrate (Life Technologies). After this, slides were immersed in TBS containing 0.9% H2O2 and 15mM NaN3 to block remaining peroxidase reactivity. The second primary antibody was probed for 1 h at ambient temperature and 555 fluorescent signal was obtained by adding HRP conjugated secondary antibody for 30 min and the signal was enhanced by using the TSA-555 substrate (Life Technologies). Previously bound antibodies were denatured by immersing the slides in 10mM Tris/1mM EDTA pH 9.0 in a PT module at 99°C for 20 min. Finally, the third primary antibody was incubated for 2 h at ambient temperature and secondary Alexa fluor-647 conjugated goat anti-mouse or -rabbit antibodies (Life Technologies) were used and sections were counterstained with DAPI (Roche, Mannheim, Germany.

Fluorescent multiplex stained TMA slides were scanned using Axio Imager.Z2 (Zeiss, Germany) with the Metafer 4 slide scanning system (MetaSystems GmbH, Germany), and quantifications were performed using Tissue Studio™ IF image analysis solution of the Definiens Developer XD 64 2.1 software (Definiens, Munich, Germany).

3.2.5. Microarray gene expression and quantitative PCR analysis (I)

Lung tumors were snap frozen and RNA was extracted using NucleoSpin RNA II kit (MACHEREY-NAGEL, Duren, Germany). Gene expression profiling was done with Illumina Mouse WT-6 version 2 expression arrays (Illumina, San Diego, CA, USA). For the quantitative real-time PCR (qPCR) analysis, cDNA was extracted from high-capacity cDNA reverse transcription kit (Life technologies, Waltham, USA), and qPCR reactions were run and analyzed on a CFX384 Touch™ Real-Time PCR Detection System (Bio-Rad, Hercules, USA).

3.2.6. Flow cytometry analysis (I)

Lung tumors were incubated with HBSS/2mg/ml collagenase 1A (Sigma Aldrich, USA) and 0,3 mg/ml dispase (Life Technologies, Thermo Fisher Scientific, USA) for 30 min at 37°C, resulting tissue homogenate was digested using gentle MACS Dissociator (Miltenyi Biotec, Germany) in DMEM/20mM Hepes and 5U/ml DNAse (Promega, USA). Thus obtained single cell suspensions were incubated with antibodies in HBSS/2%BSA buffer for 30 min at 4°C. Propidium Iodide (Sigma Aldrich, USA) was used to stain dead cells and the analysis was performed using BD Accuri flow cytometer, data analysis was done using BD Accuri C6 software (Becton, Dickinson and Company, USA).

3.2.7. Preparation and culturing of murine and human tissue slices (II, & III)

Mouse and human tumor tissue slices were prepared using vibrating blade microtome (Leica VT1200S), to ensure better quality slices vibrocheck was performed prior to slicing. Tumor-containing lung tissue was attached to the magnetic specimen holder of a Leica VT1200S, using cyanoacrylate adhesive. Lung tumor tissues were either sliced as 160 µm, or 200 µm, or 250 µm thick using speed at 0.12 mm/s and 2.5-2.7 amplitude settings. Sliced tissues were collected into 24-well plates with cold HBSS, and then placed in an inclined position on top of titanium grids inserted into culture medium in 6-well plates, which were then placed in rotating incubation units. Importantly, slices were collected in the order of slicing, and neighboring slices were compared for experimental purposes. Tumor slices were cultivated at 37°C and 5% CO2, in a humidified incubator under normoxic condition (21%). Uncultured (0 h) slices as well as those cultivated for different time points were snap frozen (*Pten* tumor slices) for western blot analysis, or fixed in 4% formaldehyde overnight at +4°C, for paraffin embedding followed by H&E and IHC analysis.

3.2.8. Drug treatments on murine NSCLC tissue slices (II, & III)

Precision-cut (200 µm) murine and human NSCLC tissue slices were placed on rotating incubation units, and were drug treated in the following medium: F-12 medium (Thermo Fisher, Waltham, MA, USA) supplemented with 2mM glutamax (Gibco), 100 U/mL penicillin, 100 µg/mL streptomycin (Gibco), and 22 mM glucose (Sigma-Aldrich, St. Louis, MO, USA). At the end of treatment period, slices were fixed in 4% formaldehyde overnight at +4°C and processed for FFPE sections, which were processed for H&E and IHC analysis.

3.3.9. Quantification of necrosis and overlapping signaling areas in tissue slices (II, & III)

Necrotic areas in the H&E stained tissue slices were analyzed by a pathologist followed by drawing of the masks on necrotic tumor regions using Adobe Photoshop CS6, as described (Davies et al., 2015). The following formula was used to calculate relative decrease in viability of the drug treated slices: (1 – viability in drug-treated/viability in DMSO control) * 100%. Analysis of phosphoprotein overlapping areas was done by drawing masks on the single stained regions in Photoshop CS6, and these masks were overlapped, and the overlapping regions were recolored using the magic wand tool in Photoshop CS6. Thus, the obtained overlapping regions were measured normalized to the total tumor area using the Photoshop histogram tool**.**

3.2.10. Tissue dissociation and epithelial cell isolation (IV)

Tumors were separated from the surrounding normal lung tissue, minced into small pieces and then subjected to enzymatic digestion in HBSS buffer containing 1% bovine serum albumin (BSA), 2 mg/ml collagenase (Sigma), and 0.3 mg/ml dispase (ThermoFisher Scientific; 17105-041) at 37ºC for 30 min with continuous rotation. Digested tissue was subjected to mechanical dissociation using gentleMACS^{TM} dissociator, and filtered through a 70 µm cell strainer. The resulting single cell suspensions were used for epithelial cell isolation using EpCAM MicroBeads (MACS Miltenyi biotec; 130-105-958).

3.2.11. Cell culture (IV)

Tumor-derived epithelial cells were either cultured on plastic with RPMI containing 10% FBS, 10mM glutamine, and penstrep, or as conditionally reprogrammed cells (CRC) as described before (Liu et al., 2012b). In brief, tumor cells were plated on 3T3 cells (feeder cells) irradiated with 11 gray in F-medium

1:3 v/v DMEM: F-12 nutrient HAM) supplemented with, 5% FBS, and reagents listed in growth factors and supplements table. 3T3 cells were maintained in DMEM supplemented with 10%FBS/10mM glutamine/penstrep. CRC cultures were passaged by differential trypsinization, first to remove the feeder cells, followed by trypsinization of the epithelial cells.

3.2.12. Colony formation assays (IV)

Murine NSCLC CRCs or normal lung (NL) CRCs at passage 7 were plated in a 6-well plates as 500 cells per well, either in CRC media or with F-media without Y-27632. To evaluate long-term effect of drugs, compounds or vehicle were added 48 h following cell seeding. At day 11 for regular assays, or day 13 for drug treated cells, colonies were fixed using a mixture of acetic acid and methanol (1:7 vol/vol) and stained with 0.5% crystal violet in methanol. For regular assays, colonies were counted manually, and the colony formation rate was calculated as the percentage of cells forming colonies per 500 cells. For drug treatment studies, analysis was done as percentage of area covered by colonies using the 'ColonyArea' Image J plugin (Guzman et al., 2014), and normalized to DMSO controls.

3.2.13. Immunofluorescence analysis (IV)

Cells cultures as CRCs were plated on top of glass coverslips, and fixed with 4% paraformaldehyde (PFA) for 15 min at ambient temperature. Fixed cells were blocked with PBS containing 3 % BSA, 0.1M Glycine, and 0.1% TritonX-100, followed by incubation with primary antibodies for 1 h. Alexa goat anti-rabbit secondary antibody (Thermo Fisher Scientific; A21244) was incubated for 30 min. at ambient temperature, followed by nuclear staining with Hoechst (1 ug/ml, Thermo Fisher Scientific). Images were acquired using a Nikon Eclipse 90i fluorescence microscope; quantifications were done using CellProfiler software.

FFPE sections (4 µm) of murine lungs treated with vehicle and CIdU or trametinib and CIdU were rehydrated, and permeabilized with 0.2% TritonX-100 in PBS. Sections were subjected to antigen retrieval using 10mM citric acid buffer (pH6) in a PT heating module (ThermoFisher Scientific) for 20 min at 99°C. To expose antigenic epitopes, DNA was denaturated using 1.5N hydrochloric acid for 40 min. at ambient temperature, followed by blocking with PBS containing 1% BSA, 10% NGS. Primary rat anti-CIdU (Biorad; OBT0030) antibody was incubated overnight at +4°C, and then with secondary anti-rat Alexa 488 (Invitrogen; A11006), and Hoechst (0,5 mg/ml). Whole slide scans of the stained samples were obtained using a Pannoramic 250 3DHISTECH digital slide scanner. Quantification of CIdU positive nuclei was done using CellProfiler software.

3.2.14. CRC 3-dimensional cultures (IV)

Tumor or NL CRCs at passage 6 or 7 were plated on top of matrigel (Corning) in chambered cover glass (Lab-Tek) at a concentration of $2.5x10^4$ cells per well in F-media (100 µl) without Y-67632. On the second day, a layer of collagen (of 2 mg/ml, Corning) was added on top of the spheroids, and allowed to solidify at 37°C for 1 h. 100 µl of F-media without Y-27632 was added on top of the solidified collagen. On the fourth day after seeding the cells, matrigel-collagen sandwich cultures were fixed with 4% PFA, processed using the Cytoblock kit (Thermo Fisher Scientific), paraffin embedded, and sectioned at 4 µm for further IHC processing.

3.2.15. Immunoblotting (I, & IV)

Snap frozen tissue references or CRC pellets were lysed using RIPA buffer, protein concentrations from the resulting protein lysate were measured using BCA kit (G Biosciences; 786-570). Western blotting was done using 20 µg of protein lysate. Membranes were blocked with Odyssey® Blocking Buffer (927-40000), and probed with primary antibody for 1 h at ambient temperature or overnight at +4°C followed by incubation with odyssey IRDye secondary antibodies. Membranes were scanned using an odyssey infrared imager.

3.2.16. Drug Sensitivity and Resistance Testing (DSRT) (IV)

Murine NSCLC tumor-derived or normal lung CRCs were subjected to DSRT according to previously published procedure (Yadav et al., 2014). For DSRT analysis a library of 299 compounds listed in Table S1 (III) was used. Drugs were dispensed using an Echo 550 Liquid Handler (Labcyte) into clear bottom 384-well plate (Corning #3712), at five different concentrations. Cells (1500 per well) were seeded into pre-plated DSRT plates using a MultiDrop Combi dispenser (Thermo Fisher Scientific), in F-media (25 ul) with or without Y-27632. Cell viability was measured using CellTiter-Glo® reagent (25 µl) (Promega) at 72 h post plating the cells using a PheraStar plate reader (BMG Labtech).

3.2.17. DSRT data analysis and interpretation (IV)

Quality assessment of DSRT screen data was done using the Z'-factors value, calculated as the raw luminescence values of drug-treated wells normalized against positive and negative controls (Yadav et al. 2015). Data from screens that passed the data quality test were used to determine the percentage inhibition of viability per drug concentration, plotted as dose-response curves by applying the

Marquardt-Levenberg algorithm implemented in an in-house developed bioinformatic pipeline 'Breeze'. Multiple parameters of each dose-response curve, including the IC50, slope, top, and lower asymptotes, were used to calculate the Drug Sensitivity Score (DSS), as described (Yadav et al, 2015). The average DSS values following treatment of normal lung cultures were used to normalize the DSS values for each tumor-derived culture, to calculate cancer cell-specific DSS (selective DSS). The sDSS values for each culture type were plotted using unsupervised hierarchical clustering with the Cluster 3.0 application (http://bonsai.hgc.jp/~mdehoon/software/cluster/), and using Euclidean distance measures of the CRC profile. Heat maps were plotted in Java TreeView (http://jtreeview.-sourceforge.net/).

3.2.18. *In vivo* drug treatments (IV)

KL or KP mice infected with Ad5-CC10-Cre or Ad5-SPC-Cre viruses were randomly assigned for treatment groups at 11-14 (for KL) or 13-25 (for KP) weeks post infection. For 24 h trametinib treatment, mice were intra peritonially (IP) treated with 1 mg/ kg trametinib in 0.9 % saline or with vehicle (1.6% DMSO in 0.9% saline). At 20 h post trametinib treatment, mice were administered with 2 mg chloro-deoxyuridine (CldU; Sigma C6891) via IP and 4 h later they were sacrificed by cervical dislocation. For combination treatments, mice were treated with vehicle equivalent of trametinib and afatinib, or with 1 mg/ kg trametinib alone in 0.9% saline via IP or with 12.5 mg/kg afatinib alone in 0.5% hydroxyl propyl methyl cellulose (HPMC), 0.1% Tween 80 in H_2O by oral gavage. Mice treated with both drugs received 1 mg/ kg trametinib and 12.5 mg/kg afatinib by IP or oral gavage, respectively. Treatment was done once daily for 3 days, and mice were sacrificed by cervical dislocation 24 h following the third treatment.

3.2.19. Statistical analysis (I, III, & IV)

Quantitative data are represented as +/- standard deviation or standard error of mean. Statistical significance calculated using t-tests were performed using two-tailed student's t-test. Survival analysis (study I) was done using the Gehan-Breslow-Wilcoxon Test. Fisher's exact test was used for the comparison of two categorical variables (human TMA analyses in study III and IV). One –way ANOVA was used for statistical comparison of more than two groups (study III). Spearman's correlation coefficient (study III) or Pearson correlation coefficient (study IV) was used to evaluate the correlations between two variables. For the data which did not pass D'Agostino-Pearson omnibus normality test, non-parametric, Kolmogorov–Smirnov test was used for statistical analysis (study I and IV).

4. RESULTS AND DISCUSSION

4.1. Cell of origin determines histotype spectrum and immune functions in NSCLC driven by mutant *Kras^{G12D}* and loss of *Lkb1*

Towards investigating the role of the cell of origin in establishing NSCLC subtypes, previous reports have utilized cell type-specific AdCre viruses or Cre-ER driven mouse strains to target CC10$^+$ club cells in the airways or SPC$^+$ AT2 cells in the alveoli and shown that both of these progenitor cell types can give rise to ACs (Mainardi et al., 2014; Sutherland et al., 2011; Sutherland et al., 2014; Xu et al., 2012). Furthermore, GEMM studies have also shown that airway basal cell-specific deletion of *Pten* together with *Tgfbr2* gives rise to SCC, however with low incidence (10-20%) and long latency (52 weeks) (Malkoski et al., 2014). In addition, using the SOX2;PC model, recent work by Berns and colleagues suggested that multiple progenitors can give rise to SCC, namely K14$^+$ cells in the bronchi, and SPC$^+$ and CC10$^+$ cells in the more distal lungs (Ferone et al., 2016). Using the KL model, Han et al showed that SPC$^+$ cells can initiate ACs, which they suggest to transdifferentiate into SCC via an ASC intermediate state. In the latter study, the human SPC promoter was used to drive Cre recombinase expression (Han et al., 2014). However, this promoter was reported to be active also in bronchiolar cells (Glasser et al., 1991), suggesting the possible involvement of bronchiolar cells in establishing tumors in the KL model. Moreover, the role of CC10$^+$ club cells in producing NSCLC histotypes, particularly in KL model which develop AC, SCC, and ASC histotype tumors, remained largely unknown. Hence, we decided to use KL mouse model to better understand the role of CC10$^+$ and SPC$^+$ lung progenitors in establishing histotype diversity and functional heterogeneity.

4.1.1. The cell of origin defines NSCLC histotype spectra and mouse survival upon activation of *Kras^{G12D}* and loss of *Lkb1*

Previous work using the KP model has shown that both CC10$^+$ and SPC$^+$ cells similarly influence the survival of the mice following AdCre infection (Sutherland et al., 2014). We asked if the progenitor cell of origin has an effect on survival of mice in the KL model. To do this, we intranasally infected 8-12 weeks old KL mice with adenovirus expressing Cre recombinase under control of the CC10 or SPC promoter: Ad5-CC10-Cre or Ad5-SPC-Cre. To confirm accurate targeting of the cell type-specific AdCre viruses, KL mice were crossed with the *Rosa26$^{mT/mG}$* reporter strain, to locate Cre-targeted cells based on membrane GFP (mGFP) expression. Consistent with previous results, IHC analysis of mGFP on lung sections following 2 and 4 weeks of Ad5-CC10-Cre and Ad5-SPC-Cre infection revealed mGFP positivity in bronchiolar and alveolar compartments, respectively. In addition, Ad5-CC10-Cre,

but not Ad5-SPC-Cre infection, also resulted in mGFP positivity in the BADJ (**I,** Fig. S1A). Virus titers were set at 1 x 10^7 pfu for Ad5-CC10-Cre and 2.5 x 10^9 pfu for Ad5-SPC-Cre to archive comparable infection rates. The numbers of $mGFP^+$, $CC10^+$ or SPC^+ cells were quantified on sequential lung sections. With these amounts of viruses, approximately 0.8% of the total lung cells were targeted at 3 and 4 weeks following Ad5-CC10-Cre and Ad5-SPC-cre infection, respectively (**I,** Fig. S1B). KL mice intranasally infected with Ad5-CC10-Cre or Ad5-SPC-Cre (n=9 for each group) were sacrificed when they showed disease symptoms (breathing difficulties and loss of body weight). Interestingly, KL mice infected with Ad5-CC10-Cre showed a significantly shorter latency compared with Ad5-SPC-Cre infected mice (median survival of 79 and 120 days respectively) (**I**, Fig. 1A), suggesting that $CC10^+$ cells may produce faster growing tumors. Next, we performed a detailed histopathological analyses of the lesions from full lung lobes of infected mice (n=5 per virus). The commonly used histotype-specific clinical biomarkers TTF1, also known as NKX 2-1, and p63 were analyzed to classify lesions into different histopathology subtypes of AC or ASC (**I**, Fig 1B) (Travis et al., 2011). Using LKB1 IHC, we first confirmed that all the lesions in KL mice originated following Ad5-CC10-Cre or Ad5-SPC-Cre infection lacked LKB1 expression, using tumors from KP mice as positive reference tissue (**I**, Fig. S1C).

Interestingly, quantification of lesions revealed that the incidence of ASCs was higher in Ad5-CC10-Cre infected mice (20/60 lesions from 5 mice) than in Ad5-SPC-Cre infected mice (3/171 lesion from 5 mice). On the other hand, Ad5-SPC-Cre infection resulted in invasive AC (IAC) (117/171), or papillary AC (PAC) (26/171) as the predominant histotypes. Of note, mucinous AC (MAC) and acinar AC (AAC) subtypes were detected specifically in Ad5-CC10-Cre infected mice (**I**, Fig. 1C, S1D, S1G and Table S1). Collectively, these results suggested that progenitor cells influence histotype spectra in KL mice, and that $CC10^+$ cells are the predominant origins of ASC.

Analysis of tumor proliferation using Ki67 IHC showed that lesions that originated from $CC10^+$ cells, more specifically PAC and AIS, showed higher proliferation compared to those derived from SPC^+ cells. In addition, the SCC regions of ASC tumors showed higher proliferation compared to the AC regions of ASCs (**I**, Fig. 1B and 1D) Analysis of tumor size revealed that ASCs were the largest (20-30 mm^2) of all the lesions (**I**, Fig. 1E). Consistent with published results, ASCs showed keratin 5 (KRT5) positivity and low or absence of SOX2 expression (Mukhopadhyay et al., 2014). Assessment of SOX2 positivity in human ASCs showed positivity in 8/12 samples, and more specifically in SCC components of ASCs. Furthermore, 7/12 ASCs showed LKB1 negativity, including 2/4 SOX2 negative tumors, indicating that SOX2 negative KL ASCs may represent a subset of clinical ASCs (**I**, Fig. S1E-F, and Table S1). To determine the precursors of end-stage tumors, we assessed the KL lungs at 6 and 9 weeks post AdCre infection. Ad5-CC10-Cre infection resulted in bronchiolar hyperplasias at 6 weeks,

and adenocarcinoma in situ (AIS), IAC, PAC, MAC, and ASC at 9 weeks post infection (w.p.i). Of note, 1/ 4 Ad5-CC10-Cre infected mice showed SCC lesions at 9 w.p.i. On the other hand, Ad5-SPC-Cre infection resulted mainly in AIS or PACs at 6 or 9 w.p.i, respectively (**I**, Fig. S1 I). We also confirmed the MAC histotype using Periodic acid-Schiff (PAS) staining, and showed that, similar to published results, PAS positive MAC tumors contained reduced numbers of NKX 2-1 positive cells compared to PACs **(I**, Fig. 1F-1G, and S2C-E) (Snyder et al., 2013). The expression of high mobility group AT-hook 2 (HMGA2), a transcription factor associated with poorly differentiated tumors (Sutherland et al., 2014), was found to be homogeneously expressed in ASCs, while other histotypes showed negative or mosaic staining **(I**, Fig. 2B). Together these results suggested that the shorter survival of Ad5-CC10-Cre infected KL mice was most likely due to the increased tendency of $CC10^{+}$ progenitors to form fast growing, larger and more poorly differentiated ASC tumors.

4.1.2. Mutant *Kras^{G12D}* and *Lkb1* loss-driven tumors show histotype-specific gene expression signatures

To investigate tumor histotype-associated molecular heterogeneity, we performed gene expression analysis of Ad5-CC10-Cre induced ASCs and Ad5-SPC-Cre induced PACs from KL mice. We decided to use PACs, as they were the largest and second most frequently detected lesion upon Ad5-SPC-Cre infection. In addition, other AC subtypes including MAC, AAC, and PACs (from Ad5-CC10-Cre infected mice) were detected in low frequency compared to ASCs, and hence could not be isolated in sufficient numbers. We isolated six tumors, two each from 3 mice infected with Ad5-CC10-Cre or Ad5-SPC-Cre viruses. Each tumor was processed for RNA isolation, protein lysates and histological analyses. We confirmed the ASC histotype of tumors by western blot analysis using anti-p63 antibody (**I**, Fig. S3B). Unsupervised clustering of the microarray results with cut-off adjusted p-value<0.01, LogFC>1 revealed 340 genes that were differentially expressed between ASCs and PACs (**I**, Fig. 2A).

We further assessed commonalities in histotype-specific gene signatures between our data and published datasets. Since there are no human ASC gene expression data available, we used human SCC vs AC comparative data and *Lkb1;Pten* loss (LP) mouse model-derived SCC vs *Kras*-AC comparative data (Kuner et al., 2009; Xu et al., 2014). Venn diagram representation of comparative gene expression analysis revealed 40 genes (29 upregulated 11 downregulated) to be commonly altered in a histotype-specific manner (**I**. Fig. 2B). Among 29 upregulated genes were SCC markers, *Trp63*, and a set of cytokeratins including *Krt5*. As expected, one of the downregulated genes included one of the AC marker napsin A (*Napsa*) (**I**, Fig. 2C). Given that ASCs showed SCC-specific gene signatures, we next assessed the similarities between the KL ASC vs PAC comparison and murine basal cell expression

(Rock et al., 2009). This analysis revealed 75 or 33 genes to be commonly up- or downregulated, respectively, in these two data sets (**I**, Fig. S3C and Table S2). Upregulated genes were related to basal cell differentiation, namely *Trp63*, basonuclin 1 (*Bnc1*), stratifin (*Sfn*), snail family zinc finger 2 (*Snai2*), and cytokeratins. In addition, pro-inflammatory cytokine interleukin 1b (*Il1b*) and its type II interleukin 1 receptor (*Illr2*) were found to be commonly upregulated in ASCs and basal cells (**I,** Table S2). Finally, we compared KL ASC vs PAC data with published data from Ad5-CMV-Cre-induced KL AC vs ASCs transcriptional analyses (Ji et al., 2007). This comparison resulted in 23 commonly deregulated genes, including SCC-specific *Trp63* and cytokeratins (**I**, Fig. S3C and Table S2).

4.1.3. Murine NSCLC show histotype-specific immune gene signature

It has been reported that Ad5-CMV-Cre induced tumors from KL mice harbor immunosuppressive microenvironment characterized by the presence of TANs and production of pro-inflammatory cytokines that suppress CTL recruitment (Koyama et al., 2016). Since our gene expression analysis showed histotype-dependent gene expression signatures, we asked if there exist histotype-specific immune gene signatures in the KL model. Ingenuity Pathway Analysis (IPA) of KL;ASC vs KL;PAC gene expression with a cut-off log FC>2 identified granulocyte adhesion and diapedesis (upregulated in ASCs: *Cxcl15, Itga2, Ccl6, Ccl7, Cldn18*), and antigen presentation (downregulated in ASCs: *Cd74, Ciita, H2-D1, H2-DMa, H2-DMb1*) as altered canonical pathways (**I**, Fig. 3A). It has been reported that in the $Kras^{G12V/+}$ model, adenovirus-induced inflammation can contribute to inflammatory infiltrates and promotes tumorigenesis (Mainardi et al., 2014). To confirm that the observed histotype-specific immune gene signature was not due to AdCre-induced inflammation, we performed gene expression analysis of selected immune genes in KL;ASCs, and PACs together with KP;ACs derived from Ad5-CC10-Cre or Ad5-SPC-Cre infection. Our results showed that indeed certain immune genes were expressed in a histotype- but not genotype-dependent manner (**I**, Fig. 3B), and excluded the possible effect of AdCre on immune gene signatures. Histotype-specific immune genes included ASC-specific upregulation of pro-inflammatory genes related to neutrophil recruitment, namely cytokine *Il1b*, *S100a8* and *S100a9*, and *Arg1*, an enzyme mediating T-cell suppression (Munder et al., 2006; Ryckman et al., 2003). Additionally, antigen presentation genes including the expression of class I major histocompatibility complex (MHC) genes (*H2-M2*, and *H2-D1*), class II MHC genes (*H2-DMa*, *H2-Ab1*, *H2-DMb1*) and class II MHC associated gene *Cd74* were downregulated in ASCs, and also the lymphocyte and monocyte chemoattractant genes *Ccl17* and *Ccl6* were downregulated in ASCs compared to ACs (**I**, Fig. 3B). Furthermore ASC histotype-specific downregulation of class I MHC genes and up regulation of *Arg1* was confirmed by quantitative real-time PCR (qPCR) (**I**, Fig. 3C). Expression of *Il1b*, one of the neutrophil chemoattractants was not statistically significant between ASCs and KP;ACs (**I**, Fig. 3C). This could possibly relate to tumor grade, as Gr-1^{+} neutrophils have

been reported to be higher in high grade KP;ACs (Faget et al., 2017). These results indicate that KL tumors show histotype-specific immune gene signatures suggestive of immunosuppression in ASCs compared to ACs

4.1.4. ASC histotype-specific recruitment of Gr-1+ CD11b+ TANs

The finding that ASCs showed gene expression signatures favorable for neutrophil recruitment prompted us to investigate the abundance of TANs in KL;ASC and KL;PACs. For this purpose, we performed quantitative IHC-based analysis for neutrophil markers, Gr-1 and Cd11b, on full lung lesions from KL Ad5-CC10-Cre or Ad5-SPC-Cre infected mice (n=5 for both groups). The results showed a clear enrichment of Gr-1^+ and $CD11b^+$ cells in ASCs compared to PACs. Furthermore, increased TAN recruitment in ASCs was accompanied with a reduced number of $CD3^+$ T cells, suggesting pro-tumorigenic effect of TANs in ASCs (**I**, Fig. 4A-B, and S3E). Additionally, we confirmed Gr-1 and Cd11b double positive cells (TANs) by flow cytometry, and the results confirmed ASC-specific recruitment of TANs. Conversely, flow cytometry analysis also showed an ASC-specific reduction in $CD3^+$ T cells (**I**, Fig. 4C-D). Consistent with varying expression of *Il1b*, IHC analysis on KP;ACs showed variability in the percentage of Gr-1^+ and $CD11b^+$ cells (**I**, Fig. S4A-B), supporting the finding that that tumor grade in KP;ACs influences TAN infiltration.

To investigate the translational relevance of our findings, we next analyzed a set of human NSCLC tumors, in a TMA comprised of ASC (N=12), PAC (N=25), and SCC (N=28) tumors, for TAN infiltration. Quantification of fluorescent multiplex staining for human TANs, $CD11b^+CD33^+HLA\text{-}Dr^-$, did not show statistically significant difference among histotypes (**I,** Fig 4F-G and S4C-D**)**. However, we observed a trend towards SCC subregion-specific infiltration of TANs in ASC tumors (**I,** Fig 4H and S4E). Consistent with the murine findings, the status of LKB1 in human NSCLC tumors did not correlate with TAN infiltration (**I,** Fig S4F-G). Taken together, these results showed an KL;ASC-specific immunosuppressive microenvironment, accompanied by increased TAN recruitment and a concomitant reduction in $CD3^+$ T cells.

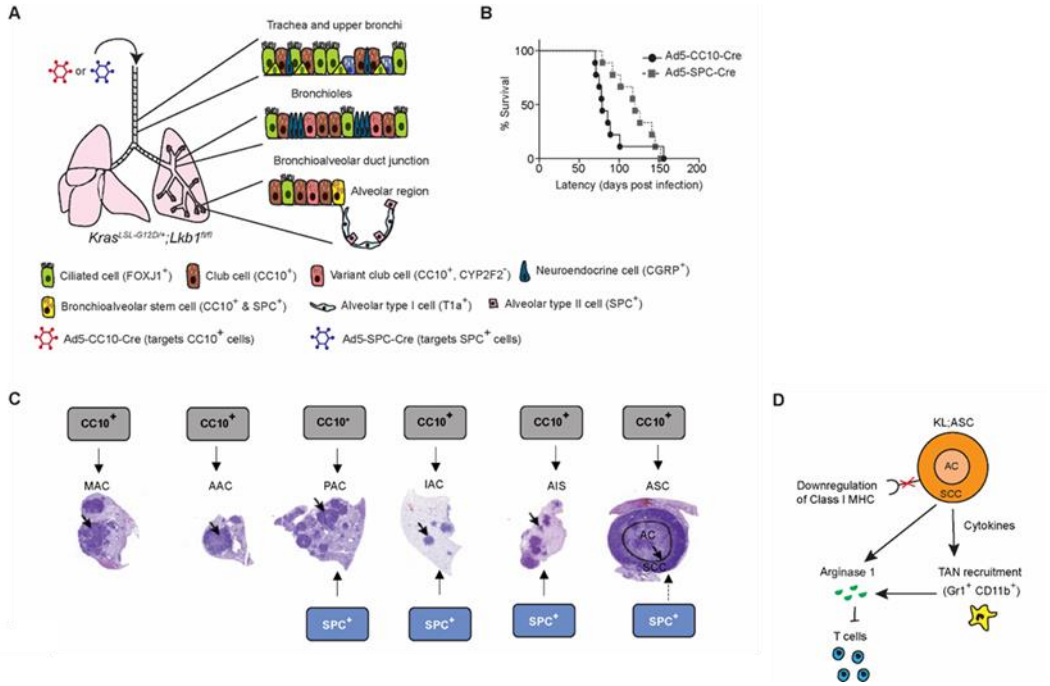

Figure 9. Schematic illustration summarizing of the role of cell of origin in determining survival of mice, histotype spectrum and histotype-specific immune microenvironment in the KL GEMM. (A) Different cell types in the distinct compartments of the adult mouse lungs. Intranasal or intratracheal administration of Ad5-CC10-Cre or Ad5-SPC-Cre viruses into KL lungs restricts genetic recombination to either $CC10^+$ or SPC^+ cells, respectively. (B) Ad5-CC10-Cre infected KL mice show a shorter survival compared to Ad5-SPC-Cre infected mice. (C) $CC10^+$ cells are the predominant progenitors of ASC, MAC, and AAC tumors, while both $CC10^+$ and SPC^+ cells can produce PAC, IAC, and AIS lesions (D) KL;ASCs show immunosuppressive features, consisting of reduced antigen presentation molecules, increased TAN infiltration and reduced intratumoral T cells.

4.2. A protocol for the generation, cultivation and analysis of precision-cut murine NSCLC tissue slices

In an IMI-funded consortium project PREDECT (http://www.predect.eu), we described an optimized workflow for the establishment, and analysis of precision-cut tumor slices derived from lung, breast, and prostate cancer models (Davies et al., 2015). We showed that, compared to filter-supports where sliced are cultivated on air-liquid interphase, rotating incubation units improved viability of short-term NSCLC slice cultures by intermittent exposure of tumor slices to oxygen and nutrients (Davies et al., 2015). However, slice cultivation on rotating incubation units is technically challenging and requires constant monitoring. We therefore developed a protocol for the generation of precision-cut murine NSCLC tissue slices using the Leica VT1200 S vibratome machine, which includes a practical video demonstration showing how to handle the rotating incubation unit followed by H&E staining and quantitative IHC analysis of cultured slices (II, Fig. 1). We also showed that thickness influences the viability of short-term (24 h) slice cultures. H&E analysis of 160 µm, 200 µm, and 250 µm thick tumor slice cultures showed that 160 µm thin slices harbor necrotic regions across the slices, likely because they are too fragile and tend to damage during slice handling. Slices of 250 µm thickness showed necrotic gradients across the slice when compared to 200 µm thin slices (II, Fig. 2A). The poor viability of thicker 250 µm slices is possibly related to insufficient oxygen and nutrient diffusion across the slices compared with thinner 200 µm slices. Due to differences in tissue stiffness, hypoxia or matrix composition, each tissue type is therefore likely to require slice thickness optimization. In addition, we demonstrated how to execute quantitative IHC analysis for well-differentiated lung AC marker, NKX2-1. This showed that, compared to 0 h slices, NKX2-1 expression was not altered in samples cultured up to 72 h, suggesting that the AC differentiation status is not affected during short-term slice cultivation (II, Fig. 2B-C). Given our findings that Kras mutant murine ACs exhibit high pERK1/2 compared to ASCs, with p4EBP1 is similarly expressed in both ACs and ASCs (III, Fig. 2A-B), we targeted these pathways to demonstrate how to select optimal drug concentrations prior to slice treatment studies. To evaluate a dose-dependent effect on targeted pathway inhibition, KL;AC slices were treated with DMSO or titrated amounts of compounds, namely 0.1 µM -1 µM dactolisib (to inhibit p4EBP1) or 0.05 µM - 0.5 µM selumetinib (to inhibit pERK1/2). The results showed that 1 µM dactolisib or 0.5 µM of selumetinib was effective in inhibiting 4EBP1 or ERK1/2 phosphorylation, respectively. In addition, as a technical bonus, such selective regulation of phosphoprotein expression indicates that tumor slices can be used to validate phosphorylation-specific antibodies. Together, this protocol demonstrated the critical steps in obtaining maximum viability of the tumor slice cultures, and analytical considerations prior to their application for pharmacological drug testing.

4.3. *Kras*^{G12D}-driven murine NSCLC show histotype-specific spatial heterogeneity in oncogenic signaling

Despite advancements in cancer therapy, successful treatments are compromised by intra- and intertumoral heterogeneity (Xue et al., 2017). Research during the past few decades have established multiple levels of tumor heterogeneity, namely genetic, phenotypic, functional, and microenvironmental heterogeneity (de Bruin et al., 2015; Turner and Reis-Filho, 2012; Xue et al., 2017). For solid cancers, an important question remains how the spatiality of oncogenic signaling activities determine functional response to therapies. Since our previous work using the KL GEMM showed a histotype-dependent immune phenotype, we next asked if the histotypes also determine oncogenic signaling. We analyzed a set of KL and KP tumors initiated by Ad5-CC10-Cre or Ad5-SPC-Cre viruses for oncogenic signaling downstream of KRAS or LKB1 (**III**, Fig. S1A). We demonstrated that certain oncogenic signaling pathways are expressed in a histotype-specific manner, with phosphorylation of AKT (pAKT; indicating PI3K pathway activity) selectively detected in ASCs and phosphorylation of ERK (pERK; indicating MAPK pathway activity) predominantly detected in ACs. Furthermore, we found that oncogenic phosphoproteins, namely pAKT, and pSRC were predominantly detected in the SCC subregions of ASCs, suggesting intratumoral spatial heterogeneity in oncogenic signaling (**III**, Fig. 2A-B). Interestingly, consistent with our murine finding, human NSCLC analysis revealed that ASC (5/13), and SCC (8/28) showed predominant pAKT expression compared to AC (1/25) (ASC comparison to AC, Fisher's test p-0.012, SCC comparison to AC, Fisher's test p-0.026), whereas pERK was more commonly detected in ACs (20/25) compared to ASC (9/13), or SCC (13/28) tumors (AC comparison to SCC, Fisher's test p-0.02). Examination of the LKB1 or TP53 status in human NSCLCs by IHC revealed that the majority of the tumors contained nuclear TP53, suggesting alteration in the TP53 pathway, while LKB1 expression varied in all the pathologies **(III**, Fig. S1B, and Table S1). In summary, these results indicated that oncogenic signaling tends to stratify according to tumor histotype and exhibits intratumoral spatial heterogeneity in murine and human NSCLC.

4.3.1. Establishment and characterization of *Kras*^{G12D}-driven murine NSCLC tissue slices to study drug responses

The fact that we identified marked intra- and intertumoral heterogeneity in PI3K/mTOR and MAPK pathway activities led us to investigate how this affects sensitivity to targeted therapies. Precision-cut tumor tissue slices are an attractive preclinical model for functional drug testing, due to the presence

of intact tumor-stroma interactions, and, more importantly, spatial aspects of drug response can be better modelled in tumor tissue slices. As a part of the PREDECT consortium project (www.predect.eu) we established KL and KP tumor tissue slices, optimized the culture conditions and assessed viability, proliferation, DNA damage, and phosphoprotein levels in uncultured (0 h) and in slices cultured up to 72 h (**III**, Fig. S2A). Slices were cultured on rotator incubation units to ensure uniform exposure to oxygen and nutrients. Assessment of the viability by H&E in cultured slices showed that viability was better maintained in the top section of the tissue (**III**, Fig. S2B and S2C). Hence, in the following experiments, all quantitative analyses were done on the top section of the tumor slices (**III**, Fig. S2A). We interrogated the slicing and culture-induced changes on cellular proliferation, DNA damage, and phosphoprotein expression. Proliferation of 0 h uncultured slices were similar to native tumors with respect to Ki67 IHC; hence we compared the proliferation in cultured samples to that of 0 h samples (**III**, Fig. S3B). While cultured AC slices showed a decrease in Ki67 positivity, ASCs showed region-specific changes: SCC regions showed a decrease in proliferation already at 24 h, and AC regions of ASCs showed an increase in proliferation after 48 h (**III**, Fig. S3C). Cultured slices accumulated more DNA damage compared to 0 h slices, as demonstrated by γH2AX positivity (**III**, Fig. S3A). Analyses of oncogenic phosphoproteins showed no significant change in 0 h slices compared to *in situ* tumors. However, ASC-specific induction of pAKT was observed in ASC slices cultivated for 24 h. While pERK1/2 showed alterations in both directions, p4EBP1 and pSRC showed a significant induction in slices of both ASC and ACs (**III**, Fig. S5A). Furthermore, *PTEN* loss-driven murine prostate cancer slices also showed similar changes in pERK1/2 upon cultivation (**III**, Fig. S7A). In addition, altered p4EBP1 and pERK1/2 expression was also seen in freshly resected human NSCLC and prostate tumors (**III**, Fig. S5B and S7B). Taken together, these results suggested that murine NSCLC tissue slices are vulnerable for culture-induced changes in proliferation and oncogenic signaling, while freshly cut (0 h) uncultured slices preserving proliferation and oncogenic functions of *in situ* tumors. Therefore, drug treatments on tumor slices must be conducted at the onset of culturing.

4.3.2. Cytotoxic response to combinatorial inhibition of the PI3K/mTOR and MAPK pathways is determined by co-expression of targeted phosphoproteins

Next, we set out to investigate how histotype-specific spatial heterogeneity in oncogenic signaling influences on sensitivity to small molecule inhibitors, namely the dual PI3K/mTOR inhibitor NVP-BEZ235 or dactolisib (dact), the MEK inhibitors AZD6244 or selumetinib (sel), and the SRC inhibitor saracatinib (sar) (**III**, Fig. 3A). Assessment of viability in neighboring DMSO and drug-treated slices (24 h) did not show significant cytotoxic responses in any of the single compound treated samples (**III**,

Fig. 3B-C). Interestingly, of the tested double combinations, only dact+sel showed considerable cytotoxic, but not cytostatic, response (**III**, Fig. 3C-D, and S10A). Since SRC activity is enriched in the SCC compartment of ASCs, we reasoned that addition of sar to the dact+sel may show SCC-specific increased sensitivity. However, our results showed that the effect of dact+sel and dact+sel+sar was very similar, and that inhibition of SRC did not increase cytotoxic effect in any of the groups tested (**III**, Fig. S10B). These results suggest that KL- and KP- derived NSCLC slices show sensitivity to combined inhibition of PI3K/mTOR and MAPK pathways. We reasoned that sensitivity to combination of dact+sel could possibly relate to prevalence of targeted pathways in the treated tissue slices. To test this, we determined baseline signaling activities, p4EBP1 and pERK1/2 (% area) in the 0 h uncultured slices, and correlated this with relative decreases in viability following 24 h dact+sel treatment. There was a significant correlation between p4EPB1 and pERK1/2 positivity in 0 h slices with cytotoxic response ($p<0.001$ for p4EBP1, and $p<0.05$ for pERK1/2) in neighboring treated slices (**III**, Fig. 4A and Table S2). Furthermore, deeper investigation of responding vs non-responding slices revealed the concomitant expression of p4EBP1 and pERK was required to elicit significant cytotoxic response (>20 decrease in viability), while expression of either of these phosphoproteins alone failed to induce cytotoxicity in treated slices (**III**, Fig 4C).

To convincingly show that co-expression of p4EBP1 and pERK1/2 guides sensitivity to dact+sel, we correlated the percentages of overlapping p4EBP1 and pERK1/2 expression areas in 0 h slices with viability decreases in dact+sel-treated samples. As expected, there was a positive correlation between the % overlapping area and viability (**III**, Fig 5A-B). Furthermore, the AC regions of ASC tumors showed increased sensitivity to dact+sel compared to SCC regions (**III**, Fig. S10C), suggesting a SCC-specific intrinsic resistance mechanism. Taken together, these results showed that in *Kras*-driven murine NSCLC slices, cytotoxic response to combined inhibition of the PI3K/mTOR and MAPK pathways depended on the co-activation of the targeted signaling pathways. In addition, the preservation of spatial aspects of oncogenic signaling may make tumor slices a valuable model for preclinical studies.

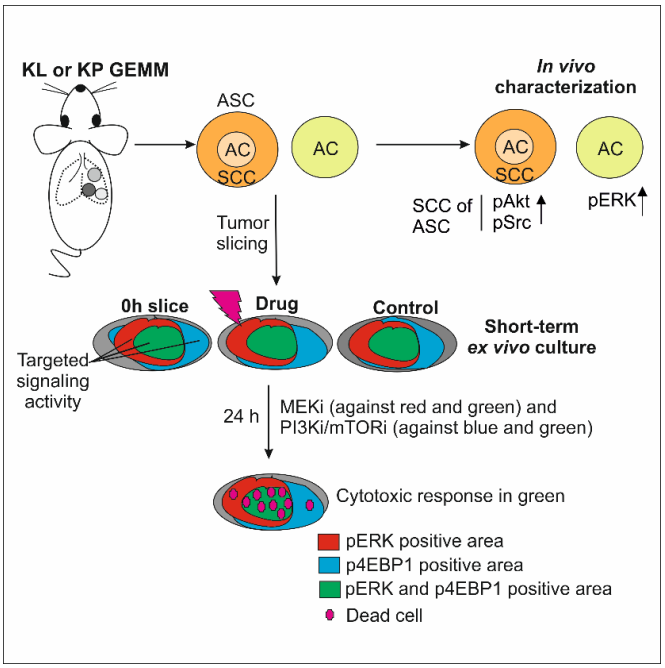

Figure 10. ***Kras*-mutant murine NSCLCs show histotype-specific oncogenic signaling, and co-expression of the targeted phosphoproteins determine sensitivity to combined drug treatment**. Spatially distributed signaling activities correlate with sensitivity to drug combinations in Kras mutant NSCLC tissue slice cultures. Oncogenic phosphoproteins pAKT and pSRC are predominant in the SCC region of ASCs, while pERK is predominant in ACs. Short-term treatment of ASC or AC tissue slice cultures with a combination of PI3K/mTOR and MEK inhibitors leads to cytotoxic response in the regions showing concomitant activation of both p4EBP1 (indicative of PI3K/mTOR pathway) and pERK (indicative of MAPK pathway). Modified from graphical abstract prepared by Katja Närhi.

4.4. Histotype-specific oncogenic signaling defines sensitivity to combinatorial MEK inhibition in *Kras^{G12D}*-driven NSCLC

Since our previous work using KL and KP GEMMs identified that tumor histotype determines immune microenvironmental heterogeneity and oncogenic signaling, we asked how *in vivo* pathology-specific functional heterogeneity informs on histotype-selective drug vulnerabilities. We hereto set out to establish KL- and KP tumor-derived cell cultures, to investigate the ability of *in vitro* cultures to model drug response of *in vivo* tumors.

4.4.1. A conditional reprogramming (CR) protocol is necessary for the establishment of KL cell cultures

To investigate NSCLC subtype-specific drug sensitivities, we first set out to establish murine NSCLC cell cultures. Epithelial cells from Ad5-CC10-Cre-induced KL;ASC (N=4), Ad5-SPC-Cre-induced KL;AC (N=3), or Ad5-CC10-Cre- or Ad5-SPC-Cre-induced KP;AC (N=4) tumors were cultured on plastic using RPMI medium, or on top of irradiated 3T3 feeder cells using F-medium supplemented with Rho kinase inhibitor (Y-27632). The latter cultures are referred to as conditionally reprogrammed cells (CRCs). Using IHC, we confirmed the histotype of the source tumors from which the cell cultures were established, by performing NKX2-1 (AC & ASC marker) and p63 (ASC marker) staining, and confirmed the lack of LKB1 expression in KL source tumors (**IV**, Fig. S1A). While KP cultures were readily established in RPMI as well as in the CR condition, establishment of KL tumor cell cultures (both ASC and AC histotypes), required the CR protocol (**IV**, Fig. 1A and S1B), indicating that tumor genotype (KL vs KP) is the major determinant influencing whether the CR protocol is required for culture establishment.

Using immunoblot analysis, we confirmed that KL- and KP-CRCs lacked LKB1 or p53, respectively, and retained features of epithelial cells (**IV**, Fig. 1B, and 1C). Interestingly, all KP-CRCs showed both vimentin and E-Cadherin positivity, while KL-CRCs were E-cadherin positive. Of note, one of the KL;ASC-CRCs, established without EpCAM purification, showed positivity for LKB1 and the stromal marker vimentin, suggesting epithelial purification is required to establish pure epithelial cultures (**IV**, Fig. 1B-1C and S1C-S1D). Next, we assessed the growth rates of the established CRCs at passage 6. In line with differential growth rates observed *in vivo*, KL;ASCs grew faster than KL;ACs (**IV**, Fig. S1E). We examined if cultures also showed a differential clonogenic potential in the presence of absence of Y-27632. This showed that KL cultures were dependent on the presence of Y-27632 for

colony formation, and exhibited a variable yet higher clonogenic potential than KL;AC cultures (**IV**, Fig. 1D and 1E). On the contrary, inclusion of Y-27632 negatively affected the clonogenic ability of KP;AC cultures (**IV**, Fig. 1D and 1E). These results suggested that murine NSCLC CRCs represent the genotype and growth characteristics of *in vivo* tumors.

To assess the representativity of CRCs to that of source tumors, we analyzed histotype-specific marker expression in CRC 2D and three dimensional (3D) cultures. Comparison of NKX2-1 and p63 expression in 2D or 3D cultures to that of the source tumors showed that p63 expression was variable yet sustained in 2D and 3D cultures of ASCs, but was absent in ACs. On the other hand, NKX2-1 expression was reduced in 2D and 3D cultures of ASCs, while it was completely lost in ACs. (**III**, Fig. S1F-H). These results suggested that AC-CRCs undergo de-differentiation by losing NKX2-1 expression, while ASC-CRCs maintain their differentiated state.

4.4.2. Identification of NSCLC subtype-specific drug vulnerabilities using drug sensitivity and resistance testing (DSRT)

To validate the robustness of the CRCs in identifying pathology- or genotype-specific drug responses, we first tested the effect of idasanutlin, an activator of p53 and inhibitor of mdm2-p53 interaction, in KL and KP cultures. Drug Sensitivity Scores (DSSs) were used to measure the drug response (Pemovska et al, 2013). As expected, KL cultures showed increased sensitivity to idasanutlin compared to KP;ACs (**IV,** Fig. S2A). Next, we performed DSRT on murine NSCLC CRCs representing KL;ASCs (N=2), KL;ACs (N=2), and KP;ACs (N=2), and on NL cultures (N=3). For each drug, tumor cell-specific sensitivities were identified by subtracting the DSS of individual tumor-derived CRCs from average DSS scores of NL;CRCs (n=3), determining selective drug sensitivity scores (sDSS) (Pemovska et al., 2013; Yadav et al., 2014). Sensitivity or resistance to a particular drug was identified as those with sDSS greater than 5 or lesser than 5, respectively (**IV,** Fig. 2A). Analysis of the DSRT data revealed that ASC cells were sensitive to 19 compounds, while ACs from both genotypes showed sensitivity to fewer drugs (**IV,** Fig. S2D). The second screening phase (phase II) included the 61 compounds for which at least one of the CRCs showed a sDSS $\geq$5 and $\leq$-5 in the initial screen (**IV,** Fig. 2A). Unsupervised hierarchical clustering of the sDSS from the phase II screen revealed four distinct compound groups (**IV,** Fig. 2B). Consistent with higher proliferative capacity, KL;ASC cultures showed increase sensitivity to antimitotic and chemotherapeutic agents. In addition, also compounds targeting proliferation, topoisomerase, BET inhibitors and HDAC inhibitors were found to be specifically effective in KL;ASC cultures (**IV,** Fig. 2B). In line with published findings, KL cultures

showed higher sensitivity to HSP90 inhibitors compared to KP cells (**IV,** Fig. 2C) (Skoulidis et al., 2015). These results tentatively suggested that murine NSCLC CRCs showed both histotype and genotype-selective drug sensitivities.

4.4.3. AC histotype-selective sensitivity to MEK inhibition

Comprehensive drug screening on GEMM tumor-derived CRCs across different genotypes and histotypes revealed that compared to other subtypes, KL;AC cultures were more sensitive to the MEK inhibitors (**IV**, Fig. 2C and S2D). To further validate this finding, eight different doses (0.5-500 nM) of MEK inhibitor trametinib were tested in all the cultures. Consistent with the previous results, KL;ACs showed increased sensitivity to trametinib among the culture subtypes tested (**IV**, Fig. 3A). To investigate signaling changes following MEK inhibition, we assessed pERK1/2 and pAKT expression in cells treated with 50 nM trametinib for 4-72 h, or with a titrated amount of trametinib (5 to 50 nM) for 48h (dose-dependent). ERK phosphorylation was successfully inhibited with 50 nM trametinib already at 4 h post treatment, and this was accompanied by increased AKT phosphorylation in all the cultures, suggesting adaptive responses to MAPK inhibition (**IV**, Fig. 3B-C and S3A-B). Consistent with our *in vivo* IHC analysis (**II**, Fig. 2A-B), western blot analysis of the source tumor tissues showed pERK to be predominant in ACs, while pAKT was higher in ASCs **(IV**, Fig. S3E). These results partially explained KL;AC-selective sensitivity to MEK inhibition.

Next, we assessed if the *in vitro* subtype-specific sensitivity to MEK inhibition was also recapitulated in *in situ* tumors. Short-term treatment (24 h) of KL and KP tumor-bearing mice with trametinib showed that ACs of both culture genotypes exhibited sensitivity to trametinib as evidenced by decreases in the percentage of proliferating cells (chloro-deoxyuridine; CIdU or Ki67 positive nuclei). Consistent with the *in vitro* results, KL;ASC tumors (both their SCC and AC subregions) were insensitive to trametinib (**IV**, Fig. 3D-H), and this could be explained by the observation that ASCs showed lower ERK activity compared to ACs (**IV**, Fig. S3C-D). Together, these result showed that, despite the presence of *Kras* mutation in all culture subtypes, murine NSCLCs showed AC-specific cytostatic effects to short-term MEK inhibition, likely due to the pronounced ERK activation in ACs compared to ASCs.

4.4.4. Inhibition of MEK together with RTKs identifies NSCLC subtype-specific drug combinations

The finding that KL;ASCs were non-responsive to trametinib, and all the culture subtypes showed adaptive activation of the PI3K/mTOR pathway following MAPK inhibition, prompted us to explore subtype-specific effective drug combinations. Several studies using *KRAS* mutant NSCLC cell lines have shown adaptive activation of various RTKs, including ERBBs, and FGFR following MAPK inhibition (Anderson et al., 2017; Kim et al., 2016; Kitai et al., 2016; Manchado et al., 2016; Massarelli et al., 2007). These adaptive pathways promote pro-survival signaling via induction of pAKT. To investigate which RTKs were involved in adaptive activation PI3K/AKT signaling, we treated cultures with pan-ERBB, FGFR, IGF1R, Axl or Met inhibitors, either alone or in combination with trametinib. This approach revealed a KL-specific (both ASC and AC cultures) sensitivity to combination treatment with MEK and pan-ERBB inhibitor (trametinib + afatinib) (**IV**, Fig. 4A-B). On the other hand, all the cultures were insensitive to MEK and FGFR inhibitor (trametinib + ponatinib) combination (**IV**. Fig. S4A-B). Together, these results indicate NSCLC subtype-specific sensitivity to combinatorial MEK and RTK inhibition, with selective sensitivity of KL cultures to combinatorial inhibition of MEK and ERBB pathways.

Combination treatment of trametinib together with ponatinib was previously shown to cause tumor regression in the KP lung cancer model (Manchado et al., 2016). Hence, the finding that none of the culture subtypes showed response to trametinib + ponatinib combination treatment, prompted us to investigate the long-term response to this combination. In addition, we asked if the culture subtype-specific response to MEK and ERBB inhibition showed durable response. Therefore, we selected the trametinib + afatinib and trametinib + ponatinib combinations to perform clonogenicity assays for NSCLC culture subtypes, and treated with single compound trametinib (5 nM), afatinib (250 nM), or ponatinib (250 nM) or their combinations. Consistent with previous results, the trametinib + afatinib combination significantly reduced the colony forming ability of KL;ASC and KL;AC, but not KP;AC cultures. Interestingly, the ponatinib combination, which was ineffective in short-term assays (**IV**, Fig. 4A and S4A-B), showed a significant reduction in colony formation exclusively in AC cultures (**IV**, Fig. 4C-D). Together, these results suggested the role of ERBBs and FGFR in KL genotype-selective and AC-histotype selective adaptive resistance mechanisms upon MEK inhibition, respectively.

To determine if KL-specific sensitivity to afatinib combination treatment was explained by activation of ERBB family receptors, we assessed pEGFR, pERBB2, and pERBB3 expression by immunoblotting, before and after trametinib treatment. In KL;ASCs, ERBB3 phosphorylation was found to be present in untreated cells, as well as following trametinib treatment. Furthermore, phosphorylation of EGFR, was found to be induced in KL cultures following trametinib treatment. In contrast, KL;AC cultures lacked pERBB3, but pERBB2 was induced following trametinib treatment. Interestingly, KP;AC cultures lacked pERBB3 expression, and baseline phosphorylation of EGFR and ERBB2 was lost upon trametinib treatment (**IV**, Fig. 4E-F and S4C-D). In line with the AC-specific sensitivity to combination MEK and FGFR inhibition, pFRS2, one of the adaptor proteins of activated FGFR1, was found to be expressed specifically in ACs, either at baseline or following trametinib treatment in KP;ACs and KL;ACs respectively (**IV**, Fig. 4E-F and S4C-D). Finally, to assess if the combinatorial inhibition of the MEK and ERBB pathways also affected cell survival, we analyzed expression of cleaved caspase-3 (CC3), a marker of apoptosis, in samples treated with trametinib (50 nM), afatinib (1000 nM), or trametinib + afatinib for 48 h. Combination treatment with trametinib + afatinib induced cell death specifically in KL cultures (**IV**, Fig. 4G). These results suggested that combinatorial inhibition of MEK together with subtype-specific RTKs effectively blocked the survival and proliferation of NSCLC cultures. Collectively, these results indicated NSCLC subtype-specific RTK activation, with intrinsic or adaptive ERBB activation being KL-selective, and AC-selective adaptive FGFR activation following MEK inhibition determining sensitivity to combinatorial MEK inhibition.

4.4.5. Histotype-specific differences in ERBB receptor activation in murine and human NSCLC

To assess if *in vitro* sensitivity to combinatorial inhibition of the MEK and ERBB pathways was explained by the activation of ERBB receptors in *in situ* tumors, we profiled *in vivo* KL;ASC (N=4 mice), KL;AC (N=3-6 mice), and KP;AC (N=7-8 mice) tumors for pEGFR, pERBB2, and pERBB3 expression. Interestingly, quantitative IHC analysis showed that activation of all three ERBB receptors was predominant in the SCC subregions of ASC tumors compared to AC tumors **(IV**, Fig. 5A-B). To determine if the pathology-specific activation of ERBB receptors was also found in clinical samples, we performed IHC for pERBBs on human NSCLC TMAs comprised of ASCs (N=13), ACs (N=25), and SCCs (N=28). In line with the murine findings, pERBB3 in human samples was predominant in ASC (4/13) and SCC (7/28) histotype lesions compared to ACs (0/25) (Fisher's test p=0.009 for ASC vs AC, p=0.02 for SCC vs AC.) In addition, activation of EGFR was significantly higher in SCCs compared to ACs, Fisher's test p=0.03 SCC vs AC (**IV**, Fig. 5C-D). Replicate cores taken from

different subregions of the same tumor showed varying positivity for activation of all tested ERBB receptors, indicating that spatial heterogeneity is also detected in human tumors (**IV,** Fig. 5D). These results suggested that NSCLCs show histotype-specific spatial heterogeneity in activation of ERBB receptors. More specifically, the SCC subregions of murine ASCs showed predominance of ERBB receptor activation compared to AC tumors.

4.4.6. Spatially-defined ERBB receptor activation determines acute cytotoxic response to combinatorial inhibition of the MAPK and ERBB pathways

Given that ERBB activation *in vivo* was prevalent in SCC subregion of ASCs, we reasoned that SCCs may show increased response to inhibition of ERBB signaling. To investigate the NSCLC subtype-specific acute response to combinatorial MEK + ERBB inhibition in *in vivo* settings, we treated KL or KP mice with TR, or AF as single agents or in combination, once daily for three days. Quantitative IHC comparisons of proliferation (Ki67), or cell death (CC3) was performed between four groups (KL;SCC of ASC, KL;AC of ASC, KL;AC, or KP;AC) of vehicle, trametinib, afatinib, or trametininb + afatinib-treated KL or KP mice. As opposed to 24 h *in vivo* trametinib treatment, MEK inhibition did not show cytostatic response in all tumor subtypes (**IV**, Fig. 3E-H and 6A-B), suggesting adaptive resistance mechanisms following MEK inhibition. However, a significant decrease in Ki67 positive proliferating cells was observed upon combinatorial MAPK and ERBB pathway inhibition in all the groups (**IV**, Fig. 6A-B). In line with the Ki67 results, residual pERK1/2 expression was detected following 72 h trametinib treatment, while combination trametinib plus afatinib treatment caused significant inhibition of pERK1/2 in all subtypes (**IV**, Fig S5A-B).

Next we assessed cytotoxic responses short-term combination treatment, using CC3 IHC. Of note, the CC3 antibody was found to stain inherent necrotic areas in vehicle-treated ASC tumors, and drug-induced or inherent-necrotic regions were indistinguishable. Hence, the percentages of CC3 positivity, marking both necrotic and apoptotic regions, per tumor area were quantified in both control and treated samples. Interestingly, the SCC regions of ASCs exhibited varying but significant cytotoxic response upon trametinib treatment (**IV,** Fig. 6C-D). Importantly, combination treatment elicited stronger cytotoxic response selectively in SCC subregion of ASCs as measured by CC3 positivity (% area) **(IV**, Fig. 6C-D). Lack of a cytotoxic response to combination treatment in ACs suggested that survival pathways in these tumors are independent of ERBB signaling. In summary, these results suggest that the *in situ* ERBB activation status associates with acute cytotoxic response to combination treatment with the pan-ERBB inhibitor afatinib and the MEK inhibitor trametinib.

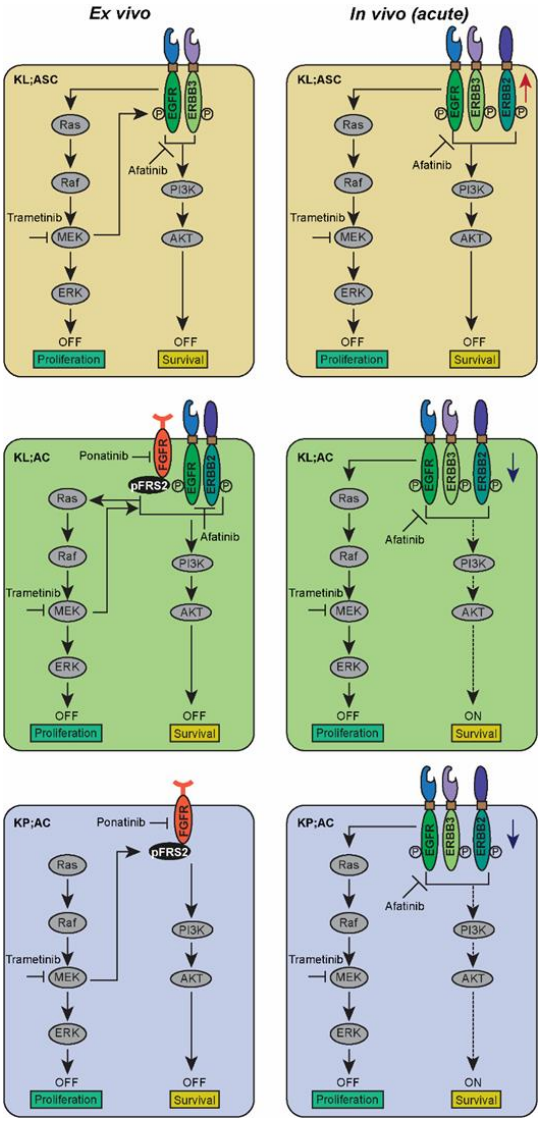

Figure 11. Subtype-specific intrinsic and adaptive signaling activities determine sensitivity to combinatorial MEK inhibition in *Kras* mutant NSCLC. MEK inhibition in *ex vivo* cultures of KL;ASC, KL;AC, or KP;AC leads to adaptive activation of the AKT in all culture subtypes. However, cultures show subtype-specific differential activation of RTKs: adaptive EGFR and intrinsic ERBB3 activation in KL;ASCs, and adaptive ERBB2, EGFR, and FGFR activation in KL;ACs, or adaptive FGFR activation in KP;ACs. Combinatorial ERBB + MAPK or FGFR1 + MAPK inhibition results in KL genotype-specific or AC histotype-specific inhibition of proliferation or survival, respectively. In contrast, short-term (72 h) combinatorial inhibition of the MAPK + ERBB pathways in KL and KP tumors results in KL;ASC-selective acute responses in terms of proliferation and survival, which is in line with the predominance of ERBB receptor activation in KL;ASC tumors compared to ACs. The dotted line represents absence or lower PI3K/AKT pathway activity in ACs compared to KL;ASC tumors. Red and blue arrows indicate predominant and lower activation of ERBB receptors in KL;ASCs and ACs, respectively.

5. CONCLUSIONS AND FUTURE PERSPECTIVES

5.1. The cell of origin defines NSCLC histotype spectra and immune microenvironment heterogeneity upon activation of *Kras^{G12D}* and loss of *Lkb1*

This thesis work demonstrates that the tumor cell of origin is crucial in determining the survival of mice, and the histotype fate of the lesions following *Kras^{G12D}* activation together with loss of *Lkb1*. Importantly, this work showed that ASCs, the most aggressive NSCLC subtype, are initiated from CC10$^+$ progenitors. The occasional ASCs produced from SPC$^+$ cells indicated possible transdifferentiation of AC-SCC via an ASC intermediate state, as reported previously (Han et al., 2014). Alternatively, rare CC10 and SPC co-expressing alveolar cells or BASCs could serve as progenitors of Ad5-SPC-Cre-derived ASCs (Rawlins et al., 2009). The finding that CC10$^+$ cells uniquely gave rise to mucinous and acinar AC subtypes could be explained by the presence of CC10$^+$ cells in different compartments of the lung, for instance a rare SPC and CC10 dual positive alveolar cells (Rawlins et al., 2009), or CC10 and mucin co-expressing bronchiolar cells (Boers et al., 1999; Rawlins et al., 2009) could serve as progenitors of Ad5-CC10-Cre-derived acinar or mucinous AC tumors, respectively. Investigation of markers specific to subsets of CC10$^+$ cells residing in anatomically distinct compartment of the lung would help in lineage-tracing the cellular origin of the diverse histotypes originated upon Ad5-CC10-Cre infection in KL mice. In addition, future studies focusing on targeting of other lung progenitors, including p63$^+$K5$^+$ cells or integrin $\alpha6^+\beta4^+$ and SPC$^-$ cells, would expand our knowledge on NSCLC subtype-specific cellular origin(s) in the KL model.

The ASCs produced from CC10$^+$ cells showed gene expression signatures similar to SCC. This finding was further supported by published reports showing the ability of club cells to form p63$^+$ cells in the lung parenchyma following influenza infection, but not bleomycin injury, and suggests a unique capacity of club cells to differentiate into basal-like cells in a context-dependent manner (Zheng et al., 2014). A study by Koyama et al suggested that immunosuppression mediated by increased TANs was specific to loss of LKB1 in the KL model (Koyama et al., 2016). Our study deepened this finding by showing that TAN infiltration and immunosuppression in KL mice is in fact ASC histotype-specific. The fast generation and bigger size of ASCs could partially be due to modulation of the immune microenvironment favorable for TAN recruitment, and reduced anti-tumor surveillance by CD3$^+$ T cells. In addition, ASCs may escape from anti-tumor immune response by downregulating antigen presentation genes, enabling faster growth of tumors. Our attempts to investigate ASC-specific expression of TANs in clinical samples did not yield convincing results due to the low number of

clinical ASCs, and possibly also because of the varied clinical history of patients with respect to co-existence of other inflammatory diseases such as COPD (Chronic obstructive pulmonary disease) and prior clinical treatments. Moreover, this study investigated myeloid cell populations in human NSCLC, and further analysis using granulocytic and monocytic MDSC-specific markers are warranted. Finally, to obtain reliable translational relevance for such TAN analyses, immune cell analysis in human NSCLC must be correlated to clinical parameters such as previous treatment history and consider the option to follow neutrophil abundance in liquid biopsies taken from the blood, so to enable the temporal tracing of immune suppressive cells. In addition, further development of strategies to specifically target TAN functions in Ad5-CC10-Cre infected KL mice, as well as in patients, is necessary to reveal if the previously observed therapeutic benefit upon TAN inhibition in KL mice is specific to ASCs (Koyama et al., 2016).

5.2. Tumor histotype but not driver genotype defines oncogenic signaling heterogeneity in *Kras^{G12D}*-driven murine NSCLC

Previous studies using murine models of lung cancer suggest that pERK activity is lower in lung SCC driven by *Lkb1;Pten* or *Sox2;Lkb1* compared to *Kras^{G12D}*-driven tumors, and this difference was attributed to absence of oncogenic *Kras*-driven MAPK pathway in SCCs (Mukhopadhyay et al., 2014; Xu et al., 2014). However, our quantitative IHC analysis of murine KL and KP tumors showed that despite being driven by oncogenic *Kras^{G12D}*, signaling downstream of *Kras* is stratified according to tumor histotype, rather than genotype. Our results demonstrated that in both murine and human NSCLCs, pAKT expression is predominant in SCC/ASC histotype lesions, while pERK is enriched in ACs. In addition, pSRC and pAKT show intratumor spatial distribution within KL;ASCs, with predominant activation in SCC subregions compared to AC. These results suggested that increased AKT and SRC activities previously observed in the KL model were mostly specific to ASC and SCC histotypes (Ji et al., 2007). Together, we demonstrated that, despite being driven by the same oncogenetic drivers, signaling activities are stratified according tumor histotypes.

5.2.1. Spatially active co-occurrence of signaling activities define cytotoxic response to combinatorial inhibition of the PI3K/mTOR and MAPK pathways in *Kras^{G12D}*-driven NSCLC tissue slices

We demonstrated that precision-cut organotypic murine NSCLC slice cultures are valuable only for short-term therapeutic studies, as the tumor slice cultures showed dynamic alterations in proliferation and signaling, particularly hyperactivation of mTORC1. By doing short-term treatment on tumor tissue slices, we showed that cytotoxic response to combined inhibition of the PI3K/mTOR and MAPK pathways was dependent on co-expression of both of the pathways being targeted. These results demonstrate the utility of tumor tissue slices in modelling spatial response to targeted therapies. Furthermore, these findings imply that spatial heterogeneity in oncogenic signaling must be taken into consideration as predictive markers in clinical settings.

Establishment of tissue slices cultures from freshly resected clinical NSCLCs is technically challenging, and in our preliminary experience, successful generation of good quality slices depends on the stiffness of the tumor tissue: harder tissues provide better quality slices, while softer tissues were not suitable for slicing. Thus, further technical refinements in slicing softer tumor tissues are needed to establish clinical tumor tissue slice cultures. Furthermore, future studies comparing the responses between tumor tissue slices established from lung cancer biopsies with that of matched patient response to the same drugs or drug combinations will reveal the applicability of this model in routine clinical settings.

5.3. Stratification of *Kras^{G12D}*-driven murine NSCLC based on *in situ* signaling activities and sensitivity to combinatorial MEK inhibition

In search of NSCLC lesion-specific drug sensitivities, we set out to establish *Kras*-driven murine NSCLC cell cultures. However, our attempts to establish conventional KL cultures was not successful, possibly due to p53-mediated growth arrest. The conditional reprograming method proved to be successful in establishing long-term KL and KP cultures with the preservation of genotype and growth properties of native tumors. DSRT analysis on murine NSCLC CRCs followed by *in vivo* validation demonstrated that KL;AC cultures and AC tumors showed increased sensitivity to the MEK inhibitor trametinib. While *in vivo* response to MEK inhibition was accurately modelled in KL;AC cultures, KP;ACs were found to be resistant to trametinib-mediated MAPK inhibition as opposed to *in situ* KP;ACs. Differential sensitivity to MEK inhibition between *in vitro* KP;AC cultures vs *in vivo* KP;AC

tumors could possibly be due to differences in end-point readout, as assessment of *in vitro* viability is based on cellular ATP levels, whereas *in vivo* effects of trametinib were measured on cell proliferation using nuclear markers. Increased sensitivity of AC tumors upon 24 h MEK inhibition could be explained by previous data showing that *Kras* copy number gain in KP tumors leads to increased dependency on the MAPK pathway (Junttila et al., 2010; Kerr et al., 2016).

A number of studies on *Kras* mutant NSCLC cell lines or *in vivo* models have reported that adaptive resistance to MEK inhibition is associated with activation of RTKs, namely ERBBs and FGFR (Kitai et al., 2016; Manchado et al., 2016; Pang and Liu, 2016; Sun et al., 2014). Our study extrapolated this finding and demonstrated that *Kras* mutant NSCLC subtype-selective intrinsic or feedback RTK activation is associated with resistance to MEK inhibition. Cell intrinsic or adaptive activation of ERBBs in KL cultures, and adaptive FGFR activation in AC cultures, is associated with resistance to MEK inhibition, and that this can be overcome by combinatorial inhibition of the MEK + ERBB pathways or MEK + FGFR1 pathways, respectively. Previously, the combined blockade of the MEK and FGFR pathways was shown to effectively induce tumor regression in the KP model (Manchado et al., 2016). However, the effect of the same combination in the KL model was not explored. Our results showed that, in addition to KP;ACs, KL-derived ACs were also responsive to this combination, indicating an AC histotype-specific sensitivity to combinatorial inhibition of the MAPK and FGFR pathways. These results highlight the utility of CRCs for the identification of NSCLC subtype-specific drug sensitivities.

It has been shown that ERBB3 has high affinity for the PI3K regulatory subunit, and is a potent activator of PI3K/AKT pathway (Hellyer et al., 1998). Our finding of absence or lower activation of ERBB3 in murine and human ACs possibly explains the lack of AKT activation in ACs, and that alternative survival pathways in tumor with low levels of ERBB3 phosphorylation may exist. Interestingly, two recent studies demonstrated the role of ERBBs in *Kras*-driven murine lung tumorigenesis, and showed an impressive anti-tumorigenic effect of long-term treatment with ERBB inhibitor alone or in combination with MEK inhibitor (Kruspig et al., 2018; Moll et al., 2018). These findings complement our finding of *in vivo* acute cytotoxic response to combinatorial MAPK and ERBB pathway inhibition, and extends this response to the SCC histopathology. Given that ASCs showed acute cytotoxic response to short-term trametinib plus afatinib combination treatment, long-term treatment with the same combination will likely show therapeutic responses in ASCs. However, long-term treatment studies are warranted to fully understand the potential of this treatment strategy in the context of *Kras*-driven mixed NSCLC histopathology models. A clinical study investigating the

combination of afatinib and MEK inhibitor selumetinib in *KRAS* mutant NSCLC is ongoing (NCT02450656), and given these findings, the outcome of this will be very interesting (Bennouna and Moreno Vera, 2016). Together, our work suggests that coupling of *in vitro* drug sensitivities with the analysis of oncogenic signaling and therapeutic responses in *in situ* tumors will aid in the selection of tumor-specific effective drug combinations

In summary, the work presented in this thesis demonstrates that while being targeted by the same genetic alterations, particularly $Kras^{G12D}$ activation and *Lkb1* loss, niche-specific lung progenitors exhibit a differential ability to establish phenotypic and immune microenvironmental heterogeneity. In addition, this work also establishes *ex vivo* models of *Kras* mutant murine NSCLCs, and demonstrates their utility in modeling spatial responses to targeted therapies, as well as in the identification of subtype-selective drug combinations. Furthermore, this work highlights that beyond understanding lung cancer at the genetic level, it is important to consider histotype-specific functions, including spatial oncogenic signaling heterogeneity, in guiding selection of effective therapies. As such, our studies start to point at an alternative way in which NSCLCs, and possibly also other tumor types, can be stratified according to etiology-related phenotypes.

ACKNOWLEDGEMENTS

This thesis work was carried out at the Institute for Molecular Medicine Finland (FIMM). I am grateful to the current and former directors of FIMM, Prof. Mark Daly, Prof. Jaakko Kaprio and Prof. Olli Kallioniemi, for providing excellent infrastructure and state-of-the-art research facilities. I thank HR and the administrative staff for supporting me all these years. I am thankful for the financial support received from the Doctoral Programme in Biomedicine (DPBM), IMI-PREDECT, Academy of Finland, K. Albin Johanssons Stiftelse Foundation, Biomedicum Helsinki Foundation, Cancer Society of Finland, Orion Research Foundation, and Maud Kuistila Foundation.

I would like to extend my deepest gratitude to my supervisor Dr. Emmy Verschuren for her generous support and encouragement throughout my PhD. Thank you, Emmy, for accepting me into your group and always leaving your door open for me no matter how busy you were. I am grateful to you for giving me the freedom to explore my ideas and making sure that I had the best possible resources to pursue my scientific questions. Your dedication, enthusiasm and positive attitude towards your work has always been an inspiration for me. This journey has been extremely educational for me because of the opportunities you made available for collaborations within and outside the lab. I am also grateful to you for fostering the transformation of myself into an independent scientist.

I would sincerely like to thank my opponent Dr. David Dankort for kindly agreeing to serve as an opponent for my thesis and for being cooperative with the defense date. I would like to thank Prof. Jaakko Kaprio for taking time out of his busy schedule to serve as the Custos for my dissertation. I am grateful to my thesis advisory members Prof. Elina Ikonen and Docent Brendan Battersby for their encouragement and support throughout my PhD. I also thank my thesis reviewers Docent Aki Manninen, and Prof. Anna-Liisa Levonen for their encouraging feedback on my thesis.

I am immensely grateful to Dr. Denis Kainov for introducing me to the FIMM research community. Thank you, Denis, for the opportunity to work with you. I could not have started my PhD if you had not recruited me in the first place. I really appreciate your help during the course of my PhD as well as during the thesis submission process.

This thesis work would not have been possible without the fruitful collaborations with my colleagues. Many thanks to Jenni Lahtela for helping me during early stages of my PhD and for providing emotional support during the difficult times. Thank you, Jenni, for being an excellent team mate on our shared publication. I am grateful to our former postdoc Katja Närhi for setting up the mouse colony and the protocols. Thank you, Katja, for guiding me through the mouse work, histology analysis and

establishment of the tumor slice cultures. I could not have completed this thesis work without learning these techniques from you. I appreciated your help outside the lab as well for our family get-togethers. I am thankful to Sarang Talwelkar for the opportunity to collaborate on the mouse CRC project. It has been very exciting to work on this project. I am very fortunate to have worked with our former postdoc Jennifer Devlin, who is one of the most organized, brilliant and kind scientists I have ever met. Thank you, Jennifer, for your generous help during my manuscript preparations and submissions, and for your continued support even after you have moved on! A big thank you to Annabrita Hemmes, I can't imagine, Anna, how I would have survived my PhD without your support. I would like to thank pathologists, Dr. Kaisa Salmenkivi, for guidance with the murine lung cancer histopathology analysis, and Dr. Mikko Mäyräpää, for helping us with the generation of human lung cancer tissue microarrays. My sincere thanks to Prof. Krister Wennerberg for advising on the CRC project. I am grateful to Dr. Simon Anders for providing valuable and critical comments on my manuscripts. I extend my thanks to Teijo Pellinen for taking the time to guide me with the 3D cell cultures. Though some of these results could not be part of my thesis, it will definitely be interesting to pursue this in future. I am thankful to Sami Blom for supporting me with the image analysis. I would also like to thank Elina Kiss for being helpful and accommodating with the *in vivo* drug treatments.

Many thanks to Margarita Walliander and Olle Hansson for helping me to troubleshoot a series of problems with Definiens. I am grateful to Kalid Saeed for helping me set up the CRC protocol in our lab. I am thankful to Susanne Hultsch for letting me use the IPA software and for guiding me with the bureaucracy of the thesis work. I would like to thank Astrid Murumägi and Katja Välimäki for kindly providing antibodies for my experiments. Special thanks to Dr. Gretchen Repasky for her advice and support during my PhD. I would like to thank current and former lab members Jie Bao, Rita C. Matos, Dat Nguyen and Erasmus student Carolina Pereira. I thank my former E-wing neighbors: Masha, Laura, Oxana, Daria, Manu, Pauliina and Yuexi for the great company. I am grateful to the Laboratory Animal Centre for breeding and maintenance of the mice, the FIMM webmicroscope facility for scanning histological slides, the FIMM High-Throughput Biomedicine facility for support with the drug screening, and the HUSLAB/Helsinki biobank for providing the human NSCLC tissue blocks.

Many thanks to my Indian friends (Helsinki Family) for the wonderful get-togethers and celebrations. Special thanks to Disha, Poojitha, Yashu, Ashwini and Dipti for organizing my surprise baby shower, and for your warmth and friendship. I thank current and former members of "desi lunch": Swapnil, Ashwini, Himanshu, Raghu, Sarang, Mahesh, Disha, Poojitha, Bala, for the delicious food, as well as for discussions on a wide range of topics. I would like to thank Sreesha and Abhilash for their friendship and for helping my family on various occasions. I am thankful to Yashu and Raghu for their company

and for being there for my family through thick and thin. I thank all the friends from Finland Kannada Association (FINKA) for the memorable gatherings. I truly appreciate your efforts to keep our language and culture alive even when we are far away from home.

My sincere thanks to all my teachers for the sharing their knowledge and guiding me through various stages of my education. I am grateful to Prof. R. Manjunath from department of Biochemistry, Indian Institute of Science (IISc), Bangalore for the opportunity to work in his research group and for the valuable research experience.

My heartfelt gratitude to my parents for their unconditional love, having faith in me and for supporting all my decisions. I am forever indebted to you for all the sacrifices you made to ensure I got the best possible education. ಅಪ್ಪ, ಅಮ್ಮ ನಿಮ್ಮ ನಿಸ್ವಾರ್ಥ ಪ್ರೀತಿ, ನನ್ನಲಿಟ್ಟ ನಂಬಿಕೆ ಹಾಗು ನನ್ನ ಎಲ್ಲ ನಿರ್ಧಾರಗಳಿಗೆ ನೀವು ಕೊಟ್ಟ ಪ್ರೋತ್ಸಾಹವೇ ನಾನು ಈ ಹಂತಕ್ಕೆ ಬರಲುಕಾರಣ. ನನ್ನ ಬೆಳವಣಿಗೆ ಮತ್ತು ಉತ್ತಮ್ಮ ಶಿಕ್ಷಣಕ್ಕಾಗಿ ನೀವು ಮಾಡಿದ ತ್ಯಾಗಕ್ಕೆ ನಾನು ಸದಾ ಚಿರಋಣಿ. My sincere thanks to Radha atte and Mohan mava for supporting my education for two years. ರಾಧಾ ಅತ್ತೆ ಮತ್ತು ಮೋಹನ್ ಮಾವ, ನನ್ನ ಉನ್ನತ ಶಿಕ್ಷಣಕ್ಕಾಗಿ ನೀವು ಮಾಡಿದ ಸಹಾಯಕ್ಕೆ ನಾನು ಸದಾ ಕೃತಜ್ಞಳಾಗಿರುತ್ತೇನೆ. I am immensely grateful to Lakshmi doddamma and Seetaramu doddappa for supporting my education and for taking care of me for 5 long years. ಲಕ್ಷ್ಮಿ ದೊಡ್ಡಮ್ಮ ಮತ್ತು ಸೀತಾರಾಮು ದೊಡ್ಡಪ್ಪ ನಿಮ್ಮ ಪ್ರೀತಿ, ಸಹಾಯ ಹಾಗು ಪ್ರೋತ್ಸಾಹಕ್ಕೆ ನಾನು ಸದಾ ಕೃತಜ್ಞಳಾಗಿರುತ್ತೇನೆ. I am grateful to my late grandmothers Bhavanamma and Ranganayakamma for their love and affection. ಪ್ರೀತಿ, ಮಮತೆ, ಹಾಗು ಆರೈಯಿಕೆ ಇಂದ ನನ್ನನ್ನು ಬೆಳಸಿದ ನನ್ನ ಅಜ್ಜಿಯರಾದ, ದಿ. ಭವಾನಮ್ಮ ಮತ್ತು ದಿ. ರಂಗನಾಯಕಮ್ಮನಿಗೆ ನನ್ನ ಅನಂತ ನಮನಗಳು. I would like to thank all my aunts and uncles from Kottige family as well as form Kalasapura family. ನನ್ನ ಬೆಳವಣಿಗೆಗೆ ಪ್ರೋತ್ಸಾಹಿಸಿದ ಕೊಟ್ಟಿಗೆ ಕುಟುಂಬ ಹಾಗು ಕಳಸಾಪುರ ಕುಟುಂಬದ ದೊಡ್ಡಪ್ಪ ದೊಡ್ಡಮ್ಮದಿರಿಗೆ, ಚಿಕ್ಕಪ್ಪ ಚಿಕ್ಕಮ್ಮಂದಿರಿಗೆ, ಹಾಗು ಅತ್ತೆ ಮಾವಂದಿರಿಗೆ ನನ್ನ ಅನಂತ ನಮನಗಳು. I would like to thank all my cousins for the good times, and for the childhood memories that I will cherish forever. Many thanks to my in-laws, kaka, chikkamma, and late Aayi for making me feel welcome to their family and for all the support and encouragement. ತಮ್ಮ ಕುಟುಂಬಕ್ಕೆ ನನ್ನನ್ನು ಸ್ವಾಗತಿಸಿ ಪ್ರೀತಿ, ವಿಶ್ವಾಸದಿಂದ ಪ್ರೋತ್ಸಾಹಿಸಿರುವ ನನ್ನ ಅತ್ತೆ ಮಾವ, ಕಾಕಾ, ಚಿಕ್ಕಮ್ಮ, ತಂಗಿ ಮತ್ತು ದಿ. ಆಯಿಗೆ ನನ್ನ ಕೃತಜ್ಞತೆಗಳು. I thank my extended family members of Hasyagar family and Bommanahalli family. ಹಾಸ್ಯಗಾರ್ ಕುಟುಂಬ ಹಾಗು ಬೊಮ್ಮನಹಳ್ಳಿ ಕುಟುಂಬಕ್ಕೆ ನನ್ನ ಅನಂತ ನಮನಗಳು. I thank my lovely daughter Inchara for bringing a positive change into our lives and for keeping the joy alive. Heartfelt thanks to my beloved husband Kiran, you are the man behind my success. Thank you for your patience and understanding. Success and failure, joy and sorrow, let's sail through them together forever, love you.

October 2018, Helsinki

Ashwini

REFERENCES

(2012). Comprehensive genomic characterization of squamous cell lung cancers. Nature 489, 519-525.

(2014). Comprehensive molecular profiling of lung adenocarcinoma. Nature *511*, 543-550.

Adjei, A.A., Mauer, A., Bruzek, L., Marks, R.S., Hillman, S., Geyer, S., Hanson, L.J., Wright, J.J., Erlichman, C., Kaufmann, S.H., *et al.* (2003). Phase II study of the farnesyl transferase inhibitor R115777 in patients with advanced non-small-cell lung cancer. Journal of clinical oncology : official journal of the American Society of Clinical Oncology *21*, 1760-1766.

Ahrendt, S.A., Decker, P.A., Alawi, E.A., Zhu Yr, Y.R., Sanchez-Cespedes, M., Yang, S.C., Haasler, G.B., Kajdacsy-Balla, A., Demeure, M.J., and Sidransky, D. (2001). Cigarette smoking is strongly associated with mutation of the K-ras gene in patients with primary adenocarcinoma of the lung. Cancer *92*, 1525-1530.

Ahrendt, S.A., Hu, Y., Buta, M., McDermott, M.P., Benoit, N., Yang, S.C., Wu, L., and Sidransky, D. (2003). p53 mutations and survival in stage I non-small-cell lung cancer: results of a prospective study. Journal of the National Cancer Institute *95*, 961-970.

Albeituni, S.H., Ding, C., and Yan, J. (2013). Hampering immune suppressors: therapeutic targeting of myeloid-derived suppressor cells in cancer. Cancer journal (Sudbury, Mass) *19*, 490-501.

Alexander, A., and Walker, C.L. (2011). The role of LKB1 and AMPK in cellular responses to stress and damage. FEBS letters *585*, 952-957.

Anand, P., Kunnumakkara, A.B., Sundaram, C., Harikumar, K.B., Tharakan, S.T., Lai, O.S., Sung, B., and Aggarwal, B.B. (2008). Cancer is a preventable disease that requires major lifestyle changes. Pharmaceutical research *25*, 2097-2116.

Anderson, G.R., Winter, P.S., Lin, K.H., Nussbaum, D.P., Cakir, M., Stein, E.M., Soderquist, R.S., Crawford, L., Leeds, J.C., Newcomb, R., *et al.* (2017). A Landscape of Therapeutic Cooperativity in KRAS Mutant Cancers Reveals Principles for Controlling Tumor Evolution. Cell reports *20*, 999-1015.

Appella, E., and Anderson, C.W. (2001). Post-translational modifications and activation of p53 by genotoxic stresses. European journal of biochemistry *268*, 2764-2772.

Arteaga, C.L., and Engelman, J.A. (2014). ERBB receptors: from oncogene discovery to basic science to mechanism-based cancer therapeutics. Cancer cell *25*, 282-303.

Baas, A.F., Boudeau, J., Sapkota, G.P., Smit, L., Medema, R., Morrice, N.A., Alessi, D.R., and Clevers, H.C. (2003). Activation of the tumour suppressor kinase LKB1 by the STE20-like pseudokinase STRAD. The EMBO journal *22*, 3062-3072.

Baas, A.F., Kuipers, J., van der Wel, N.N., Batlle, E., Koerten, H.K., Peters, P.J., and Clevers, H.C. (2004). Complete polarization of single intestinal epithelial cells upon activation of LKB1 by STRAD. Cell *116*, 457-466.

Balmain, A. (2001). Cancer genetics: from Boveri and Mendel to microarrays. Nature reviews Cancer *1*, 77-82.

Bass, A.J., Watanabe, H., Mermel, C.H., Yu, S., Perner, S., Verhaak, R.G., Kim, S.Y., Wardwell, L., Tamayo, P., Gat-Viks, I., *et al.* (2009). SOX2 is an amplified lineage-survival oncogene in lung and esophageal squamous cell carcinomas. Nature genetics *41*, 1238-1242.

Beglyarova, N., Banina, E., Zhou, Y., Mukhamadeeva, R., Andrianov, G., Bobrov, E., Lysenko, E., Skobeleva, N., Gabitova, L., Restifo, D., *et al.* (2016). Screening of Conditionally Reprogrammed Patient-Derived Carcinoma Cells Identifies

ERCC3-MYC Interactions as a Target in Pancreatic Cancer. Clinical cancer research : an official journal of the American Association for Cancer Research *22*, 6153-6163.

Bennouna, J., and Moreno Vera, S.R. (2016). Afatinib-based combination regimens for the treatment of solid tumors: rationale, emerging strategies and recent progress. Future oncology (London, England) *12*, 355-372.

Berger, A.H., Brooks, A.N., Wu, X., Shrestha, Y., Chouinard, C., Piccioni, F., Bagul, M., Kamburov, A., Imielinski, M., Hogstrom, L., *et al.* (2017). High-throughput Phenotyping of Lung Cancer Somatic Mutations. Cancer cell *32*, 884.

Bergethon, K., Shaw, A.T., Ou, S.H., Katayama, R., Lovly, C.M., McDonald, N.T., Massion, P.P., Siwak-Tapp, C., Gonzalez, A., Fang, R., *et al.* (2012). ROS1 rearrangements define a unique molecular class of lung cancers. Journal of clinical oncology : official journal of the American Society of Clinical Oncology *30*, 863-870.

Bernhardt, E.B., and Jalal, S.I. (2016). Small Cell Lung Cancer. Cancer treatment and research *170*, 301-322.

Bieging, K.T., Mello, S.S., and Attardi, L.D. (2014). Unravelling mechanisms of p53-mediated tumour suppression. Nature reviews Cancer *14*, 359-370.

Bishop, J.A., Teruya-Feldstein, J., Westra, W.H., Pelosi, G., Travis, W.D., and Rekhtman, N. (2012). p40 (DeltaNp63) is superior to p63 for the diagnosis of pulmonary squamous cell carcinoma. Modern pathology : an official journal of the United States and Canadian Academy of Pathology, Inc *25*, 405-415.

Black, C.C., Turk, M.J., Dragnev, K., and Rigas, J.R. (2013). Adenocarcinoma contains more immune tolerance regulatory t-cell lymphocytes (versus squamous carcinoma) in non-small-cell lung cancer. Lung *191*, 265-270.

Blanpain, C. (2013). Tracing the cellular origin of cancer. Nature cell biology *15*, 126-134.

Blumenschein, G.R., Jr., Smit, E.F., Planchard, D., Kim, D.W., Cadranel, J., De Pas, T., Dunphy, F., Udud, K., Ahn, M.J., Hanna, N.H., *et al.* (2015). A randomized phase II study of the MEK1/MEK2 inhibitor trametinib (GSK1120212) compared with docetaxel in KRAS-mutant advanced non-small-cell lung cancer (NSCLC)dagger. Annals of oncology : official journal of the European Society for Medical Oncology *26*, 894-901.

Boch, C., Kollmeier, J., Roth, A., Stephan-Falkenau, S., Misch, D., Gruning, W., Bauer, T.T., and Mairinger, T. (2013). The frequency of EGFR and KRAS mutations in non-small cell lung cancer (NSCLC): routine screening data for central Europe from a cohort study. BMJ Open *3*.

Boers, J.E., Ambergen, A.W., and Thunnissen, F.B. (1999). Number and proliferation of clara cells in normal human airway epithelium. American journal of respiratory and critical care medicine *159*, 1585-1591.

Borghaei, H., Paz-Ares, L., Horn, L., Spigel, D.R., Steins, M., Ready, N.E., Chow, L.Q., Vokes, E.E., Felip, E., Holgado, E., *et al.* (2015). Nivolumab versus Docetaxel in Advanced Nonsquamous Non-Small-Cell Lung Cancer. The New England journal of medicine *373*, 1627-1639.

Boudeau, J., Baas, A.F., Deak, M., Morrice, N.A., Kieloch, A., Schutkowski, M., Prescott, A.R., Clevers, H.C., and Alessi, D.R. (2003). MO25alpha/beta interact with STRADalpha/beta enhancing their ability to bind, activate and localize LKB1 in the cytoplasm. The EMBO journal *22*, 5102-5114.

Bousquet, J., and Meunier, J.M. (1962). [Organotypic culture, on natural and artificial media, of fragments of the adult rat hypophysis]. Comptes rendus des seances de la Societe de biologie et de ses filiales *156*, 65-67.

Brahmer, J., Reckamp, K.L., Baas, P., Crino, L., Eberhardt, W.E., Poddubskaya, E., Antonia, S., Pluzanski, A., Vokes, E.E., Holgado, E., *et al.* (2015). Nivolumab versus Docetaxel in Advanced Squamous-Cell Non-Small-Cell Lung Cancer. The New England journal of medicine *373*, 123-135.

Bronte, G., Rizzo, S., La Paglia, L., Adamo, V., Siragusa, S., Ficorella, C., Santini, D., Bazan, V., Colucci, G., Gebbia, N., *et al.* (2010). Driver mutations and differential sensitivity to targeted therapies: a new approach to the treatment of lung adenocarcinoma. Cancer Treat Rev *36 Suppl 3*, S21-29.

Brugarolas, J., Chandrasekaran, C., Gordon, J.I., Beach, D., Jacks, T., and Hannon, G.J. (1995). Radiation-induced cell cycle arrest compromised by p21 deficiency. Nature *377*, 552-557.

Buckpitt, A., Chang, A.M., Weir, A., Van Winkle, L., Duan, X., Philpot, R., and Plopper, C. (1995). Relationship of cytochrome P450 activity to Clara cell cytotoxicity. IV. Metabolism of naphthalene and naphthalene oxide in microdissected airways from mice, rats, and hamsters. Molecular pharmacology *47*, 74-81.

Busch, S.E., Hanke, M.L., Kargl, J., Metz, H.E., MacPherson, D., and Houghton, A.M. (2016). Lung Cancer Subtypes Generate Unique Immune Responses. Journal of immunology (Baltimore, Md : 1950) *197*, 4493-4503.

Calles, A., Sholl, L.M., Rodig, S.J., Pelton, A.K., Hornick, J.L., Butaney, M., Lydon, C., Dahlberg, S.E., Oxnard, G.R., Jackman, D.M., *et al.* (2015). Immunohistochemical Loss of LKB1 Is a Biomarker for More Aggressive Biology in KRAS-Mutant Lung Adenocarcinoma. Clinical cancer research : an official journal of the American Association for Cancer Research *21*, 2851-2860.

Campbell, J.D., Alexandrov, A., Kim, J., Wala, J., Berger, A.H., Pedamallu, C.S., Shukla, S.A., Guo, G., Brooks, A.N., Murray, B.A., *et al.* (2016). Distinct patterns of somatic genome alterations in lung adenocarcinomas and squamous cell carcinomas. Nature genetics *48*, 607-616.

Carranza-Torres, I.E., Guzman-Delgado, N.E., Coronado-Martinez, C., Banuelos-Garcia, J.I., Viveros-Valdez, E., Moran-Martinez, J., and Carranza-Rosales, P. (2015). Organotypic culture of breast tumor explants as a multicellular system for the screening of natural compounds with antineoplastic potential. BioMed research international *2015*, 618021.

Carretero, J., Shimamura, T., Rikova, K., Jackson, A.L., Wilkerson, M.D., Borgman, C.L., Buttarazzi, M.S., Sanofsky, B.A., McNamara, K.L., Brandstetter, K.A., *et al.* (2010). Integrative genomic and proteomic analyses identify targets for Lkb1-deficient metastatic lung tumors. Cancer cell *17*, 547-559.

Carter, C.A., Rajan, A., Keen, C., Szabo, E., Khozin, S., Thomas, A., Brzezniak, C., Guha, U., Doyle, L.A., Steinberg, S.M., *et al.* (2016). Selumetinib with and without erlotinib in KRAS mutant and KRAS wild-type advanced nonsmall-cell lung cancer. Annals of oncology : official journal of the European Society for Medical Oncology *27*, 693-699.

Casey, P.J., Solski, P.A., Der, C.J., and Buss, J.E. (1989). p21ras is modified by a farnesyl isoprenoid. Proceedings of the National Academy of Sciences of the United States of America *86*, 8323-8327.

Casey, S.C., Vaccari, M., Al-Mulla, F., Al-Temaimi, R., Amedei, A., Barcellos-Hoff, M.H., Brown, D.G., Chapellier, M., Christopher, J., Curran, C.S., *et al.* (2015). The effect of environmental chemicals on the tumor microenvironment. Carcinogenesis *36 Suppl 1*, S160-183.

Castellano, E., and Santos, E. (2011). Functional specificity of ras isoforms: so similar but so different. Genes & cancer *2*, 216-231.

Chakrabarty, A., Sanchez, V., Kuba, M.G., Rinehart, C., and Arteaga, C.L. (2012). Feedback upregulation of HER3 (ErbB3) expression and activity attenuates antitumor effect of PI3K inhibitors. Proceedings of the National Academy of Sciences of the United States of America *109*, 2718-2723.

Chandarlapaty, S., Sawai, A., Scaltriti, M., Rodrik-Outmezguine, V., Grbovic-Huezo, O., Serra, V., Majumder, P.K., Baselga, J., and Rosen, N. (2011). AKT inhibition relieves feedback suppression of receptor tyrosine kinase expression and activity. Cancer cell *19*, 58-71.

Chapman, H.A., Li, X., Alexander, J.P., Brumwell, A., Lorizio, W., Tan, K., Sonnenberg, A., Wei, Y., and Vu, T.H. (2011). Integrin alpha6beta4 identifies an adult distal lung epithelial population with regenerative potential in mice. The Journal of clinical investigation *121*, 2855-2862.

Chen, F., and Fine, A. (2016). Stem Cells in Lung Injury and Repair. The American journal of pathology *186*, 2544-2550.

Chen, Z., Cheng, K., Walton, Z., Wang, Y., Ebi, H., Shimamura, T., Liu, Y., Tupper, T., Ouyang, J., Li, J., *et al.* (2012). A murine lung cancer co-clinical trial identifies genetic modifiers of therapeutic response. Nature *483*, 613-617.

Chen, Z., Fillmore, C.M., Hammerman, P.S., Kim, C.F., and Wong, K.K. (2014). Non-small-cell lung cancers: a heterogeneous set of diseases. Nature reviews Cancer *14*, 535-546.

Choi, Y.L., Soda, M., Yamashita, Y., Ueno, T., Takashima, J., Nakajima, T., Yatabe, Y., Takeuchi, K., Hamada, T., Haruta, H., *et al.* (2010). EML4-ALK mutations in lung cancer that confer resistance to ALK inhibitors. The New England journal of medicine *363*, 1734-1739.

Citri, A., Skaria, K.B., and Yarden, Y. (2003). The deaf and the dumb: the biology of ErbB-2 and ErbB-3. Experimental cell research *284*, 54-65.

Corcoran, R.B., Ebi, H., Turke, A.B., Coffee, E.M., Nishino, M., Cogdill, A.P., Brown, R.D., Della Pelle, P., Dias-Santagata, D., Hung, K.E., *et al.* (2012). EGFR-mediated re-activation of MAPK signaling contributes to insensitivity of BRAF mutant colorectal cancers to RAF inhibition with vemurafenib. Cancer discovery *2*, 227-235.

Costa, D.B., Shaw, A.T., Ou, S.H., Solomon, B.J., Riely, G.J., Ahn, M.J., Zhou, C., Shreeve, S.M., Selaru, P., Polli, A., *et al.* (2015). Clinical Experience With Crizotinib in Patients With Advanced ALK-Rearranged Non-Small-Cell Lung Cancer and Brain Metastases. Journal of clinical oncology : official journal of the American Society of Clinical Oncology *33*, 1881-1888.

Cox, A.D., Fesik, S.W., Kimmelman, A.C., Luo, J., and Der, C.J. (2014). Drugging the undruggable RAS: Mission possible? Nature reviews Drug discovery *13*, 828-851.

Crystal, A.S., Shaw, A.T., Sequist, L.V., Friboulet, L., Niederst, M.J., Lockerman, E.L., Frias, R.L., Gainor, J.F., Amzallag, A., Greninger, P., *et al.* (2014). Patient-derived models of acquired resistance can identify effective drug combinations for cancer. Science (New York, NY) *346*, 1480-1486.

Curry, N.L., Mino-Kenudson, M., Oliver, T.G., Yilmaz, O.H., Yilmaz, V.O., Moon, J.Y., Jacks, T., Sabatini, D.M., and Kalaany, N.Y. (2013). Pten-null tumors cohabiting the same lung display differential AKT activation and sensitivity to dietary restriction. Cancer discovery *3*, 908-921.

D'Amico, D., Carbone, D., Mitsudomi, T., Nau, M., Fedorko, J., Russell, E., Johnson, B., Buchhagen, D., Bodner, S., Phelps, R., *et al.* (1992). High frequency of somatically acquired p53 mutations in small-cell lung cancer cell lines and tumors. Oncogene *7*, 339-346.

Dankort, D., Filenova, E., Collado, M., Serrano, M., Jones, K., and McMahon, M. (2007). A new mouse model to explore the initiation, progression, and therapy of BRAFV600E-induced lung tumors. Genes & development *21*, 379-384.

Das, A., Cheng, R.R., Hilbert, M.L., Dixon-Moh, Y.N., Decandio, M., Vandergrift, W.A., 3rd, Banik, N.L., Lindhorst, S.M., Cachia, D., Varma, A.K., *et al.* (2015). Synergistic Effects of Crizotinib and Temozolomide in Experimental FIG-ROS1 Fusion-Positive Glioblastoma. Cancer growth and metastasis *8*, 51-60.

Davies, E.J., Dong, M., Gutekunst, M., Narhi, K., van Zoggel, H.J., Blom, S., Nagaraj, A., Metsalu, T., Oswald, E., Erkens-Schulze, S., *et al.* (2015). Capturing complex tumour biology in vitro: histological and molecular characterisation of precision cut slices. Scientific reports *5*, 17187.

de Bruin, E.C., McGranahan, N., and Swanton, C. (2015). Analysis of intratumor heterogeneity unravels lung cancer evolution. Molecular & cellular oncology *2*, e985549.

DeCaprio, J.A., Ludlow, J.W., Figge, J., Shew, J.Y., Huang, C.M., Lee, W.H., Marsilio, E., Paucha, E., and Livingston, D.M. (1988). SV40 large tumor antigen forms a specific complex with the product of the retinoblastoma susceptibility gene. Cell *54*, 275-283.

Denissenko, M.F., Pao, A., Tang, M., and Pfeifer, G.P. (1996). Preferential formation of benzo[a]pyrene adducts at lung cancer mutational hotspots in P53. Science (New York, NY) *274*, 430-432.

Der, C.J., Krontiris, T.G., and Cooper, G.M. (1982). Transforming genes of human bladder and lung carcinoma cell lines are homologous to the ras genes of Harvey and Kirsten sarcoma viruses. Proceedings of the National Academy of Sciences of the United States of America *79*, 3637-3640.

Dhanasekaran, S.M., Balbin, O.A., Chen, G., Nadal, E., Kalyana-Sundaram, S., Pan, J., Veeneman, B., Cao, X., Malik, R., Vats, P., *et al.* (2014). Transcriptome meta-analysis of lung cancer reveals recurrent aberrations in NRG1 and Hippo pathway genes. Nature communications *5*, 5893.

Diem, S., Schmid, S., Krapf, M., Flatz, L., Born, D., Jochum, W., Templeton, A.J., and Fruh, M. (2017). Neutrophil-to-Lymphocyte ratio (NLR) and Platelet-to-Lymphocyte ratio (PLR) as prognostic markers in patients with non-small cell lung cancer (NSCLC) treated with nivolumab. Lung cancer (Amsterdam, Netherlands) *111*, 176-181.

Dietz, S., Harms, A., Endris, V., Eichhorn, F., Kriegsmann, M., Longuespee, R., Stenzinger, A., Sultmann, H., Warth, A., and Kazdal, D. (2017). Spatial distribution of EGFR and KRAS mutation frequencies correlates with histological growth patterns of lung adenocarcinomas. International journal of cancer *141*, 1841-1848.

Dobbelstein, M., and Roth, J. (1998). The large T antigen of simian virus 40 binds and inactivates p53 but not p73. The Journal of general virology *79 (Pt 12)*, 3079-3083.

Doebele, R.C., Pilling, A.B., Aisner, D.L., Kutateladze, T.G., Le, A.T., Weickhardt, A.J., Kondo, K.L., Linderman, D.J., Heasley, L.E., Franklin, W.A., *et al.* (2012). Mechanisms of resistance to crizotinib in patients with ALK gene rearranged non-small cell lung cancer. Clinical cancer research : an official journal of the American Association for Cancer Research *18*, 1472-1482.

Donehower, L.A., Harvey, M., Slagle, B.L., McArthur, M.J., Montgomery, C.A., Jr., Butel, J.S., and Bradley, A. (1992). Mice deficient for p53 are developmentally normal but susceptible to spontaneous tumours. Nature *356*, 215-221.

Downward, J., Yarden, Y., Mayes, E., Scrace, G., Totty, N., Stockwell, P., Ullrich, A., Schlessinger, J., and Waterfield, M.D. (1984). Close similarity of epidermal growth factor receptor and v-erb-B oncogene protein sequences. Nature *307*, 521-527.

Drosten, M., Simon-Carrasco, L., Hernandez-Porras, I., Lechuga, C.G., Blasco, M.T., Jacob, H.K., Fabbiano, S., Potenza, N., Bustelo, X.R., Guerra, C., *et al.* (2017). H-Ras and K-Ras Oncoproteins Induce Different Tumor Spectra When Driven by the Same Regulatory Sequences. Cancer research *77*, 707-718.

Dunn, G.P., Bruce, A.T., Ikeda, H., Old, L.J., and Schreiber, R.D. (2002). Cancer immunoediting: from immunosurveillance to tumor escape. Nature immunology *3*, 991-998.

DuPage, M., Cheung, A.F., Mazumdar, C., Winslow, M.M., Bronson, R., Schmidt, L.M., Crowley, D., Chen, J., and Jacks, T. (2011). Endogenous T cell responses to antigens expressed in lung adenocarcinomas delay malignant tumor progression. Cancer cell *19*, 72-85.

Dykens, J.A., Jamieson, J., Marroquin, L., Nadanaciva, S., Billis, P.A., and Will, Y. (2008). Biguanide-induced mitochondrial dysfunction yields increased lactate production and cytotoxicity of aerobically-poised HepG2 cells and human hepatocytes in vitro. Toxicology and applied pharmacology *233*, 203-210.

Eberhard, D.A., Johnson, B.E., Amler, L.C., Goddard, A.D., Heldens, S.L., Herbst, R.S., Ince, W.L., Janne, P.A., Januario, T., Johnson, D.H., *et al.* (2005). Mutations in the epidermal growth factor receptor and in KRAS are predictive and prognostic indicators in patients with non-small-cell lung cancer treated with chemotherapy alone and in combination with erlotinib. Journal of clinical oncology : official journal of the American Society of Clinical Oncology *23*, 5900-5909.

Egan, D.F., Shackelford, D.B., Mihaylova, M.M., Gelino, S., Kohnz, R.A., Mair, W., Vasquez, D.S., Joshi, A., Gwinn, D.M., Taylor, R., *et al.* (2011). Phosphorylation of ULK1 (hATG1) by AMP-activated protein kinase connects energy sensing to mitophagy. Science (New York, NY) *331*, 456-461.

Ehrhardt, A., Bartels, T., Geick, A., Klocke, R., Paul, D., and Halter, R. (2001). Development of pulmonary bronchiolo-alveolar adenocarcinomas in transgenic mice overexpressing murine c-myc and epidermal growth factor in alveolar type II pneumocytes. British journal of cancer *84*, 813-818.

el-Deiry, W.S., Kern, S.E., Pietenpol, J.A., Kinzler, K.W., and Vogelstein, B. (1992). Definition of a consensus binding site for p53. Nature genetics *1*, 45-49.

Elliott, L.A., Doherty, G.A., Sheahan, K., and Ryan, E.J. (2017). Human Tumor-Infiltrating Myeloid Cells: Phenotypic and Functional Diversity. Frontiers in immunology *8*, 86.

Engelman, J.A., Chen, L., Tan, X., Crosby, K., Guimaraes, A.R., Upadhyay, R., Maira, M., McNamara, K., Perera, S.A., Song, Y., *et al.* (2008). Effective use of PI3K and MEK inhibitors to treat mutant Kras G12D and PIK3CA H1047R murine lung cancers. Nature medicine *14*, 1351-1356.

Facchinetti, F., Bluthgen, M.V., Tergemina-Clain, G., Faivre, L., Pignon, J.P., Planchard, D., Remon, J., Soria, J.C., Lacroix, L., and Besse, B. (2017a). LKB1/STK11 mutations in non-small cell lung cancer patients: Descriptive analysis and prognostic value. Lung cancer (Amsterdam, Netherlands) *112*, 62-68.

Facchinetti, F., Proto, C., Minari, R., Garassino, M., and Tiseo, M. (2017b). Mechanisms of Resistance to Target Therapies in Non-small Cell Lung Cancer. Handbook of experimental pharmacology.

Facciabene, A., Motz, G.T., and Coukos, G. (2012). T-regulatory cells: key players in tumor immune escape and angiogenesis. Cancer research *72*, 2162-2171.

Faget, J., Groeneveld, S., Boivin, G., Sankar, M., Zangger, N., Garcia, M., Guex, N., Zlobec, I., Steiner, L., Piersigilli, A., *et al.* (2017). Neutrophils and Snail Orchestrate the Establishment of a Pro-tumor Microenvironment in Lung Cancer. Cell reports *21*, 3190-3204.

Falls, D.L. (2003). Neuregulins: functions, forms, and signaling strategies. Experimental cell research *284*, 14-30.

Fehrenbacher, L., Spira, A., Ballinger, M., Kowanetz, M., Vansteenkiste, J., Mazieres, J., Park, K., Smith, D., Artal-Cortes, A., Lewanski, C., *et al.* (2016). Atezolizumab versus docetaxel for patients with previously treated non-small-cell lung cancer (POPLAR): a multicentre, open-label, phase 2 randomised controlled trial. Lancet (London, England) *387*, 1837-1846.

Ferlay, J., Soerjomataram, I., Dikshit, R., Eser, S., Mathers, C., Rebelo, M., Parkin, D.M., Forman, D., and Bray, F. (2015). Cancer incidence and mortality worldwide: sources, methods and major patterns in GLOBOCAN 2012. International journal of cancer *136*, E359-386.

Fernandez-Cuesta, L., Plenker, D., Osada, H., Sun, R., Menon, R., Leenders, F., Ortiz-Cuaran, S., Peifer, M., Bos, M., Dassler, J., *et al.* (2014). CD74-NRG1 fusions in lung adenocarcinoma. Cancer discovery *4*, 415-422.

Ferone, G., Song, J.Y., Sutherland, K.D., Bhaskaran, R., Monkhorst, K., Lambooij, J.P., Proost, N., Gargiulo, G., and Berns, A. (2016). SOX2 Is the Determining Oncogenic Switch in Promoting Lung Squamous Cell Carcinoma from Different Cells of Origin. Cancer cell *30*, 519-532.

Finlay, C.A., Hinds, P.W., and Levine, A.J. (1989). The p53 proto-oncogene can act as a suppressor of transformation. Cell *57*, 1083-1093.

Fisher, G.H., Wellen, S.L., Klimstra, D., Lenczowski, J.M., Tichelaar, J.W., Lizak, M.J., Whitsett, J.A., Koretsky, A., and Varmus, H.E. (2001). Induction and apoptotic regression of lung adenocarcinomas by regulation of a K-Ras transgene in the presence and absence of tumor suppressor genes. Genes & development *15*, 3249-3262.

Fleming, T.J., Fleming, M.L., and Malek, T.R. (1993). Selective expression of Ly-6G on myeloid lineage cells in mouse bone marrow. RB6-8C5 mAb to granulocyte-differentiation antigen (Gr-1) detects members of the Ly-6 family. Journal of immunology (Baltimore, Md : 1950) *151*, 2399-2408.

Forbes, S.A., Bindal, N., Bamford, S., Cole, C., Kok, C.Y., Beare, D., Jia, M., Shepherd, R., Leung, K., Menzies, A., *et al.* (2011). COSMIC: mining complete cancer genomes in the Catalogue of Somatic Mutations in Cancer. Nucleic acids research *39*, D945-950.

Friboulet, L., Li, N., Katayama, R., Lee, C.C., Gainor, J.F., Crystal, A.S., Michellys, P.Y., Awad, M.M., Yanagitani, N., Kim, S., *et al.* (2014). The ALK inhibitor ceritinib overcomes crizotinib resistance in non-small cell lung cancer. Cancer discovery *4*, 662-673.

Fridman, W.H., Dieu-Nosjean, M.C., Pages, F., Cremer, I., Damotte, D., Sautes-Fridman, C., and Galon, J. (2013). The immune microenvironment of human tumors: general significance and clinical impact. Cancer microenvironment : official journal of the International Cancer Microenvironment Society *6*, 117-122.

Fuller, S.J., Sivarajah, K., and Sugden, P.H. (2008). ErbB receptors, their ligands, and the consequences of their activation and inhibition in the myocardium. Journal of molecular and cellular cardiology *44*, 831-854.

Furrukh, M. (2013). Tobacco Smoking and Lung Cancer: Perception-changing facts. Sultan Qaboos University medical journal *13*, 345-358.

Gabrielson, E. (2006). Worldwide trends in lung cancer pathology. Respirology (Carlton, Vic) *11*, 533-538.

Gabrilovich, D.I. (2017). Myeloid-Derived Suppressor Cells. Cancer immunology research *5*, 3-8.

Gabrilovich, D.I., and Nagaraj, S. (2009). Myeloid-derived suppressor cells as regulators of the immune system. Nature reviews Immunology *9*, 162-174.

Ganesan, A.P., Johansson, M., Ruffell, B., Yagui-Beltran, A., Lau, J., Jablons, D.M., and Coussens, L.M. (2013). Tumor-infiltrating regulatory T cells inhibit endogenous cytotoxic T cell

responses to lung adenocarcinoma. Journal of immunology (Baltimore, Md : 1950) *191*, 2009-2017.

Gao, H., Korn, J.M., Ferretti, S., Monahan, J.E., Wang, Y., Singh, M., Zhang, C., Schnell, C., Yang, G., Zhang, Y., *et al.* (2015). High-throughput screening using patient-derived tumor xenografts to predict clinical trial drug response. Nature medicine *21*, 1318-1325.

Gao, X., Dai, M., Li, Q., Wang, Z., Lu, Y., and Song, Z. (2017). HMGA2 regulates lung cancer proliferation and metastasis. Thoracic cancer *8*, 501-510.

Gao, Y., Zhang, W., Han, X., Li, F., Wang, X., Wang, R., Fang, Z., Tong, X., Yao, S., Li, F., *et al.* (2014). YAP inhibits squamous transdifferentiation of Lkb1-deficient lung adenocarcinoma through ZEB2-dependent DNp63 repression. Nature communications *5*, 4629.

Garnett, S., Dutchak, K.L., McDonough, R.V., and Dankort, D. (2017). p53 loss does not permit escape from Braf(V600E)-induced senescence in a mouse model of lung cancer. Oncogene *36*, 6325-6335.

Garrett, T.P., McKern, N.M., Lou, M., Elleman, T.C., Adams, T.E., Lovrecz, G.O., Kofler, M., Jorissen, R.N., Nice, E.C., Burgess, A.W., *et al.* (2003). The crystal structure of a truncated ErbB2 ectodomain reveals an active conformation, poised to interact with other ErbB receptors. Molecular cell *11*, 495-505.

Garrido, F., Ruiz-Cabello, F., Cabrera, T., Perez-Villar, J.J., Lopez-Botet, M., Duggan-Keen, M., and Stern, P.L. (1997). Implications for immunosurveillance of altered HLA class I phenotypes in human tumours. Immunology today *18*, 89-95.

Gautschi, O., Huegli, B., Ziegler, A., Gugger, M., Heighway, J., Ratschiller, D., Mack, P.C., Gumerlock, P.H., Kung, H.J., Stahel, R.A., *et al.* (2007). Origin and prognostic value of circulating KRAS mutations in lung cancer patients. Cancer letters *254*, 265-273.

Geick, A., Redecker, P., Ehrhardt, A., Klocke, R., Paul, D., and Halter, R. (2001). Uteroglobin promoter-targeted c-MYC expression in transgenic mice cause hyperplasia of Clara cells and malignant transformation of T-lymphoblasts and tubular epithelial cells. Transgenic research *10*, 501-511.

George, J., Lim, J.S., Jang, S.J., Cun, Y., Ozretic, L., Kong, G., Leenders, F., Lu, X., Fernandez-Cuesta, L., Bosco, G., *et al.* (2015). Comprehensive genomic profiles of small cell lung cancer. Nature *524*, 47-53.

Gerdes, M.J., Sevinsky, C.J., Sood, A., Adak, S., Bello, M.O., Bordwell, A., Can, A., Corwin, A., Dinn, S., Filkins, R.J., *et al.* (2013). Highly multiplexed single-cell analysis of formalin-fixed, paraffin-embedded cancer tissue. Proceedings of the National Academy of Sciences of the United States of America *110*, 11982-11987.

Gerlach, M.M., Merz, F., Wichmann, G., Kubick, C., Wittekind, C., Lordick, F., Dietz, A., and Bechmann, I. (2014). Slice cultures from head and neck squamous cell carcinoma: a novel test system for drug susceptibility and mechanisms of resistance. British journal of cancer *110*, 479-488.

Gerlinger, M., Rowan, A.J., Horswell, S., Math, M., Larkin, J., Endesfelder, D., Gronroos, E., Martinez, P., Matthews, N., Stewart, A., *et al.* (2012). Intratumor heterogeneity and branched evolution revealed by multiregion sequencing. The New England journal of medicine *366*, 883-892.

Gettinger, S.N., Horn, L., Gandhi, L., Spigel, D.R., Antonia, S.J., Rizvi, N.A., Powderly, J.D., Heist, R.S., Carvajal, R.D., Jackman, D.M., *et al.* (2015). Overall Survival and Long-Term Safety of Nivolumab (Anti-Programmed Death 1 Antibody, BMS-936558, ONO-4538) in Patients With Previously Treated Advanced Non-Small-Cell Lung Cancer. Journal of clinical oncology : official journal of the American Society of Clinical Oncology *33*, 2004-2012.

Giangreco, A., Reynolds, S.D., and Stripp, B.R. (2002). Terminal bronchioles harbor a unique airway stem cell population that localizes to the bronchoalveolar duct junction. The American journal of pathology *161*, 173-182.

Giardiello, F.M., Welsh, S.B., Hamilton, S.R., Offerhaus, G.J., Gittelsohn, A.M., Booker, S.V., Krush, A.J., Yardley, J.H., and Luk, G.D. (1987). Increased risk of cancer in the Peutz-Jeghers syndrome. The New England journal of medicine *316*, 1511-1514.

Gierut, J.J., Jacks, T.E., and Haigis, K.M. (2014). In vivo delivery of lenti-Cre or adeno-Cre into mice using intranasal instillation. Cold Spring Harbor protocols *2014*, 307-309.

Glasser, S.W., Korfhagen, T.R., Wert, S.E., Bruno, M.D., McWilliams, K.M., Vorbroker, D.K., and Whitsett, J.A. (1991). Genetic element from human surfactant protein SP-C gene confers bronchiolar-alveolar cell specificity in transgenic mice. The American journal of physiology *261*, L349-356.

Goldstraw, P., Chansky, K., Crowley, J., Rami-Porta, R., Asamura, H., Eberhardt, W.E., Nicholson, A.G., Groome, P., Mitchell, A., and Bolejack, V. (2016). The IASLC Lung Cancer Staging Project: Proposals for Revision of the TNM Stage Groupings in the Forthcoming (Eighth) Edition of the TNM Classification for Lung Cancer. Journal of thoracic oncology : official publication of the International Association for the Study of Lung Cancer *11*, 39-51.

Gordon, J.W., Scangos, G.A., Plotkin, D.J., Barbosa, J.A., and Ruddle, F.H. (1980). Genetic transformation of mouse embryos by microinjection of purified DNA. Proceedings of the National Academy of Sciences of the United States of America *77*, 7380-7384.

Gordon, T., and Bosland, M. (2009). Strain-dependent differences in susceptibility to lung cancer in inbred mice exposed to mainstream cigarette smoke. Cancer letters *275*, 213-220.

Gray, N. (2006). The consequences of the unregulated cigarette. Tobacco control *15*, 405-408.

Greshock, J., Bachman, K.E., Degenhardt, Y.Y., Jing, J., Wen, Y.H., Eastman, S., McNeil, E., Moy, C., Wegrzyn, R., Auger, K., *et al.* (2010). Molecular target class is predictive of in vitro response profile. Cancer research *70*, 3677-3686.

Gridelli, C., Rossi, A., Carbone, D.P., Guarize, J., Karachaliou, N., Mok, T., Petrella, F., Spaggiari, L., and Rosell, R. (2015). Non-small-cell lung cancer. Nature reviews Disease primers *1*, 15009.

Guy, P.M., Platko, J.V., Cantley, L.C., Cerione, R.A., and Carraway, K.L., 3rd (1994). Insect cell-expressed p180erbB3 possesses an impaired tyrosine kinase activity. Proceedings of the National Academy of Sciences of the United States of America *91*, 8132-8136.

Gwinn, D.M., Shackelford, D.B., Egan, D.F., Mihaylova, M.M., Mery, A., Vasquez, D.S., Turk, B.E., and Shaw, R.J. (2008). AMPK phosphorylation of raptor mediates a metabolic checkpoint. Molecular cell *30*, 214-226.

Gysin, S., Salt, M., Young, A., and McCormick, F. (2011). Therapeutic strategies for targeting ras proteins. Genes & cancer *2*, 359-372.

Hagiwara, K., McMenamin, M.G., Miura, K., and Harris, C.C. (1999). Mutational analysis of the p63/p73L/p51/p40/CUSP/KET gene in human cancer cell lines using intronic primers. Cancer research *59*, 4165-4169.

Halvorsen, A.R., Silwal-Pandit, L., Meza-Zepeda, L.A., Vodak, D., Vu, P., Sagerup, C., Hovig, E., Myklebost, O., Borresen-Dale, A.L., Brustugun, O.T., *et al.* (2016). TP53 Mutation Spectrum in Smokers and Never Smoking Lung Cancer Patients. Frontiers in genetics *7*, 85.

Han, X., Li, F., Fang, Z., Gao, Y., Li, F., Fang, R., Yao, S., Sun, Y., Li, L., Zhang, W., *et al.* (2014). Transdifferentiation of lung adenocarcinoma in mice with Lkb1 deficiency to squamous cell carcinoma. Nature communications *5*, 3261.

Hanahan, D., and Coussens, L.M. (2012). Accessories to the crime: functions of cells recruited to the tumor microenvironment. Cancer cell *21*, 309-322.

Hanahan, D., and Weinberg, R.A. (2000). The hallmarks of cancer. Cell *100*, 57-70.
Hanahan, D., and Weinberg, R.A. (2011). Hallmarks of cancer: the next generation. Cell *144*, 646-674.
Hao, J.J., Lin, D.C., Dinh, H.Q., Mayakonda, A., Jiang, Y.Y., Chang, C., Jiang, Y., Lu, C.C., Shi, Z.Z., Xu, X., *et al.* (2016). Spatial intratumoral heterogeneity and temporal clonal evolution in esophageal squamous cell carcinoma. Nature genetics *48*, 1500-1507.
Hardie, D.G. (2007). AMP-activated/SNF1 protein kinases: conserved guardians of cellular energy. Nature reviews Molecular cell biology *8*, 774-785.
Harvey, J.J. (1964). AN UNIDENTIFIED VIRUS WHICH CAUSES THE RAPID PRODUCTION OF TUMOURS IN MICE. Nature *204*, 1104-1105.
Hawley, S.A., Ross, F.A., Chevtzoff, C., Green, K.A., Evans, A., Fogarty, S., Towler, M.C., Brown, L.J., Ogunbayo, O.A., Evans, A.M., *et al.* (2010). Use of cells expressing gamma subunit variants to identify diverse mechanisms of AMPK activation. Cell metabolism *11*, 554-565.
Hearle, N., Schumacher, V., Menko, F.H., Olschwang, S., Boardman, L.A., Gille, J.J., Keller, J.J., Westerman, A.M., Scott, R.J., Lim, W., *et al.* (2006). Frequency and spectrum of cancers in the Peutz-Jeghers syndrome. Clinical cancer research : an official journal of the American Association for Cancer Research *12*, 3209-3215.
Hecht, S.S. (2012). Lung carcinogenesis by tobacco smoke. International journal of cancer *131*, 2724-2732.
Hellyer, N.J., Cheng, K., and Koland, J.G. (1998). ErbB3 (HER3) interaction with the p85 regulatory subunit of phosphoinositide 3-kinase. The Biochemical journal *333 (Pt 3)*, 757-763.
Hemminki, A. (1999). The molecular basis and clinical aspects of Peutz-Jeghers syndrome. Cellular and molecular life sciences : CMLS *55*, 735-750.
Hemminki, A., Markie, D., Tomlinson, I., Avizienyte, E., Roth, S., Loukola, A., Bignell, G., Warren, W., Aminoff, M., Hoglund, P., *et al.* (1998). A serine/threonine kinase gene defective in Peutz-Jeghers syndrome. Nature *391*, 184-187.
Hemminki, A., Tomlinson, I., Markie, D., Jarvinen, H., Sistonen, P., Bjorkqvist, A.M., Knuutila, S., Salovaara, R., Bodmer, W., Shibata, D., *et al.* (1997). Localization of a susceptibility locus for Peutz-Jeghers syndrome to 19p using comparative genomic hybridization and targeted linkage analysis. Nature genetics *15*, 87-90.
Hendler, F.J., and Ozanne, B.W. (1984). Human squamous cell lung cancers express increased epidermal growth factor receptors. The Journal of clinical investigation *74*, 647-651.
Herbst, R.S., Baas, P., Kim, D.W., Felip, E., Perez-Gracia, J.L., Han, J.Y., Molina, J., Kim, J.H., Arvis, C.D., Ahn, M.J., *et al.* (2016). Pembrolizumab versus docetaxel for previously treated, PD-L1-positive, advanced non-small-cell lung cancer (KEYNOTE-010): a randomised controlled trial. Lancet (London, England) *387*, 1540-1550.
Herriges, M., and Morrisey, E.E. (2014). Lung development: orchestrating the generation and regeneration of a complex organ. Development (Cambridge, England) *141*, 502-513.
Hezel, A.F., and Bardeesy, N. (2008). LKB1; linking cell structure and tumor suppression. Oncogene *27*, 6908-6919.
Hinds, P., Finlay, C., and Levine, A.J. (1989). Mutation is required to activate the p53 gene for cooperation with the ras oncogene and transformation. Journal of virology *63*, 739-746.
Hirsch, F.R., Varella-Garcia, M., Bunn, P.A., Jr., Di Maria, M.V., Veve, R., Bremmes, R.M., Baron, A.E., Zeng, C., and Franklin, W.A. (2003). Epidermal growth factor receptor in non-small-cell lung carcinomas: correlation between gene copy number and protein expression and impact on prognosis. Journal of clinical oncology : official journal of the American Society of Clinical Oncology *21*, 3798-3807.

Hirsch, F.R., Varella-Garcia, M., Franklin, W.A., Veve, R., Chen, L., Helfrich, B., Zeng, C., Baron, A., and Bunn, P.A., Jr. (2002). Evaluation of HER-2/neu gene amplification and protein expression in non-small cell lung carcinomas. British journal of cancer *86*, 1449-1456.

Ho, V.M., Schaffer, B.E., Karnezis, A.N., Park, K.S., and Sage, J. (2009). The retinoblastoma gene Rb and its family member p130 suppress lung adenocarcinoma induced by oncogenic K-Ras. Oncogene *28*, 1393-1399.

Hobbs, G.A., Der, C.J., and Rossman, K.L. (2016). RAS isoforms and mutations in cancer at a glance. Journal of cell science *129*, 1287-1292.

Hollstein, M., Sidransky, D., Vogelstein, B., and Harris, C.C. (1991). p53 mutations in human cancers. Science (New York, NY) *253*, 49-53.

Horio, Y., Chen, A., Rice, P., Roth, J.A., Malkinson, A.M., and Schrump, D.S. (1996). Ki-ras and p53 mutations are early and late events, respectively, in urethane-induced pulmonary carcinogenesis in A/J mice. Molecular carcinogenesis *17*, 217-223.

Hu, W., Feng, Z., and Levine, A.J. (2012). The Regulation of Multiple p53 Stress Responses is Mediated through MDM2. Genes & cancer *3*, 199-208.

Huang, A., Zhang, B., Wang, B., Zhang, F., Fan, K.X., and Guo, Y.J. (2013). Increased CD14(+)HLA-DR (-/low) myeloid-derived suppressor cells correlate with extrathoracic metastasis and poor response to chemotherapy in non-small cell lung cancer patients. Cancer immunology, immunotherapy : CII *62*, 1439-1451.

Ihle, N.T., Byers, L.A., Kim, E.S., Saintigny, P., Lee, J.J., Blumenschein, G.R., Tsao, A., Liu, S., Larsen, J.E., Wang, J., *et al.* (2012). Effect of KRAS oncogene substitutions on protein behavior: implications for signaling and clinical outcome. Journal of the National Cancer Institute *104*, 228-239.

Inoki, K., Zhu, T., and Guan, K.L. (2003). TSC2 mediates cellular energy response to control cell growth and survival. Cell *115*, 577-590.

Iwanaga, K., Yang, Y., Raso, M.G., Ma, L., Hanna, A.E., Thilaganathan, N., Moghaddam, S., Evans, C.M., Li, H., Cai, W.W., *et al.* (2008). Pten inactivation accelerates oncogenic K-ras-initiated tumorigenesis in a mouse model of lung cancer. Cancer research *68*, 1119-1127.

Jackman, D.M., Yeap, B.Y., Sequist, L.V., Lindeman, N., Holmes, A.J., Joshi, V.A., Bell, D.W., Huberman, M.S., Halmos, B., Rabin, M.S., *et al.* (2006). Exon 19 deletion mutations of epidermal growth factor receptor are associated with prolonged survival in non-small cell lung cancer patients treated with gefitinib or erlotinib. Clinical cancer research : an official journal of the American Association for Cancer Research *12*, 3908-3914.

Jackson, E.L., Olive, K.P., Tuveson, D.A., Bronson, R., Crowley, D., Brown, M., and Jacks, T. (2005). The differential effects of mutant p53 alleles on advanced murine lung cancer. Cancer research *65*, 10280-10288.

Jackson, E.L., Willis, N., Mercer, K., Bronson, R.T., Crowley, D., Montoya, R., Jacks, T., and Tuveson, D.A. (2001). Analysis of lung tumor initiation and progression using conditional expression of oncogenic K-ras. Genes & development *15*, 3243-3248.

Janes, M.R., Zhang, J., Li, L.S., Hansen, R., Peters, U., Guo, X., Chen, Y., Babbar, A., Firdaus, S.J., Darjania, L., *et al.* (2018). Targeting KRAS Mutant Cancers with a Covalent G12C-Specific Inhibitor. Cell *172*, 578-589.e517.

Janne, P.A., Shaw, A.T., Pereira, J.R., Jeannin, G., Vansteenkiste, J., Barrios, C., Franke, F.A., Grinsted, L., Zazulina, V., Smith, P., *et al.* (2013). Selumetinib plus docetaxel for KRAS-mutant advanced non-small-cell lung cancer: a randomised, multicentre, placebo-controlled, phase 2 study. The Lancet Oncology *14*, 38-47.

Jenne, D.E., Reimann, H., Nezu, J., Friedel, W., Loff, S., Jeschke, R., Muller, O., Back, W., and Zimmer, M. (1998). Peutz-Jeghers syndrome is caused by mutations in a novel serine threonine kinase. Nature genetics *18*, 38-43.

Ji, H., Li, D., Chen, L., Shimamura, T., Kobayashi, S., McNamara, K., Mahmood, U., Mitchell, A., Sun, Y., Al-Hashem, R., *et al.* (2006a). The impact of human EGFR kinase domain mutations on lung tumorigenesis and in vivo sensitivity to EGFR-targeted therapies. Cancer cell *9*, 485-495.

Ji, H., Ramsey, M.R., Hayes, D.N., Fan, C., McNamara, K., Kozlowski, P., Torrice, C., Wu, M.C., Shimamura, T., Perera, S.A., *et al.* (2007). LKB1 modulates lung cancer differentiation and metastasis. Nature *448*, 807-810.

Ji, H., Zhao, X., Yuza, Y., Shimamura, T., Li, D., Protopopov, A., Jung, B.L., McNamara, K., Xia, H., Glatt, K.A., *et al.* (2006b). Epidermal growth factor receptor variant III mutations in lung tumorigenesis and sensitivity to tyrosine kinase inhibitors. Proceedings of the National Academy of Sciences of the United States of America *103*, 7817-7822.

Jin, G., Kim, M.J., Jeon, H.S., Choi, J.E., Kim, D.S., Lee, E.B., Cha, S.I., Yoon, G.S., Kim, C.H., Jung, T.H., *et al.* (2010). PTEN mutations and relationship to EGFR, ERBB2, KRAS, and TP53 mutations in non-small cell lung cancers. Lung cancer (Amsterdam, Netherlands) *69*, 279-283.

Jishage, K., Nezu, J., Kawase, Y., Iwata, T., Watanabe, M., Miyoshi, A., Ose, A., Habu, K., Kake, T., Kamada, N., *et al.* (2002). Role of Lkb1, the causative gene of Peutz-Jegher's syndrome, in embryogenesis and polyposis. Proceedings of the National Academy of Sciences of the United States of America *99*, 8903-8908.

Johnson, L., Mercer, K., Greenbaum, D., Bronson, R.T., Crowley, D., Tuveson, D.A., and Jacks, T. (2001). Somatic activation of the K-ras oncogene causes early onset lung cancer in mice. Nature *410*, 1111-1116.

Joseph, D., Puttaswamy, R.K., and Krovvidi, H. (2013). Non-respiratory functions of the lung. Continuing Education in Anaesthesia Critical Care & Pain *13*, 98-102.

Joshi, A., Zanwar, S., Noronha, V., Patil, V.M., Chougule, A., Kumar, R., Janu, A., Mahajan, A., Kapoor, A., and Prabhash, K. (2017). EGFR mutation in squamous cell carcinoma of the lung: does it carry the same connotation as in adenocarcinomas? OncoTargets and therapy *10*, 1859-1863.

Joshi, N.S., Akama-Garren, E.H., Lu, Y., Lee, D.Y., Chang, G.P., Li, A., DuPage, M., Tammela, T., Kerper, N.R., Farago, A.F., *et al.* (2015). Regulatory T Cells in Tumor-Associated Tertiary Lymphoid Structures Suppress Anti-tumor T Cell Responses. Immunity *43*, 579-590.

Julien, S., Merino-Trigo, A., Lacroix, L., Pocard, M., Goere, D., Mariani, P., Landron, S., Bigot, L., Nemati, F., Dartigues, P., *et al.* (2012). Characterization of a large panel of patient-derived tumor xenografts representing the clinical heterogeneity of human colorectal cancer. Clinical cancer research : an official journal of the American Association for Cancer Research *18*, 5314-5328.

Junttila, M.R., and de Sauvage, F.J. (2013). Influence of tumour micro-environment heterogeneity on therapeutic response. Nature *501*, 346-354.

Junttila, M.R., Karnezis, A.N., Garcia, D., Madriles, F., Kortlever, R.M., Rostker, F., Brown Swigart, L., Pham, D.M., Seo, Y., Evan, G.I., *et al.* (2010). Selective activation of p53-mediated tumour suppression in high-grade tumours. Nature *468*, 567-571.

Kar, A., and Gutierrez-Hartmann, A. (2013). Molecular mechanisms of ETS transcription factor-mediated tumorigenesis. Critical reviews in biochemistry and molecular biology *48*, 522-543.

Katayama, R., Shaw, A.T., Khan, T.M., Mino-Kenudson, M., Solomon, B.J., Halmos, B., Jessop, N.A., Wain, J.C., Yeo, A.T., Benes, C., *et al.* (2012). Mechanisms of acquired

crizotinib resistance in ALK-rearranged lung Cancers. Science translational medicine *4*, 120ra117.

Kellar, A., Egan, C., and Morris, D. (2015). Preclinical Murine Models for Lung Cancer: Clinical Trial Applications. BioMed research international *2015*, 621324.

Kemphues, K.J., Priess, J.R., Morton, D.G., and Cheng, N.S. (1988). Identification of genes required for cytoplasmic localization in early C. elegans embryos. Cell *52*, 311-320.

Kerr, E.M., Gaude, E., Turrell, F.K., Frezza, C., and Martins, C.P. (2016). Mutant Kras copy number defines metabolic reprogramming and therapeutic susceptibilities. Nature *531*, 110-113.

Khosravi, R., Maya, R., Gottlieb, T., Oren, M., Shiloh, Y., and Shkedy, D. (1999). Rapid ATM-dependent phosphorylation of MDM2 precedes p53 accumulation in response to DNA damage. Proceedings of the National Academy of Sciences of the United States of America *96*, 14973-14977.

Khuder, S.A. (2001). Effect of cigarette smoking on major histological types of lung cancer: a meta-analysis. Lung cancer (Amsterdam, Netherlands) *31*, 139-148.

Kilic, A., Landreneau, R.J., Luketich, J.D., Pennathur, A., and Schuchert, M.J. (2011). Density of tumor-infiltrating lymphocytes correlates with disease recurrence and survival in patients with large non-small-cell lung cancer tumors. The Journal of surgical research *167*, 207-210.

Kim, C.F., Jackson, E.L., Woolfenden, A.E., Lawrence, S., Babar, I., Vogel, S., Crowley, D., Bronson, R.T., and Jacks, T. (2005). Identification of bronchioalveolar stem cells in normal lung and lung cancer. Cell *121*, 823-835.

Kim, E.K., Kim, K.A., Lee, C.Y., and Shim, H.S. (2017). The frequency and clinical impact of HER2 alterations in lung adenocarcinoma. PloS one *12*, e0171280.

Kim, J.Y., Welsh, E.A., Fang, B., Bai, Y., Kinose, F., Eschrich, S.A., Koomen, J.M., and Haura, E.B. (2016). Phosphoproteomics Reveals MAPK Inhibitors Enhance MET- and EGFR-Driven AKT Signaling in KRAS-Mutant Lung Cancer. Molecular cancer research : MCR *14*, 1019-1029.

Kirsten, W.H., and Mayer, L.A. (1967). Morphologic responses to a murine erythroblastosis virus. Journal of the National Cancer Institute *39*, 311-335.

Kishimoto, Y., Murakami, Y., Shiraishi, M., Hayashi, K., and Sekiya, T. (1992). Aberrations of the p53 tumor suppressor gene in human non-small cell carcinomas of the lung. Cancer research *52*, 4799-4804.

Kitai, H., Ebi, H., Tomida, S., Floros, K.V., Kotani, H., Adachi, Y., Oizumi, S., Nishimura, M., Faber, A.C., and Yano, S. (2016). Epithelial-to-Mesenchymal Transition Defines Feedback Activation of Receptor Tyrosine Kinase Signaling Induced by MEK Inhibition in KRAS-Mutant Lung Cancer. Cancer discovery *6*, 754-769.

Kiviharju-af Hallstrom, T.M., Jaamaa, S., Monkkonen, M., Peltonen, K., Andersson, L.C., Medema, R.H., Peehl, D.M., and Laiho, M. (2007). Human prostate epithelium lacks Wee1A-mediated DNA damage-induced checkpoint enforcement. Proceedings of the National Academy of Sciences of the United States of America *104*, 7211-7216.

Klapper, L.N., Glathe, S., Vaisman, N., Hynes, N.E., Andrews, G.C., Sela, M., and Yarden, Y. (1999). The ErbB-2/HER2 oncoprotein of human carcinomas may function solely as a shared coreceptor for multiple stroma-derived growth factors. Proceedings of the National Academy of Sciences of the United States of America *96*, 4995-5000.

Knudson, A.G. (2001). Two genetic hits (more or less) to cancer. Nature reviews Cancer *1*, 157-162.

Koera, K., Nakamura, K., Nakao, K., Miyoshi, J., Toyoshima, K., Hatta, T., Otani, H., Aiba, A., and Katsuki, M. (1997). K-ras is essential for the development of the mouse embryo. Oncogene *15*, 1151-1159.

Koerfer, J., Kallendrusch, S., Merz, F., Wittekind, C., Kubick, C., Kassahun, W.T., Schumacher, G., Moebius, C., Gassler, N., Schopow, N., *et al.* (2016). Organotypic slice cultures of human gastric and esophagogastric junction cancer. Cancer medicine *5*, 1444-1453.

Koinis, F., Vetsika, E.K., Aggouraki, D., Skalidaki, E., Koutoulaki, A., Gkioulmpasani, M., Georgoulias, V., and Kotsakis, A. (2016). Effect of First-Line Treatment on Myeloid-Derived Suppressor Cells' Subpopulations in the Peripheral Blood of Patients with Non-Small Cell Lung Cancer. Journal of thoracic oncology : official publication of the International Association for the Study of Lung Cancer *11*, 1263-1272.

Koivunen, J.P., Kim, J., Lee, J., Rogers, A.M., Park, J.O., Zhao, X., Naoki, K., Okamoto, I., Nakagawa, K., Yeap, B.Y., *et al.* (2008). Mutations in the LKB1 tumour suppressor are frequently detected in tumours from Caucasian but not Asian lung cancer patients. British journal of cancer *99*, 245-252.

Koyama, S., Akbay, E.A., Li, Y.Y., Aref, A.R., Skoulidis, F., Herter-Sprie, G.S., Buczkowski, K.A., Liu, Y., Awad, M.M., Denning, W.L., *et al.* (2016). STK11/LKB1 Deficiency Promotes Neutrophil Recruitment and Proinflammatory Cytokine Production to Suppress T-cell Activity in the Lung Tumor Microenvironment. Cancer research *76*, 999-1008.

Kress, M., May, E., Cassingena, R., and May, P. (1979). Simian virus 40-transformed cells express new species of proteins precipitable by anti-simian virus 40 tumor serum. Journal of virology *31*, 472-483.

Krumdieck, C.L. (2013). Development of a live tissue microtome: reflections of an amateur machinist. Xenobiotica; the fate of foreign compounds in biological systems *43*, 2-7.

Kruspig, B., Monteverde, T., Neidler, S., Hock, A., Kerr, E., Nixon, C., Clark, W., Hedley, A., Laing, S., Coffelt, S.B., *et al.* (2018). The ERBB network facilitates KRAS-driven lung tumorigenesis. Science translational medicine *10*.

Kuner, R., Muley, T., Meister, M., Ruschhaupt, M., Buness, A., Xu, E.C., Schnabel, P., Warth, A., Poustka, A., Sultmann, H., *et al.* (2009). Global gene expression analysis reveals specific patterns of cell junctions in non-small cell lung cancer subtypes. Lung cancer (Amsterdam, Netherlands) *63*, 32-38.

Kurppa, K.J., Denessiouk, K., Johnson, M.S., and Elenius, K. (2016). Activating ERBB4 mutations in non-small cell lung cancer. Oncogene *35*, 1283-1291.

Lane, D.P., and Crawford, L.V. (1979). T antigen is bound to a host protein in SV40-transformed cells. Nature *278*, 261-263.

Lassen, U., Osterlind, K., Hansen, M., Dombernowsky, P., Bergman, B., and Hansen, H.H. (1995). Long-term survival in small-cell lung cancer: posttreatment characteristics in patients surviving 5 to 18+ years--an analysis of 1,714 consecutive patients. Journal of clinical oncology : official journal of the American Society of Clinical Oncology *13*, 1215-1220.

Lee, C.L., Moding, E.J., Huang, X., Li, Y., Woodlief, L.Z., Rodrigues, R.C., Ma, Y., and Kirsch, D.G. (2012). Generation of primary tumors with Flp recombinase in FRT-flanked p53 mice. Disease models & mechanisms *5*, 397-402.

Lee, J., Kim, S., Kim, P., Liu, X., Lee, T., Kim, K.M., Do, I.G., Park, J.O., Park, S.H., Jang, J., *et al.* (2013). A novel proteomics-based clinical diagnostics technology identifies heterogeneity in activated signaling pathways in gastric cancers. PloS one *8*, e54644.

Lee, K.F., Simon, H., Chen, H., Bates, B., Hung, M.C., and Hauser, C. (1995). Requirement for neuregulin receptor erbB2 in neural and cardiac development. Nature *378*, 394-398.

Lee, W.C., Diao, L., Wang, J., Zhang, J., Roarty, E.B., Varghese, S., Chow, C.W., Fujimoto, J., Behrens, C., Cascone, T., *et al.* (2018). Multiregion gene expression profiling reveals heterogeneity in molecular subtypes and immunotherapy response signatures in lung

cancer. Modern pathology : an official journal of the United States and Canadian Academy of Pathology, Inc.

Leeman, K.T., Fillmore, C.M., and Kim, C.F. (2014). Lung stem and progenitor cells in tissue homeostasis and disease. Current topics in developmental biology *107*, 207-233.

Lefrancais, E., Ortiz-Munoz, G., Caudrillier, A., Mallavia, B., Liu, F., Sayah, D.M., Thornton, E.E., Headley, M.B., David, T., Coughlin, S.R., *et al.* (2017). The lung is a site of platelet biogenesis and a reservoir for haematopoietic progenitors. Nature *544*, 105-109.

Levrero, M., De Laurenzi, V., Costanzo, A., Gong, J., Wang, J.Y., and Melino, G. (2000). The p53/p63/p73 family of transcription factors: overlapping and distinct functions. Journal of cell science *113 (Pt 10)*, 1661-1670.

Li, C., Sun, Y., Fang, R., Han, X., Luo, X., Wang, R., Pan, Y., Hu, H., Zhang, Y., Pao, W., *et al.* (2012). Lung adenocarcinomas with HER2-activating mutations are associated with distinct clinical features and HER2/EGFR copy number gains. Journal of thoracic oncology : official publication of the International Association for the Study of Lung Cancer *7*, 85-89.

Li, F., Han, X., Li, F., Wang, R., Wang, H., Gao, Y., Wang, X., Fang, Z., Zhang, W., Yao, S., *et al.* (2015a). LKB1 Inactivation Elicits a Redox Imbalance to Modulate Non-small Cell Lung Cancer Plasticity and Therapeutic Response. Cancer cell *27*, 698-711.

Li, F., He, J., Wei, J., Cho, W.C., and Liu, X. (2015b). Diversity of epithelial stem cell types in adult lung. Stem cells international *2015*, 728307.

Li, L., Wei, Y., Van Winkle, L., Zhang, Q.Y., Zhou, X., Hu, J., Xie, F., Kluetzman, K., and Ding, X. (2011). Generation and characterization of a Cyp2f2-null mouse and studies on the role of CYP2F2 in naphthalene-induced toxicity in the lung and nasal olfactory mucosa. The Journal of pharmacology and experimental therapeutics *339*, 62-71.

Li, S., Liu, S., Deng, J., Akbay, E.A., Hai, J., Ambrogio, C., Zhang, L., Zhou, F., Jenkins, R.W., Adeegbe, D.O., *et al.* (2018). Assessing Therapeutic Efficacy of MEK Inhibition in a KRAS G12C-Driven Mouse Model of Lung Cancer. Clinical cancer research : an official journal of the American Association for Cancer Research.

Li, Y., Li, F., Jiang, F., Lv, X., Zhang, R., Lu, A., and Zhang, G. (2016). A Mini-Review for Cancer Immunotherapy: Molecular Understanding of PD-1/PD-L1 Pathway & Translational Blockade of Immune Checkpoints. International journal of molecular sciences *17*.

Litvak, A.M., Paik, P.K., Woo, K.M., Sima, C.S., Hellmann, M.D., Arcila, M.E., Ladanyi, M., Rudin, C.M., Kris, M.G., and Riely, G.J. (2014). Clinical characteristics and course of 63 patients with BRAF mutant lung cancers. Journal of thoracic oncology : official publication of the International Association for the Study of Lung Cancer *9*, 1669-1674.

Liu, C.Y., Wang, Y.M., Wang, C.L., Feng, P.H., Ko, H.W., Liu, Y.H., Wu, Y.C., Chu, Y., Chung, F.T., Kuo, C.H., *et al.* (2010). Population alterations of L-arginase- and inducible nitric oxide synthase-expressed CD11b+/CD14(-)/CD15+/CD33+ myeloid-derived suppressor cells and CD8+ T lymphocytes in patients with advanced-stage non-small cell lung cancer. Journal of cancer research and clinical oncology *136*, 35-45.

Liu, H., Zhang, T., Ye, J., Li, H., Huang, J., Li, X., Wu, B., Huang, X., and Hou, J. (2012a). Tumor-infiltrating lymphocytes predict response to chemotherapy in patients with advance non-small cell lung cancer. Cancer immunology, immunotherapy : CII *61*, 1849-1856.

Liu, J., Cho, S.N., Akkanti, B., Jin, N., Mao, J., Long, W., Chen, T., Zhang, Y., Tang, X., Wistub, II, *et al.* (2015). ErbB2 Pathway Activation upon Smad4 Loss Promotes Lung Tumor Growth and Metastasis. Cell reports.

Liu, X., Krawczyk, E., Suprynowicz, F.A., Palechor-Ceron, N., Yuan, H., Dakic, A., Simic, V., Zheng, Y.L., Sripadhan, P., Chen, C., *et al.* (2017). Conditional reprogramming and

long-term expansion of normal and tumor cells from human biospecimens. Nature protocols *12*, 439-451.

Liu, X., Ory, V., Chapman, S., Yuan, H., Albanese, C., Kallakury, B., Timofeeva, O.A., Nealon, C., Dakic, A., Simic, V., *et al.* (2012b). ROCK inhibitor and feeder cells induce the conditional reprogramming of epithelial cells. Am J Pathol *180*, 599-607.

Liu, Y., Marks, K., Cowley, G.S., Carretero, J., Liu, Q., Nieland, T.J., Xu, C., Cohoon, T.J., Gao, P., Zhang, Y., *et al.* (2013). Metabolic and functional genomic studies identify deoxythymidylate kinase as a target in LKB1-mutant lung cancer. Cancer discovery *3*, 870-879.

Liu, Y., Zhang, J., Li, L., Yin, G., Zhang, J., Zheng, S., Cheung, H., Wu, N., Lu, N., Mao, X., *et al.* (2016). Genomic heterogeneity of multiple synchronous lung cancer. Nature communications *7*, 13200.

Loeb, K.R., and Loeb, L.A. (2000). Significance of multiple mutations in cancer. Carcinogenesis *21*, 379-385.

Loffredo Sampaolo, C. (1956). [Chick embryo heart in organotypic culture]. Bollettino della Societa italiana di biologia sperimentale *32*, 1580-1582.

Lynch, T.J., Bell, D.W., Sordella, R., Gurubhagavatula, S., Okimoto, R.A., Brannigan, B.W., Harris, P.L., Haserlat, S.M., Supko, J.G., Haluska, F.G., *et al.* (2004). Activating mutations in the epidermal growth factor receptor underlying responsiveness of non-small-cell lung cancer to gefitinib. The New England journal of medicine *350*, 2129-2139.

Maeurer, M.J., Gollin, S.M., Martin, D., Swaney, W., Bryant, J., Castelli, C., Robbins, P., Parmiani, G., Storkus, W.J., and Lotze, M.T. (1996). Tumor escape from immune recognition: lethal recurrent melanoma in a patient associated with downregulation of the peptide transporter protein TAP-1 and loss of expression of the immunodominant MART-1/Melan-A antigen. The Journal of clinical investigation *98*, 1633-1641.

Mainardi, S., Mijimolle, N., Francoz, S., Vicente-Duenas, C., Sanchez-Garcia, I., and Barbacid, M. (2014). Identification of cancer initiating cells in K-Ras driven lung adenocarcinoma. Proceedings of the National Academy of Sciences of the United States of America *111*, 255-260.

Majumder, B., Baraneedharan, U., Thiyagarajan, S., Radhakrishnan, P., Narasimhan, H., Dhandapani, M., Brijwani, N., Pinto, D.D., Prasath, A., Shanthappa, B.U., *et al.* (2015). Predicting clinical response to anticancer drugs using an ex vivo platform that captures tumour heterogeneity. Nature communications *6*, 6169.

Malkoski, S.P., Cleaver, T.G., Thompson, J.J., Sutton, W.P., Haeger, S.M., Rodriguez, K.J., Lu, S.L., Merrick, D., and Wang, X.J. (2014). Role of PTEN in basal cell derived lung carcinogenesis. Molecular carcinogenesis *53*, 841-846.

Malkoski, S.P., Haeger, S.M., Cleaver, T.G., Rodriguez, K.J., Li, H., Lu, S.L., Feser, W.J., Baron, A.E., Merrick, D., Lighthall, J.G., *et al.* (2012). Loss of transforming growth factor beta type II receptor increases aggressive tumor behavior and reduces survival in lung adenocarcinoma and squamous cell carcinoma. Clinical cancer research : an official journal of the American Association for Cancer Research *18*, 2173-2183.

Manchado, E., Weissmueller, S., Morris, J.P.t., Chen, C.C., Wullenkord, R., Lujambio, A., de Stanchina, E., Poirier, J.T., Gainor, J.F., Corcoran, R.B., *et al.* (2016). A combinatorial strategy for treating KRAS-mutant lung cancer. Nature *534*, 647-651.

Manning, G., Whyte, D.B., Martinez, R., Hunter, T., and Sudarsanam, S. (2002). The protein kinase complement of the human genome. Science (New York, NY) *298*, 1912-1934.

Mao, L., Lee, J.S., Kurie, J.M., Fan, Y.H., Lippman, S.M., Lee, J.J., Ro, J.Y., Broxson, A., Yu, R., Morice, R.C., *et al.* (1997). Clonal genetic alterations in the lungs of current and former smokers. Journal of the National Cancer Institute *89*, 857-862.

Marshall, E.A., Ng, K.W., Kung, S.H., Conway, E.M., Martinez, V.D., Halvorsen, E.C., Rowbotham, D.A., Vucic, E.A., Plumb, A.W., Becker-Santos, D.D., *et al.* (2016). Emerging roles of T helper 17 and regulatory T cells in lung cancer progression and metastasis. Molecular cancer *15*, 67.

Martin, S.G., and St Johnston, D. (2003). A role for Drosophila LKB1 in anterior-posterior axis formation and epithelial polarity. Nature *421*, 379-384.

Marvel, D., and Gabrilovich, D.I. (2015). Myeloid-derived suppressor cells in the tumor microenvironment: expect the unexpected. The Journal of clinical investigation *125*, 3356-3364.

Massarelli, E., Varella-Garcia, M., Tang, X., Xavier, A.C., Ozburn, N.C., Liu, D.D., Bekele, B.N., Herbst, R.S., and Wistuba, II (2007). KRAS mutation is an important predictor of resistance to therapy with epidermal growth factor receptor tyrosine kinase inhibitors in non-small-cell lung cancer. Clinical cancer research : an official journal of the American Association for Cancer Research *13*, 2890-2896.

Matsumoto, S., Iwakawa, R., Takahashi, K., Kohno, T., Nakanishi, Y., Matsuno, Y., Suzuki, K., Nakamoto, M., Shimizu, E., Minna, J.D., *et al.* (2007). Prevalence and specificity of LKB1 genetic alterations in lung cancers. Oncogene *26*, 5911-5918.

McCubrey, J.A., Steelman, L.S., Chappell, W.H., Abrams, S.L., Montalto, G., Cervello, M., Nicoletti, F., Fagone, P., Malaponte, G., Mazzarino, M.C., *et al.* (2012). Mutations and deregulation of Ras/Raf/MEK/ERK and PI3K/PTEN/Akt/mTOR cascades which alter therapy response. Oncotarget *3*, 954-987.

McLure, K.G., and Lee, P.W. (1998). How p53 binds DNA as a tetramer. The EMBO journal *17*, 3342-3350.

Meijer, T.G., Naipal, K.A., Jager, A., and van Gent, D.C. (2017). Ex vivo tumor culture systems for functional drug testing and therapy response prediction. Future science OA *3*, Fso190.

Melino, G., De Laurenzi, V., and Vousden, K.H. (2002). p73: Friend or foe in tumorigenesis. Nature reviews Cancer *2*, 605-615.

Merz, F., Gaunitz, F., Dehghani, F., Renner, C., Meixensberger, J., Gutenberg, A., Giese, A., Schopow, K., Hellwig, C., Schafer, M., *et al.* (2013). Organotypic slice cultures of human glioblastoma reveal different susceptibilities to treatments. Neuro-oncology *15*, 670-681.

Meuwissen, R., and Berns, A. (2005). Mouse models for human lung cancer. Genes & development *19*, 643-664.

Meuwissen, R., Linn, S.C., Linnoila, R.I., Zevenhoven, J., Mooi, W.J., and Berns, A. (2003). Induction of small cell lung cancer by somatic inactivation of both Trp53 and Rb1 in a conditional mouse model. Cancer cell *4*, 181-189.

Meuwissen, R., Linn, S.C., van der Valk, M., Mooi, W.J., and Berns, A. (2001). Mouse model for lung tumorigenesis through Cre/lox controlled sporadic activation of the K-Ras oncogene. Oncogene *20*, 6551-6558.

Meylan, E., Dooley, A.L., Feldser, D.M., Shen, L., Turk, E., Ouyang, C., and Jacks, T. (2009). Requirement for NF-kappaB signalling in a mouse model of lung adenocarcinoma. Nature *462*, 104-107.

Midha, A., Dearden, S., and McCormack, R. (2015). EGFR mutation incidence in non-small-cell lung cancer of adenocarcinoma histology: a systematic review and global map by ethnicity (mutMapII). American journal of cancer research *5*, 2892-2911.

Miettinen, P.J., Berger, J.E., Meneses, J., Phung, Y., Pedersen, R.A., Werb, Z., and Derynck, R. (1995). Epithelial immaturity and multiorgan failure in mice lacking epidermal growth factor receptor. Nature *376*, 337-341.

Miller, V.A., Kris, M.G., Shah, N., Patel, J., Azzoli, C., Gomez, J., Krug, L.M., Pao, W., Rizvi, N., Pizzo, B., *et al.* (2004). Bronchioloalveolar pathologic subtype and smoking history

predict sensitivity to gefitinib in advanced non-small-cell lung cancer. Journal of clinical oncology : official journal of the American Society of Clinical Oncology *22*, 1103-1109.

Mills, A.A., Zheng, B., Wang, X.J., Vogel, H., Roop, D.R., and Bradley, A. (1999). p63 is a p53 homologue required for limb and epidermal morphogenesis. Nature *398*, 708-713.

Mitsudomi, T., Viallet, J., Mulshine, J.L., Linnoila, R.I., Minna, J.D., and Gazdar, A.F. (1991). Mutations of ras genes distinguish a subset of non-small-cell lung cancer cell lines from small-cell lung cancer cell lines. Oncogene *6*, 1353-1362.

Moll, H.P., Pranz, K., Musteanu, M., Grabner, B., Hruschka, N., Mohrherr, J., Aigner, P., Stiedl, P., Brcic, L., Laszlo, V., *et al.* (2018). Afatinib restrains K-RAS-driven lung tumorigenesis. Science translational medicine *10*.

Momcilovic, M., McMickle, R., Abt, E., Seki, A., Simko, S.A., Magyar, C., Stout, D.B., Fishbein, M.C., Walser, T.C., Dubinett, S.M., *et al.* (2015). Heightening Energetic Stress Selectively Targets LKB1-Deficient Non-Small Cell Lung Cancers. Cancer research *75*, 4910-4922.

Moran, T., Palmero, R., Provencio, M., Insa, A., Majem, M., Reguart, N., Bosch-Barrera, J., Isla, D., Costa, E.C., Lee, C., *et al.* (2017). A phase Ib trial of continuous once-daily oral afatinib plus sirolimus in patients with epidermal growth factor receptor mutation-positive non-small cell lung cancer and/or disease progression following prior erlotinib or gefitinib. Lung cancer (Amsterdam, Netherlands) *108*, 154-160.

Morgan, K.M., Riedlinger, G.M., Rosenfeld, J., Ganesan, S., and Pine, S.R. (2017). Patient-Derived Xenograft Models of Non-Small Cell Lung Cancer and Their Potential Utility in Personalized Medicine. Frontiers in oncology *7*, 2.

Moya-Horno, I., Viteri, S., Karachaliou, N., and Rosell, R. (2018). Combination of immunotherapy with targeted therapies in advanced non-small cell lung cancer (NSCLC). Therapeutic advances in medical oncology *10*, 1758834017745012.

Mukhopadhyay, A., Berrett, K.C., Kc, U., Clair, P.M., Pop, S.M., Carr, S.R., Witt, B.L., and Oliver, T.G. (2014). Sox2 cooperates with Lkb1 loss in a mouse model of squamous cell lung cancer. Cell reports *8*, 40-49.

Multhoff, G., Molls, M., and Radons, J. (2011). Chronic inflammation in cancer development. Frontiers in immunology *2*, 98.

Mumenthaler, S.M., Foo, J., Choi, N.C., Heise, N., Leder, K., Agus, D.B., Pao, W., Michor, F., and Mallick, P. (2015). The Impact of Microenvironmental Heterogeneity on the Evolution of Drug Resistance in Cancer Cells. Cancer informatics *14*, 19-31.

Munder, M., Schneider, H., Luckner, C., Giese, T., Langhans, C.D., Fuentes, J.M., Kropf, P., Mueller, I., Kolb, A., Modolell, M., *et al.* (2006). Suppression of T-cell functions by human granulocyte arginase. Blood *108*, 1627-1634.

Naipal, K.A., Verkaik, N.S., Ameziane, N., van Deurzen, C.H., Ter Brugge, P., Meijers, M., Sieuwerts, A.M., Martens, J.W., O'Connor, M.J., Vrieling, H., *et al.* (2014). Functional ex vivo assay to select homologous recombination-deficient breast tumors for PARP inhibitor treatment. Clinical cancer research : an official journal of the American Association for Cancer Research *20*, 4816-4826.

Naipal, K.A., Verkaik, N.S., Sanchez, H., van Deurzen, C.H., den Bakker, M.A., Hoeijmakers, J.H., Kanaar, R., Vreeswijk, M.P., Jager, A., and van Gent, D.C. (2016). Tumor slice culture system to assess drug response of primary breast cancer. BMC Cancer *16*, 78.

Nakagawa, K., Yasumitu, T., Fukuhara, K., Shiono, H., and Kikui, M. (2003). Poor prognosis after lung resection for patients with adenosquamous carcinoma of the lung. The Annals of thoracic surgery *75*, 1740-1744.

Nomura, M., Shigematsu, H., Li, L., Suzuki, M., Takahashi, T., Estess, P., Siegelman, M., Feng, Z., Kato, H., Marchetti, A., *et al.* (2007). Polymorphisms, mutations, and amplification of the EGFR gene in non-small cell lung cancers. PLoS medicine *4*, e125.

Nowell, P.C. (1976). The clonal evolution of tumor cell populations. Science (New York, NY) *194*, 23-28.

Novikova, D.S., Garabadzhiu, A.V., Melino, G., Barlev, N.A., and Tribulovich, V.G. (2015). AMP-activated protein kinase: structure, function, and role in pathological processes. Biochemistry Biokhimiia *80*, 127-144.

Ochocki, J.D., and Simon, M.C. (2013). Nutrient-sensing pathways and metabolic regulation in stem cells. The Journal of cell biology *203*, 23-33.

Okudela, K., Suzuki, M., Kageyama, S., Bunai, T., Nagura, K., Igarashi, H., Takamochi, K., Suzuki, K., Yamada, T., Niwa, H., *et al.* (2007). PIK3CA mutation and amplification in human lung cancer. Pathology international *57*, 664-671.

Olivier, M., Eeles, R., Hollstein, M., Khan, M.A., Harris, C.C., and Hainaut, P. (2002). The IARC TP53 database: new online mutation analysis and recommendations to users. Human mutation *19*, 607-614.

Ostrand-Rosenberg, S., and Sinha, P. (2009). Myeloid-derived suppressor cells: linking inflammation and cancer. Journal of immunology (Baltimore, Md : 1950) *182*, 4499-4506.

Ou, S.H., Kwak, E.L., Siwak-Tapp, C., Dy, J., Bergethon, K., Clark, J.W., Camidge, D.R., Solomon, B.J., Maki, R.G., Bang, Y.J., *et al.* (2011). Activity of crizotinib (PF02341066), a dual mesenchymal-epithelial transition (MET) and anaplastic lymphoma kinase (ALK) inhibitor, in a non-small cell lung cancer patient with de novo MET amplification. Journal of thoracic oncology : official publication of the International Association for the Study of Lung Cancer *6*, 942-946.

Owen, M.R., Doran, E., and Halestrap, A.P. (2000). Evidence that metformin exerts its anti-diabetic effects through inhibition of complex 1 of the mitochondrial respiratory chain. The Biochemical journal *348 Pt 3*, 607-614.

Palmer, A.C., and Sorger, P.K. (2017). Combination Cancer Therapy Can Confer Benefit via Patient-to-Patient Variability without Drug Additivity or Synergy. Cell *171*, 1678-1691.e1613.

Pang, X., and Liu, M. (2016). A combination therapy for KRAS-mutant lung cancer by targeting synthetic lethal partners of mutant KRAS. Chinese journal of cancer *35*, 92.

Pao, W., Miller, V., Zakowski, M., Doherty, J., Politi, K., Sarkaria, I., Singh, B., Heelan, R., Rusch, V., Fulton, L., *et al.* (2004). EGF receptor gene mutations are common in lung cancers from "never smokers" and are associated with sensitivity of tumors to gefitinib and erlotinib. Proceedings of the National Academy of Sciences of the United States of America *101*, 13306-13311.

Pao, W., Wang, T.Y., Riely, G.J., Miller, V.A., Pan, Q., Ladanyi, M., Zakowski, M.F., Heelan, R.T., Kris, M.G., and Varmus, H.E. (2005). KRAS mutations and primary resistance of lung adenocarcinomas to gefitinib or erlotinib. PLoS medicine *2*, e17.

Papageorgiou, A., Stravoravdi, P., Sahpazidou, D., Natsis, K., Chrysogelou, E., and Toliou, T. (2000). Effect of navelbine on inhibition of tumor growth, cellular differentiation and estrogen receptor status on Lewis lung carcinoma. Chemotherapy *46*, 188-194.

Parada, L.F., Tabin, C.J., Shih, C., and Weinberg, R.A. (1982). Human EJ bladder carcinoma oncogene is homologue of Harvey sarcoma virus ras gene. Nature *297*, 474-478.

Peifer, M., Fernandez-Cuesta, L., Sos, M.L., George, J., Seidel, D., Kasper, L.H., Plenker, D., Leenders, F., Sun, R., Zander, T., *et al.* (2012). Integrative genome analyses identify key somatic driver mutations of small-cell lung cancer. Nature genetics *44*, 1104-1110.

Pemovska, T., Kontro, M., Yadav, B., Edgren, H., Eldfors, S., Szwajda, A., Almusa, H., Bespalov, M.M., Ellonen, P., Elonen, E., *et al.* (2013). Individualized systems medicine strategy to tailor treatments for patients with chemorefractory acute myeloid leukemia. Cancer discovery *3*, 1416-1429.

Perera, S.A., Li, D., Shimamura, T., Raso, M.G., Ji, H., Chen, L., Borgman, C.L., Zaghlul, S., Brandstetter, K.A., Kubo, S., *et al.* (2009). HER2YVMA drives rapid development of adenosquamous lung tumors in mice that are sensitive to BIBW2992 and rapamycin combination therapy. Proceedings of the National Academy of Sciences of the United States of America *106*, 474-479.

Pfeifer, G.P., Denissenko, M.F., Olivier, M., Tretyakova, N., Hecht, S.S., and Hainaut, P. (2002). Tobacco smoke carcinogens, DNA damage and p53 mutations in smoking-associated cancers. Oncogene *21*, 7435-7451.

Pfirschke, C., Engblom, C., Rickelt, S., Cortez-Retamozo, V., Garris, C., Pucci, F., Yamazaki, T., Poirier-Colame, V., Newton, A., Redouane, Y., *et al.* (2016). Immunogenic Chemotherapy Sensitizes Tumors to Checkpoint Blockade Therapy. Immunity *44*, 343-354.

Pillay, J., Tak, T., Kamp, V.M., and Koenderman, L. (2013). Immune suppression by neutrophils and granulocytic myeloid-derived suppressor cells: similarities and differences. Cellular and molecular life sciences : CMLS *70*, 3813-3827.

Pirie, K., Peto, R., Green, J., Reeves, G.K., and Beral, V. (2016). Lung cancer in never smokers in the UK Million Women Study. International journal of cancer *139*, 347-354.

Politi, K., Ayeni, D., and Lynch, T. (2015). The Next Wave of EGFR Tyrosine Kinase Inhibitors Enter the Clinic. Cancer cell *27*, 751-753.

Politi, K., Zakowski, M.F., Fan, P.D., Schonfeld, E.A., Pao, W., and Varmus, H.E. (2006). Lung adenocarcinomas induced in mice by mutant EGF receptors found in human lung cancers respond to a tyrosine kinase inhibitor or to down-regulation of the receptors. Genes & development *20*, 1496-1510.

Port, J.L.F., Muthalagu, N., Raja, M., Ceteci, F., Monteverde, T., Kruspig, B., Hedley, A., Kalna, G., Lilla, S., Neilson, L., *et al.* (2018). Colorectal tumors require NUAK1 for protection from oxidative stress. Cancer discovery.

Powrozek, T., Krawczyk, P., Ramlau, R., Sura, S., Wojas-Krawczyk, K., Kucharczyk, T., Walczyna, B., Szumilo, J., Szyszka-Barth, K., Milecki, P., *et al.* (2014). EGFR gene mutations in patients with adenosquamous lung carcinoma. Asia-Pacific journal of clinical oncology *10*, 340-345.

Prahallad, A., Sun, C., Huang, S., Di Nicolantonio, F., Salazar, R., Zecchin, D., Beijersbergen, R.L., Bardelli, A., and Bernards, R. (2012). Unresponsiveness of colon cancer to BRAF(V600E) inhibition through feedback activation of EGFR. Nature *483*, 100-103.

Prior, I.A., and Hancock, J.F. (2012). Ras trafficking, localization and compartmentalized signalling. Seminars in cell & developmental biology *23*, 145-153.

Rask, L., Fregil, M., Hogdall, E., Mitchelmore, C., and Eriksen, J. (2013). Development of a metastatic fluorescent Lewis Lung carcinoma mouse model: identification of mRNAs and microRNAs involved in tumor invasion. Gene *517*, 72-81.

Rawlins, E.L., Okubo, T., Xue, Y., Brass, D.M., Auten, R.L., Hasegawa, H., Wang, F., and Hogan, B.L. (2009). The role of Scgb1a1+ Clara cells in the long-term maintenance and repair of lung airway, but not alveolar, epithelium. Cell stem cell *4*, 525-534.

Repasky, G.A., Chenette, E.J., and Der, C.J. (2004). Renewing the conspiracy theory debate: does Raf function alone to mediate Ras oncogenesis? Trends in cell biology *14*, 639-647.

Reya, T., Morrison, S.J., Clarke, M.F., and Weissman, I.L. (2001). Stem cells, cancer, and cancer stem cells. Nature *414*, 105-111.

Rittmeyer, A., Barlesi, F., Waterkamp, D., Park, K., Ciardiello, F., von Pawel, J., Gadgeel, S.M., Hida, T., Kowalski, D.M., Dols, M.C., *et al.* (2017). Atezolizumab versus docetaxel in patients with previously treated non-small-cell lung cancer (OAK): a phase 3, open-label, multicentre randomised controlled trial. Lancet (London, England) *389*, 255-265.

Rocco, G., Morabito, A., Leone, A., Muto, P., Fiore, F., and Budillon, A. (2016). Management of non-small cell lung cancer in the era of personalized medicine. The international journal of biochemistry & cell biology *78*, 173-179.

Rock, J.R., Barkauskas, C.E., Cronce, M.J., Xue, Y., Harris, J.R., Liang, J., Noble, P.W., and Hogan, B.L. (2011). Multiple stromal populations contribute to pulmonary fibrosis without evidence for epithelial to mesenchymal transition. Proceedings of the National Academy of Sciences of the United States of America *108*, E1475-1483.

Rock, J.R., Onaitis, M.W., Rawlins, E.L., Lu, Y., Clark, C.P., Xue, Y., Randell, S.H., and Hogan, B.L. (2009). Basal cells as stem cells of the mouse trachea and human airway epithelium. Proceedings of the National Academy of Sciences of the United States of America *106*, 12771-12775.

Rock, J.R., Randell, S.H., and Hogan, B.L. (2010). Airway basal stem cells: a perspective on their roles in epithelial homeostasis and remodeling. Disease models & mechanisms *3*, 545-556.

Rodriguez, P.C., and Ochoa, A.C. (2008). Arginine regulation by myeloid derived suppressor cells and tolerance in cancer: mechanisms and therapeutic perspectives. Immunological reviews *222*, 180-191.

Rodriguez, P.C., Zea, A.H., Culotta, K.S., Zabaleta, J., Ochoa, J.B., and Ochoa, A.C. (2002). Regulation of T cell receptor CD3zeta chain expression by L-arginine. The Journal of biological chemistry *277*, 21123-21129.

Rosell, R., Carcereny, E., Gervais, R., Vergnenegre, A., Massuti, B., Felip, E., Palmero, R., Garcia-Gomez, R., Pallares, C., Sanchez, J.M., *et al.* (2012). Erlotinib versus standard chemotherapy as first-line treatment for European patients with advanced EGFR mutation-positive non-small-cell lung cancer (EURTAC): a multicentre, open-label, randomised phase 3 trial. The Lancet Oncology *13*, 239-246.

Rosell, R., Karachaliou, N., Morales-Espinosa, D., Costa, C., Molina, M.A., Sansano, I., Gasco, A., Viteri, S., Massuti, B., Wei, J., *et al.* (2013). Adaptive resistance to targeted therapies in cancer. Translational lung cancer research *2*, 152-159.

Rosell, R., Moran, T., Queralt, C., Porta, R., Cardenal, F., Camps, C., Majem, M., Lopez-Vivanco, G., Isla, D., Provencio, M., *et al.* (2009). Screening for epidermal growth factor receptor mutations in lung cancer. The New England journal of medicine *361*, 958-967.

Rudin, C.M., Durinck, S., Stawiski, E.W., Poirier, J.T., Modrusan, Z., Shames, D.S., Bergbower, E.A., Guan, Y., Shin, J., Guillory, J., *et al.* (2012). Comprehensive genomic analysis identifies SOX2 as a frequently amplified gene in small-cell lung cancer. Nature genetics *44*, 1111-1116.

Ruiz-Ceja, K.A., and Chirino, Y.I. (2017). Current FDA-approved treatments for non-small cell lung cancer and potential biomarkers for its detection. Biomedicine & pharmacotherapy = Biomedecine & pharmacotherapie *90*, 24-37.

Ryckman, C., Vandal, K., Rouleau, P., Talbot, M., and Tessier, P.A. (2003). Proinflammatory activities of S100: proteins S100A8, S100A9, and S100A8/A9 induce neutrophil chemotaxis and adhesion. Journal of immunology (Baltimore, Md : 1950) *170*, 3233-3242.

Sadowski, P.D. (1995). The Flp recombinase of the 2-microns plasmid of Saccharomyces cerevisiae. Progress in nucleic acid research and molecular biology *51*, 53-91.

Saeed, K., Rahkama, V., Eldfors, S., Bychkov, D., Mpindi, J.P., Yadav, B., Paavolainen, L., Aittokallio, T., Heckman, C., Wennerberg, K., *et al.* (2017). Comprehensive Drug Testing of Patient-derived Conditionally Reprogrammed Cells from Castration-resistant Prostate Cancer. European urology *71*, 319-327.

Sakai, Y., Sasahira, T., Ohmori, H., Yoshida, K., and Kuniyasu, H. (2006). Conjugated linoleic acid reduced metastasized LL2 tumors in mouse peritoneum. Virchows Archiv : an international journal of pathology *449*, 341-347.

Sanchez-Cespedes, M. (2007). A role for LKB1 gene in human cancer beyond the Peutz-Jeghers syndrome. Oncogene *26*, 7825-7832.

Sanchez-Cespedes, M., Parrella, P., Esteller, M., Nomoto, S., Trink, B., Engles, J.M., Westra, W.H., Herman, J.G., and Sidransky, D. (2002). Inactivation of LKB1/STK11 is a common event in adenocarcinomas of the lung. Cancer research *62*, 3659-3662.

Santos, E., Tronick, S.R., Aaronson, S.A., Pulciani, S., and Barbacid, M. (1982). T24 human bladder carcinoma oncogene is an activated form of the normal human homologue of BALB- and Harvey-MSV transforming genes. Nature *298*, 343-347.

Sasaki, H., Yokota, K., Hikosaka, Y., Moriyama, S., Yano, M., and Fujii, Y. (2012). Increased Sox2 copy number in lung squamous cell carcinomas. Experimental and therapeutic medicine *3*, 44-48.

Sasaki, T., Koivunen, J., Ogino, A., Yanagita, M., Nikiforow, S., Zheng, W., Lathan, C., Marcoux, J.P., Du, J., Okuda, K., *et al.* (2011). A novel ALK secondary mutation and EGFR signaling cause resistance to ALK kinase inhibitors. Cancer research *71*, 6051-6060.

Sasaki, T., Rodig, S.J., Chirieac, L.R., and Janne, P.A. (2010). The biology and treatment of EML4-ALK non-small cell lung cancer. European journal of cancer (Oxford, England : 1990) *46*, 1773-1780.

Schaber, M.D., O'Hara, M.B., Garsky, V.M., Mosser, S.C., Bergstrom, J.D., Moores, S.L., Marshall, M.S., Friedman, P.A., Dixon, R.A., and Gibbs, J.B. (1990). Polyisoprenylation of Ras in vitro by a farnesyl-protein transferase. The Journal of biological chemistry *265*, 14701-14704.

Schmid, K., Oehl, N., Wrba, F., Pirker, R., Pirker, C., and Filipits, M. (2009). EGFR/KRAS/BRAF mutations in primary lung adenocarcinomas and corresponding locoregional lymph node metastases. Clinical cancer research : an official journal of the American Association for Cancer Research *15*, 4554-4560.

Schramek, D., Kotsinas, A., Meixner, A., Wada, T., Elling, U., Pospisilik, J.A., Neely, G.G., Zwick, R.H., Sigl, V., Forni, G., *et al.* (2011). The stress kinase MKK7 couples oncogenic stress to p53 stability and tumor suppression. Nature genetics *43*, 212-219.

Serizawa, M., Takahashi, T., Yamamoto, N., and Koh, Y. (2013). Genomic aberrations associated with erlotinib resistance in non-small cell lung cancer cells. Anticancer research *33*, 5223-5233.

Shackelford, D.B., Abt, E., Gerken, L., Vasquez, D.S., Seki, A., Leblanc, M., Wei, L., Fishbein, M.C., Czernin, J., Mischel, P.S., *et al.* (2013). LKB1 inactivation dictates therapeutic response of non-small cell lung cancer to the metabolism drug phenformin. Cancer cell *23*, 143-158.

Shaw, A.T., Kim, D.W., Nakagawa, K., Seto, T., Crino, L., Ahn, M.J., De Pas, T., Besse, B., Solomon, B.J., Blackhall, F., *et al.* (2013). Crizotinib versus chemotherapy in advanced ALK-positive lung cancer. The New England journal of medicine *368*, 2385-2394.

Shepherd, F.A., Rodrigues Pereira, J., Ciuleanu, T., Tan, E.H., Hirsh, V., Thongprasert, S., Campos, D., Maoleekoonpiroj, S., Smylie, M., Martins, R., *et al.* (2005). Erlotinib in previously treated non-small-cell lung cancer. The New England journal of medicine *353*, 123-132.

Shi, X., Wu, H., Lu, J., Duan, H., Liu, X., and Liang, Z. (2016). Screening for major driver oncogene alterations in adenosquamous lung carcinoma using PCR coupled with next-generation and Sanger sequencing methods. Scientific reports *6*, 22297.

Shojaee, S., and Nana-Sinkam, P. (2017). Recent advances in the management of non-small cell lung cancer. F1000Research *6*, 2110.

Siegel, R.L., Miller, K.D., and Jemal, A. (2018). Cancer statistics, 2018. CA: a cancer journal for clinicians *68*, 7-30.

Singh, A., Misra, V., Thimmulappa, R.K., Lee, H., Ames, S., Hoque, M.O., Herman, J.G., Baylin, S.B., Sidransky, D., Gabrielson, E., *et al.* (2006). Dysfunctional KEAP1-NRF2 interaction in non-small-cell lung cancer. PLoS medicine *3*, e420.

Singh, M., Lima, A., Molina, R., Hamilton, P., Clermont, A.C., Devasthali, V., Thompson, J.D., Cheng, J.H., Bou Reslan, H., Ho, C.C., *et al.* (2010). Assessing therapeutic responses in Kras mutant cancers using genetically engineered mouse models. Nature biotechnology *28*, 585-593.

Singh, S.R. (2012). Stem cell niche in tissue homeostasis, aging and cancer. Current medicinal chemistry *19*, 5965-5974.

Sinha, P., Okoro, C., Foell, D., Freeze, H.H., Ostrand-Rosenberg, S., and Srikrishna, G. (2008). Proinflammatory S100 proteins regulate the accumulation of myeloid-derived suppressor cells. Journal of immunology (Baltimore, Md : 1950) *181*, 4666-4675.

Skoulidis, F., Byers, L.A., Diao, L., Papadimitrakopoulou, V.A., Tong, P., Izzo, J., Behrens, C., Kadara, H., Parra, E.R., Canales, J.R., *et al.* (2015). Co-occurring genomic alterations define major subsets of KRAS-mutant lung adenocarcinoma with distinct biology, immune profiles, and therapeutic vulnerabilities. Cancer discovery *5*, 860-877.

Smith, E.L., Zamarin, D., and Lesokhin, A.M. (2014). Harnessing the immune system for cancer therapy. Current opinion in oncology *26*, 600-607.

Snyder, E.L., Watanabe, H., Magendantz, M., Hoersch, S., Chen, T.A., Wang, D.G., Crowley, D., Whittaker, C.A., Meyerson, M., Kimura, S., *et al.* (2013). Nkx2-1 represses a latent gastric differentiation program in lung adenocarcinoma. Molecular cell *50*, 185-199.

Soda, M., Choi, Y.L., Enomoto, M., Takada, S., Yamashita, Y., Ishikawa, S., Fujiwara, S., Watanabe, H., Kurashina, K., Hatanaka, H., *et al.* (2007). Identification of the transforming EML4-ALK fusion gene in non-small-cell lung cancer. Nature *448*, 561-566.

Soda, M., Takada, S., Takeuchi, K., Choi, Y.L., Enomoto, M., Ueno, T., Haruta, H., Hamada, T., Yamashita, Y., Ishikawa, Y., *et al.* (2008). A mouse model for EML4-ALK-positive lung cancer. Proceedings of the National Academy of Sciences of the United States of America *105*, 19893-19897.

Song, X., Krelin, Y., Dvorkin, T., Bjorkdahl, O., Segal, S., Dinarello, C.A., Voronov, E., and Apte, R.N. (2005). CD11b+/Gr-1+ immature myeloid cells mediate suppression of T cells in mice bearing tumors of IL-1beta-secreting cells. Journal of immunology (Baltimore, Md : 1950) *175*, 8200-8208.

Song, Z., Lin, B., Shao, L., and Zhang, Y. (2013). Therapeutic efficacy of gefitinib and erlotinib in patients with advanced lung adenosquamous carcinoma. Journal of the Chinese Medical Association : JCMA *76*, 481-485.

Sordella, R., Bell, D.W., Haber, D.A., and Settleman, J. (2004). Gefitinib-sensitizing EGFR mutations in lung cancer activate anti-apoptotic pathways. Science (New York, NY) *305*, 1163-1167.

Soria, J.C., Felip, E., Cobo, M., Lu, S., Syrigos, K., Lee, K.H., Goker, E., Georgoulias, V., Li, W., Isla, D., *et al.* (2015). Afatinib versus erlotinib as second-line treatment of patients with advanced squamous cell carcinoma of the lung (LUX-Lung 8): an open-label randomised controlled phase 3 trial. The Lancet Oncology *16*, 897-907.

Sos, M.L., Michel, K., Zander, T., Weiss, J., Frommolt, P., Peifer, M., Li, D., Ullrich, R., Koker, M., Fischer, F., *et al.* (2009). Predicting drug susceptibility of non-small cell lung cancers based on genetic lesions. The Journal of clinical investigation *119*, 1727-1740.

Sousa, S.F., Fernandes, P.A., and Ramos, M.J. (2008). Farnesyltransferase inhibitors: a detailed chemical view on an elusive biological problem. Current medicinal chemistry *15*, 1478-1492.

Spagnolo, D.M., Gyanchandani, R., Al-Kofahi, Y., Stern, A.M., Lezon, T.R., Gough, A., Meyer, D.E., Ginty, F., Sarachan, B., Fine, J., *et al.* (2016). Pointwise mutual information quantifies intratumor heterogeneity in tissue sections labeled with multiple fluorescent biomarkers. Journal of pathology informatics *7*, 47.

St Clair, S., and Manfredi, J.J. (2006). The dual specificity phosphatase Cdc25C is a direct target for transcriptional repression by the tumor suppressor p53. Cell cycle (Georgetown, Tex) *5*, 709-713.

Steiner, P., Joynes, C., Bassi, R., Wang, S., Tonra, J.R., Hadari, Y.R., and Hicklin, D.J. (2007). Tumor growth inhibition with cetuximab and chemotherapy in non-small cell lung cancer xenografts expressing wild-type and mutated epidermal growth factor receptor. Clinical cancer research : an official journal of the American Association for Cancer Research *13*, 1540-1551.

Stephens, P., Hunter, C., Bignell, G., Edkins, S., Davies, H., Teague, J., Stevens, C., O'Meara, S., Smith, R., Parker, A., *et al.* (2004). Lung cancer: intragenic ERBB2 kinase mutations in tumours. Nature *431*, 525-526.

Sternberg, N., and Hamilton, D. (1981). Bacteriophage P1 site-specific recombination. I. Recombination between loxP sites. Journal of molecular biology *150*, 467-486.

Subramanian, J., and Govindan, R. (2007). Lung cancer in never smokers: a review. Journal of clinical oncology : official journal of the American Society of Clinical Oncology *25*, 561-570.

Subramanian, J., and Govindan, R. (2013). Molecular profile of lung cancer in never smokers. EJC supplements : EJC : official journal of EORTC, European Organization for Research and Treatment of Cancer [et al] *11*, 248-253.

Sugaya, M., Takenoyama, M., Osaki, T., Yasuda, M., Nagashima, A., Sugio, K., and Yasumoto, K. (2002). Establishment of 15 cancer cell lines from patients with lung cancer and the potential tools for immunotherapy. Chest *122*, 282-288.

Sullivan, I., and Planchard, D. (2016). ALK inhibitors in non-small cell lung cancer: the latest evidence and developments. Therapeutic advances in medical oncology *8*, 32-47.

Sun, C., Hobor, S., Bertotti, A., Zecchin, D., Huang, S., Galimi, F., Cottino, F., Prahallad, A., Grernrum, W., Tzani, A., *et al.* (2014). Intrinsic resistance to MEK inhibition in KRAS mutant lung and colon cancer through transcriptional induction of ERBB3. Cell reports *7*, 86-93.

Sun, S., Schiller, J.H., and Gazdar, A.F. (2007). Lung cancer in never smokers--a different disease. Nature reviews Cancer *7*, 778-790.

Sutherland, K.D., Proost, N., Brouns, I., Adriaensen, D., Song, J.Y., and Berns, A. (2011). Cell of origin of small cell lung cancer: inactivation of Trp53 and Rb1 in distinct cell types of adult mouse lung. Cancer cell *19*, 754-764.

Sutherland, K.D., Song, J.Y., Kwon, M.C., Proost, N., Zevenhoven, J., and Berns, A. (2014). Multiple cells-of-origin of mutant K-Ras-induced mouse lung adenocarcinoma. Proceedings of the National Academy of Sciences of the United States of America *111*, 4952-4957.

Suzuki, A., Kusakai, G., Kishimoto, A., Lu, J., Ogura, T., and Esumi, H. (2003). ARK5 suppresses the cell death induced by nutrient starvation and death receptors via inhibition of

caspase 8 activation, but not by chemotherapeutic agents or UV irradiation. Oncogene *22*, 6177-6182.

Suzuki, Y., Orita, M., Shiraishi, M., Hayashi, K., and Sekiya, T. (1990). Detection of ras gene mutations in human lung cancers by single-strand conformation polymorphism analysis of polymerase chain reaction products. Oncogene *5*, 1037-1043.

Takagi, Y., Osada, H., Kuroishi, T., Mitsudomi, T., Kondo, M., Niimi, T., Saji, S., Gazdar, A.F., Takahashi, T., Minna, J.D., *et al.* (1998). p53 mutations in non-small-cell lung cancers occurring in individuals without a past history of active smoking. British journal of cancer *77*, 1568-1572.

Takahashi, T., Sonobe, M., Kobayashi, M., Yoshizawa, A., Menju, T., Nakayama, E., Mino, N., Iwakiri, S., Sato, K., Miyahara, R., *et al.* (2010). Clinicopathologic features of non-small-cell lung cancer with EML4-ALK fusion gene. Annals of surgical oncology *17*, 889-897.

Takahashi, T., Takahashi, T., Suzuki, H., Hida, T., Sekido, Y., Ariyoshi, Y., and Ueda, R. (1991). The p53 gene is very frequently mutated in small-cell lung cancer with a distinct nucleotide substitution pattern. Oncogene *6*, 1775-1778.

Taneja, T.K., and Sharma, S.K. (2004). Markers of small cell lung cancer. World journal of surgical oncology *2*, 10.

Terry, J., Leung, S., Laskin, J., Leslie, K.O., Gown, A.M., and Ionescu, D.N. (2010). Optimal immunohistochemical markers for distinguishing lung adenocarcinomas from squamous cell carcinomas in small tumor samples. The American journal of surgical pathology *34*, 1805-1811.

Thomas, K.R., and Capecchi, M.R. (1987). Site-directed mutagenesis by gene targeting in mouse embryo-derived stem cells. Cell *51*, 503-512.

Threadgill, D.W., Dlugosz, A.A., Hansen, L.A., Tennenbaum, T., Lichti, U., Yee, D., LaMantia, C., Mourton, T., Herrup, K., Harris, R.C., *et al.* (1995). Targeted disruption of mouse EGF receptor: effect of genetic background on mutant phenotype. Science (New York, NY) *269*, 230-234.

Thun, M.J., Hannan, L.M., Adams-Campbell, L.L., Boffetta, P., Buring, J.E., Feskanich, D., Flanders, W.D., Jee, S.H., Katanoda, K., Kolonel, L.N., *et al.* (2008). Lung cancer occurrence in never-smokers: an analysis of 13 cohorts and 22 cancer registry studies. PLoS medicine *5*, e185.

Tiainen, M., Ylikorkala, A., and Makela, T.P. (1999). Growth suppression by Lkb1 is mediated by a G(1) cell cycle arrest. Proceedings of the National Academy of Sciences of the United States of America *96*, 9248-9251.

Tidcombe, H., Jackson-Fisher, A., Mathers, K., Stern, D.F., Gassmann, M., and Golding, J.P. (2003). Neural and mammary gland defects in ErbB4 knockout mice genetically rescued from embryonic lethality. Proceedings of the National Academy of Sciences of the United States of America *100*, 8281-8286.

Tochigi, N., Dacic, S., Nikiforova, M., Cieply, K.M., and Yousem, S.A. (2011). Adenosquamous carcinoma of the lung: a microdissection study of KRAS and EGFR mutational and amplification status in a western patient population. American journal of clinical pathology *135*, 783-789.

Travis, W.D., Brambilla, E., Noguchi, M., Nicholson, A.G., Geisinger, K., Yatabe, Y., Ishikawa, Y., Wistuba, I., Flieder, D.B., Franklin, W., *et al.* (2013). Diagnosis of lung cancer in small biopsies and cytology: implications of the 2011 International Association for the Study of Lung Cancer/American Thoracic Society/European Respiratory Society classification. Archives of pathology & laboratory medicine *137*, 668-684.

Travis, W.D., Brambilla, E., Noguchi, M., Nicholson, A.G., Geisinger, K., Yatabe, Y., Powell, C.A., Beer, D., Riely, G., Garg, K., *et al.* (2011). International Association for the Study of

Lung Cancer/American Thoracic Society/European Respiratory Society: international multidisciplinary classification of lung adenocarcinoma: executive summary. Proceedings of the American Thoracic Society *8*, 381-385.

Tsai, F.D., Lopes, M.S., Zhou, M., Court, H., Ponce, O., Fiordalisi, J.J., Gierut, J.J., Cox, A.D., Haigis, K.M., and Philips, M.R. (2015). K-Ras4A splice variant is widely expressed in cancer and uses a hybrid membrane-targeting motif. Proceedings of the National Academy of Sciences of the United States of America *112*, 779-784.

Tsao, M.S., Sakurada, A., Cutz, J.C., Zhu, C.Q., Kamel-Reid, S., Squire, J., Lorimer, I., Zhang, T., Liu, N., Daneshmand, M., *et al.* (2005). Erlotinib in lung cancer - molecular and clinical predictors of outcome. The New England journal of medicine *353*, 133-144.

Tsimberidou, A.M., Rudek, M.A., Hong, D., Ng, C.S., Blair, J., Goldsweig, H., and Kurzrock, R. (2010). Phase 1 first-in-human clinical study of S-trans,trans-farnesylthiosalicylic acid (salirasib) in patients with solid tumors. Cancer chemotherapy and pharmacology *65*, 235-241.

Tu, S., Bhagat, G., Cui, G., Takaishi, S., Kurt-Jones, E.A., Rickman, B., Betz, K.S., Penz-Oesterreicher, M., Bjorkdahl, O., Fox, J.G., *et al.* (2008). Overexpression of interleukin-1beta induces gastric inflammation and cancer and mobilizes myeloid-derived suppressor cells in mice. Cancer cell *14*, 408-419.

Turke, A.B., Song, Y., Costa, C., Cook, R., Arteaga, C.L., Asara, J.M., and Engelman, J.A. (2012). MEK inhibition leads to PI3K/AKT activation by relieving a negative feedback on ERBB receptors. Cancer research *72*, 3228-3237.

Turner, N.C., and Reis-Filho, J.S. (2012). Genetic heterogeneity and cancer drug resistance. The Lancet Oncology *13*, e178-185.

Ugocsai, K., Mandoky, L., Tiszlavicz, L., and Molnar, J. (2005). Investigation of HER2 overexpression in non-small cell lung cancer. Anticancer research *25*, 3061-3066.

Vaahtomeri, K., and Makela, T.P. (2011). Molecular mechanisms of tumor suppression by LKB1. FEBS letters *585*, 944-951.

Vahakangas, K.H., Bennett, W.P., Castren, K., Welsh, J.A., Khan, M.A., Blomeke, B., Alavanja, M.C., and Harris, C.C. (2001). p53 and K-ras mutations in lung cancers from former and never-smoking women. Cancer research *61*, 4350-4356.

Vaira, V., Fedele, G., Pyne, S., Fasoli, E., Zadra, G., Bailey, D., Snyder, E., Faversani, A., Coggi, G., Flavin, R., *et al.* (2010). Preclinical model of organotypic culture for pharmacodynamic profiling of human tumors. Proceedings of the National Academy of Sciences of the United States of America *107*, 8352-8356.

Wang, L., Zhu, B., Zhang, M., and Wang, X. (2017). Roles of immune microenvironment heterogeneity in therapy-associated biomarkers in lung cancer. Seminars in cell & developmental biology *64*, 90-97.

Wang, T., Nelson, R.A., Bogardus, A., and Grannis, F.W., Jr. (2010). Five-year lung cancer survival: which advanced stage nonsmall cell lung cancer patients attain long-term survival? Cancer *116*, 1518-1525.

Varghese, A.M., Zakowski, M.F., Yu, H.A., Won, H.H., Riely, G.J., Krug, L.M., Kris, M.G., Rekhtman, N., Ladanyi, M., Wang, L., *et al.* (2014). Small-cell lung cancers in patients who never smoked cigarettes. Journal of thoracic oncology : official publication of the International Association for the Study of Lung Cancer *9*, 892-896.

Vassella, E., Langsch, S., Dettmer, M.S., Schlup, C., Neuenschwander, M., Frattini, M., Gugger, M., and Schafer, S.C. (2015). Molecular profiling of lung adenosquamous carcinoma: hybrid or genuine type? Oncotarget *6*, 23905-23916.

Wculek, S.K., and Malanchi, I. (2015). Neutrophils support lung colonization of metastasis-initiating breast cancer cells. Nature *528*, 413-417.

Weiss, J., Sos, M.L., Seidel, D., Peifer, M., Zander, T., Heuckmann, J.M., Ullrich, R.T., Menon, R., Maier, S., Soltermann, A., *et al.* (2010). Frequent and focal FGFR1 amplification associates with therapeutically tractable FGFR1 dependency in squamous cell lung cancer. Science translational medicine *2*, 62ra93.

Wennerberg, K., Rossman, K.L., and Der, C.J. (2005). The Ras superfamily at a glance. Journal of cell science *118*, 843-846.

Westcott, P.M., and To, M.D. (2013). The genetics and biology of KRAS in lung cancer. Chinese journal of cancer *32*, 63-70.

Wingo, S.N., Gallardo, T.D., Akbay, E.A., Liang, M.C., Contreras, C.M., Boren, T., Shimamura, T., Miller, D.S., Sharpless, N.E., Bardeesy, N., *et al.* (2009). Somatic LKB1 mutations promote cervical cancer progression. PloS one *4*, e5137.

Virmani, A.K., Fong, K.M., Kodagoda, D., McIntire, D., Hung, J., Tonk, V., Minna, J.D., and Gazdar, A.F. (1998). Allelotyping demonstrates common and distinct patterns of chromosomal loss in human lung cancer types. Genes, chromosomes & cancer *21*, 308-319.

Wong, D.W., Leung, E.L., So, K.K., Tam, I.Y., Sihoe, A.D., Cheng, L.C., Ho, K.K., Au, J.S., Chung, L.P., and Pik Wong, M. (2009). The EML4-ALK fusion gene is involved in various histologic types of lung cancers from nonsmokers with wild-type EGFR and KRAS. Cancer *115*, 1723-1733.

Wong, M.C.S., Lao, X.Q., Ho, K.F., Goggins, W.B., and Tse, S.L.A. (2017). Incidence and mortality of lung cancer: global trends and association with socioeconomic status. Scientific reports *7*, 14300.

Woodard, G.A., Jones, K.D., and Jablons, D.M. (2016). Lung Cancer Staging and Prognosis. Cancer treatment and research *170*, 47-75.

Wu, K., Chang, Q., Lu, Y., Qiu, P., Chen, B., Thakur, C., Sun, J., Li, L., Kowluru, A., and Chen, F. (2013). Gefitinib resistance resulted from STAT3-mediated Akt activation in lung cancer cells. Oncotarget *4*, 2430-2438.

Xiao, Z., Jiang, Q., Willette-Brown, J., Xi, S., Zhu, F., Burkett, S., Back, T., Song, N.Y., Datla, M., Sun, Z., *et al.* (2013). The pivotal role of IKKalpha in the development of spontaneous lung squamous cell carcinomas. Cancer cell *23*, 527-540.

Xu, C., Fillmore, C.M., Koyama, S., Wu, H., Zhao, Y., Chen, Z., Herter-Sprie, G.S., Akbay, E.A., Tchaicha, J.H., Altabef, A., *et al.* (2014). Loss of Lkb1 and Pten leads to lung squamous cell carcinoma with elevated PD-L1 expression. Cancer cell *25*, 590-604.

Xu, X., Rock, J.R., Lu, Y., Futtner, C., Schwab, B., Guinney, J., Hogan, B.L., and Onaitis, M.W. (2012). Evidence for type II cells as cells of origin of K-Ras-induced distal lung adenocarcinoma. Proceedings of the National Academy of Sciences of the United States of America *109*, 4910-4915.

Xue, Y., Hou, S., Ji, H., and Han, X. (2017). Evolution from genetics to phenotype: reinterpretation of NSCLC plasticity, heterogeneity, and drug resistance. Protein & cell *8*, 178-190.

Yadav, B., Pemovska, T., Szwajda, A., Kulesskiy, E., Kontro, M., Karjalainen, R., Majumder, M.M., Malani, D., Murumagi, A., Knowles, J., *et al.* (2014). Quantitative scoring of differential drug sensitivity for individually optimized anticancer therapies. Scientific reports *4*, 5193.

Yamamoto, H., Shigematsu, H., Nomura, M., Lockwood, W.W., Sato, M., Okumura, N., Soh, J., Suzuki, M., Wistuba, II, Fong, K.M., *et al.* (2008). PIK3CA mutations and copy number gains in human lung cancers. Cancer research *68*, 6913-6921.

Yang, A., Walker, N., Bronson, R., Kaghad, M., Oosterwegel, M., Bonnin, J., Vagner, C., Bonnet, H., Dikkes, P., Sharpe, A., *et al.* (2000). p73-deficient mice have neurological, pheromonal and inflammatory defects but lack spontaneous tumours. Nature *404*, 99-103.

Yang, G., Rosen, D.G., Zhang, Z., Bast, R.C., Jr., Mills, G.B., Colacino, J.A., Mercado-Uribe, I., and Liu, J. (2006). The chemokine growth-regulated oncogene 1 (Gro-1) links RAS signaling to the senescence of stromal fibroblasts and ovarian tumorigenesis. Proceedings of the National Academy of Sciences of the United States of America *103*, 16472-16477.

Yang, M.-J., Hsu, C.-K., Chang, H.-J., Yen, L.-C., Tsao, D.-A., Chiu, H.-H., Huang, Y.-T., Chen, Y.-F., Wang, J.-Y., and Lin, S.-R. (2009). The KRAS Mutation is Highly Correlated With EGFR Alterations in Patients With Non-small Cell Lung Cancer, Vol 1.

Yang, P., Cerhan, J.R., Vierkant, R.A., Olson, J.E., Vachon, C.M., Limburg, P.J., Parker, A.S., Anderson, K.E., and Sellers, T.A. (2002). Adenocarcinoma of the lung is strongly associated with cigarette smoking: further evidence from a prospective study of women. American journal of epidemiology *156*, 1114-1122.

Yarden, Y., and Sliwkowski, M.X. (2001). Untangling the ErbB signalling network. Nature reviews Molecular cell biology *2*, 127-137.

Ye, X.Z., Yu, S.C., and Bian, X.W. (2010). Contribution of myeloid-derived suppressor cells to tumor-induced immune suppression, angiogenesis, invasion and metastasis. Journal of genetics and genomics = Yi chuan xue bao *37*, 423-430.

Ylikorkala, A., Rossi, D.J., Korsisaari, N., Luukko, K., Alitalo, K., Henkemeyer, M., and Makela, T.P. (2001). Vascular abnormalities and deregulation of VEGF in Lkb1-deficient mice. Science (New York, NY) *293*, 1323-1326.

Youn, J.I., Nagaraj, S., Collazo, M., and Gabrilovich, D.I. (2008). Subsets of myeloid-derived suppressor cells in tumor-bearing mice. Journal of immunology (Baltimore, Md : 1950) *181*, 5791-5802.

Yuan, H., Myers, S., Wang, J., Zhou, D., Woo, J.A., Kallakury, B., Ju, A., Bazylewicz, M., Carter, Y.M., Albanese, C., *et al.* (2012). Use of reprogrammed cells to identify therapy for respiratory papillomatosis. The New England journal of medicine *367*, 1220-1227.

Yuan, Y. (2016). Spatial Heterogeneity in the Tumor Microenvironment. Cold Spring Harbor perspectives in medicine *6*.

Yun, C.H., Mengwasser, K.E., Toms, A.V., Woo, M.S., Greulich, H., Wong, K.K., Meyerson, M., and Eck, M.J. (2008). The T790M mutation in EGFR kinase causes drug resistance by increasing the affinity for ATP. Proceedings of the National Academy of Sciences of the United States of America *105*, 2070-2075.

Zhang, X., Gureasko, J., Shen, K., Cole, P.A., and Kuriyan, J. (2006). An allosteric mechanism for activation of the kinase domain of epidermal growth factor receptor. Cell *125*, 1137-1149.

Zhang, Z., Lee, J.C., Lin, L., Olivas, V., Au, V., LaFramboise, T., Abdel-Rahman, M., Wang, X., Levine, A.D., Rho, J.K., *et al.* (2012). Activation of the AXL kinase causes resistance to EGFR-targeted therapy in lung cancer. Nature genetics *44*, 852-860.

Zheng, D., Yin, L., and Chen, J. (2014). Evidence for Scgb1a1(+) cells in the generation of p63(+) cells in the damaged lung parenchyma. American journal of respiratory cell and molecular biology *50*, 595-604.

Zilfou, J.T., and Lowe, S.W. (2009). Tumor suppressive functions of p53. Cold Spring Harbor perspectives in biology *1*, a001883.

Zimmermann, M., Lampe, J., Lange, S., Smirnow, I., Konigsrainer, A., Hann-von-Weyhern, C., Fend, F., Gregor, M., Bitzer, M., and Lauer, U.M. (2009). Improved reproducibility in preparing precision-cut liver tissue slices. Cytotechnology *61*, 145-152.

Zuo, W., Zhang, T., Wu, D.Z., Guan, S.P., Liew, A.A., Yamamoto, Y., Wang, X., Lim, S.J., Vincent, M., Lessard, M., *et al.* (2015). p63(+)Krt5(+) distal airway stem cells are essential for lung regeneration. Nature *517*, 616-620.